COMPARISON OF CLEANING PERFORMANCE FOR ROW CLEANERS ON A STRIP-TILLAGE IMPLEMENT

A Thesis Submitted to the College of Graduate Studies and Research
in Partial Fulfillment of the Requirements for the Degree of
Master of Science
in the Department of Chemical and Biological Engineering
University of Saskatchewan
Saskatoon

By

Ryan Roberge

PERMISSION TO USE

In presenting this thesis in partial fulfillment of the requirements for a Master of Science degree from the University of Saskatchewan, I agree that the Libraries of this University may make it freely available for inspection. I further agree that permission for copying of this thesis in any manner, in whole or in part, for scholarly purposes may be granted by the professor who supervised my thesis work or, in his absence, by the Head of the Department of Chemical and Biological Engineering or the Dean of the College of Engineering. It is understood that any copying or publication or use of this thesis or parts thereof for financial gain shall not be allowed without my written permission. It is also understood that due recognition shall be given to me and to the University of Saskatchewan in any scholarly use which may be made of any material in my thesis.

Requests for permission to copy or to make other use of material in thesis in whole or in part should be addressed to:

Head of the Department of Chemical and Biological Engineering
University of Saskatchewan
Saskatoon, Saskatchewan, S7N 5A9

OR

Dean
College of Graduate Studies and Research
University of Saskatchewan
107 Administration Place
Saskatoon, Saskatchewan S7N 5A2
Canada

'I hereby grant to University of Saskatchewan and/or its agents the non-exclusive license to archive and make accessible, under the conditions specified below, my thesis, dissertation, or project report in whole or in part in all forms of media, now or for the duration of my copyright ownership. I retain all other ownership rights to the copyright

of the thesis, dissertation or project report. I also reserve the right to use in future works (such as articles or books) all or part of this thesis, dissertation, or project report.

I hereby certify that, if appropriate, I have obtained and attached hereto a written permission statement from the owner(s) of each third party copyrighted matter that is included in my thesis, dissertation, or project report, allowing distribution as specified below. I certify that the version I submitted is the same as that approved by my advisory committee.'

ABSTRACT

Strip-tillage implements remove the residue from previous crops and form a seedbed ready for planting. An experiment was conducted to evaluate 5 row-cleaning devices. The proportion of residue removed by the implement was used as the performance indicator. Each of the 5 devices was evaluated at 2 speeds and orientations on the implement. The devices were tested in two blocks (fields) of corn residue (one high residue and one medium residue), and one field of wheat residue. An analysis was conducted, using a mixed-effects model, to compare the performance of the cleaners operating in the different conditions. All cleaners performed well, with no statistical difference in mean performance. All row cleaners performed more consistently in wheat residue, compared with performance in corn residue. Numerically, the consistency of the different cleaners was different, with one configuration performing less consistently than the other four. Edge-effects of the outside row unit of the implement had, in most cases, an insignificant effect on the row unit's cleaning performance.

ACKNOWLEDGMENTS

Even though only one name appears on the front page of this thesis, there are many people without whose time, guidance and expertise, this project would not have been completed. I've always found it difficult to put feelings into words, but here's my best shot...

Firstly, to my supervisor, Dr. Trever Crowe, from whom I've had the privilege to learn and grow as an undergraduate student, a summer-student, and a graduate student. I consider myself very lucky to have worked with you on so many levels. Thank you for taking me under your wing as a graduate student, for the leadership and guidance you have given me along the road to the completion of the graduate degree, and for mentoring me to become an ever-better researcher and engineer.

Dr. Martin Roberge has also had a great influence on my research career. I would like to thank you for the opportunities you've given me to work with you as a summer student throughout my undergraduate career and extending me the opportunity to pursue this research project for my graduate work. Throughout the time I've known you, you have often used the word 'passion' in discussions. Thank-you for sharing your passion of agricultural equipment research with me and instilling a passion for research and engineering within me.

I would like to thank Dr. Scott Noble for sitting on my advisory committee, providing advice about the thesis, our 'problem-solving' discussions, and allowing me to experience university education from the instructor's position as opposed to the student's. Helping you throughout the 'Electrical Power' labs as a teaching assistant has given me a new and different perspective on the learning experience.

I know time is something we often find ourselves short of and I want you to know how much I appreciate the time you have all (Drs. Crowe, Roberge, and Noble) devoted to me throughout this project - from meetings and discussions to document reviewing.

Jacky Payne played a critical role in the execution of this research. Without you, I would have been unable to complete the field trials. Thank-you for organizing and constructing the

prototype equipment for the tests, for your time and patience throughout the period we were in Texas, for sharing your extensive agronomic knowledge and expertise with me, and introducing me to authentic Texas-style BBQ... I would like to thank Tracey Meiners and Tim Olson from CNH Goodfield for providing me the opportunity to perform research on strip-tillage equipment produced at the Goodfield facility and for providing financial & logistical support through CNH for the project.

As part of my graduate studies, I had the opportunity to take a class about experiment design and statistical analysis from Dr. Eric Lamb in the Department of Plant Sciences at the University of Saskatchewan. The practical methods I learned (along with extra advice from Dr. Lamb along the way...) helped greatly when the time came to analyze the field data I had collected. Thank-you for your advice and interest in my graduate research.

I would like to acknowledge David Ford of Dumas, TX for the use of his equipment, land, and time to complete this research. We couldn't have asked for a better research collaborator.

I would like to thank NSERC, the Department of Agricultural & Bioresource Engineering (now the Department of Chemical and Biological Engineering) at the University of Saskatchewan, and CNH Canada Ltd. for financial support for graduate student scholarships, research capital, and accommodation costs for the CIGR World Congress in Québec City to present this research.

Lastly, but most importantly, I would like to thank my family. Mom & dad, thank-you for supporting me in so many ways throughout this part of my life, and passing on your values and your parent's values to me. Merissa, thanks for putting up with a brother who comes home to tell you boring stories (i.e. how his statistical code doesn't work...) and for being a good roomie at 1425. Sarah - what can I say... You inspire me every day to do the best I can do. Thank-you for the motivation, support, and love you've given me through this dance. I can't wait for the next one...

- Ryan

TABLE OF CONTENTS

LIST OF TABLES

LIST OF FIGURES

1.0 INTRODUCTION

Strip-tillage is an agronomic practice used in minimum tillage row-crop production in the United States and Canada. It can be defined as, "any row-crop cultural practice that restricts soil and residue disturbance to less than 25% of the field area" (Morrison, 2002). The tillage can be shallow or deep, and within each of these two categories it may be minimal or intense. The configurations chosen from the above-listed options will depend upon the type of soil, the climate, the crop and the management scheme in the farming operation. (Morrison, 2002) Generally, the portion of the field that is tilled becomes the seedbed (berm) for the crop while a vast majority of the accumulated surface residue is moved to the inter-row zones as shown in Figure 1.1. Fertilizer is usually applied at the same time and can be in the form of solid (ie. urea or phosphate), liquid (i.e. urea ammonium nitrate) or gas (anhydrous ammonia), with the latter being the most common type. Strip-tillage and fertilizer application operations are often completed in the fall, followed by seeding in spring, however both the strip-till and seeding operations may be performed in the spring.

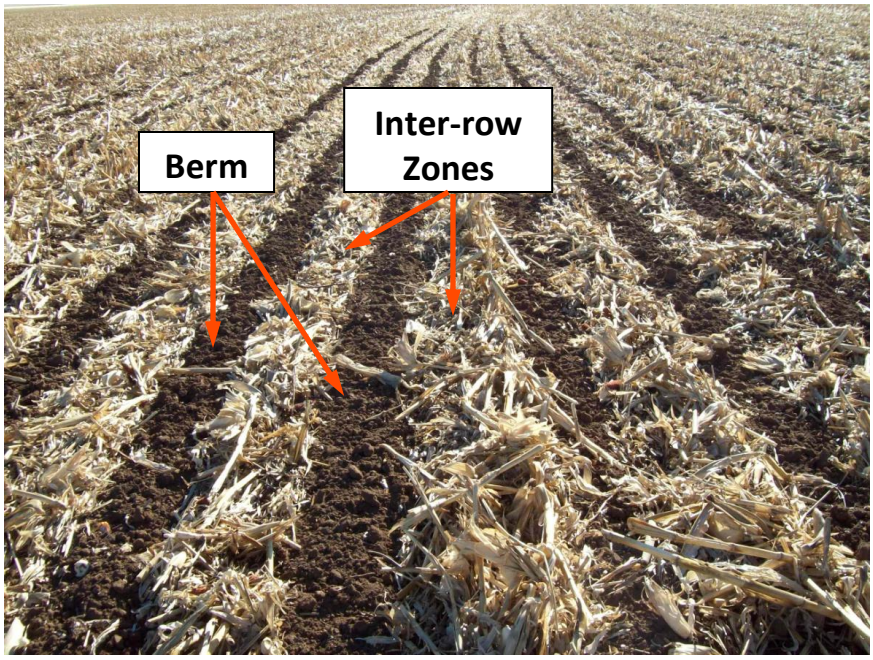

Figure 1.1. A corn field which has undergone the strip-tillage operation showing the berms as long dark vertical lines of soil and the corn residue which has been moved to the inter-row zones.

The adoption of strip tillage as a mainstream field management practice is growing across the American Midwest. It is difficult to associate an increase in strip-tillage with a specific factor, however the combination of a variety of factors may be playing a role. As the costs of fuel, labor and equipment rise, farmers and farm managers are constantly looking for ways to reduce or at least hold production costs to current levels, while also seeking more agronomically sound and environmentally friendly practices. With strip-tillage, cost savings are realized because there are at least two fewer field passes as compared to conventional tillage (Wolkowski, 2000). Studies by Al-Kaisi et al. (2005) have indicated that by using strip-tillage, the amount of soil organic carbon (SOC) increased by 11.4% as compared to a moldboard plow tillage treatment after three years. Similar results in this study were also apparent with soil organic nitrogen (SON). Increasing SOC and SON improve the quality of the soil and could potentially lead to a higher quality, higher yielding crop. Using strip tillage also has significant effects on soil temperature and moisture content. Various studies by Swan et al. (1996), Azooz et al. (1995), Wolkowski et al. (2000), and Licht and Al-Kaisi (2005) have come to similar conclusions. Strip-tillage increased the soil temperature as compared to no-till conditions allowing for faster plant germination and better early growth. This is important as it allows the crop to advance ahead of weeds in the competition for limited resources, potentially facilitating better yields and an earlier harvest date. With regards to soil moisture content or soil moisture retention, strip-tillage was able to better conserve moisture than conventional tillage due to reduced evaporation rates. This meant that more plant-available water (PAW) is present to support crop growth.

1.1 Strip Tillage Field Implements

The Goodfield, Illinois, CNH manufacturing facility constructs strip-tillage machines in both 3-point mounted and pull-type models with 0.76-m (30-in) row spacings. The layout of a typical strip tillage row unit is shown in Figure 1.2, and a commercial Case IH machine is shown in Figure 1.3. From front to rear, the row units employed in these machines consist of:

1. a leading coulter to cut residue and create a path for the mole knife,
2. a row-cleaner to move the residue to the inter-row zone that is permitted to float over the ground via a parallel linkage, operating directly in front of the mole knife,
3. a mole knife used to fracture & loosen the soil and apply fertilizer,

4. a pair of berm-building disks mounted so as to capture the soil thrown aside and bring it back together to form a seedbed ridge or berm and
5. a rolling basket to firm and shape the ridge into a proper berm.

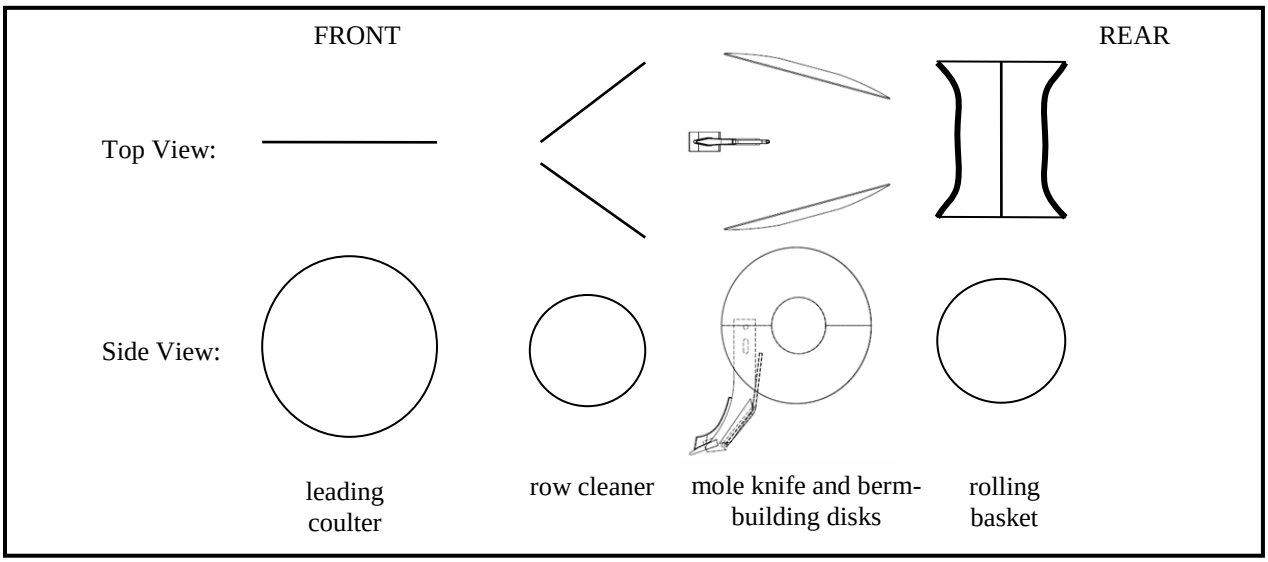

Figure 1.2. Top and side view schematic of a typical strip tillage row unit.

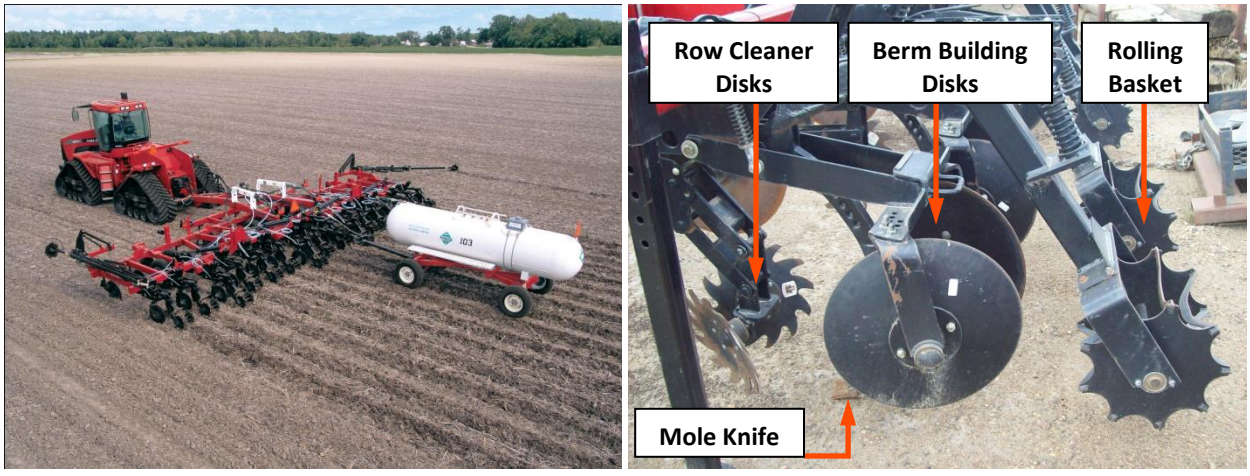

(a) **(b)**

Figure 1.3. 'a' strip tillage equipment working in the field (CNH, 2010 [used with perimission]). 'b' side view of a single strip-tillage row unit (leading coulter not shown).

1.2 Differing Philosophies on Dealing with Residue

Companies who manufacture strip tillage implements have differing views on the management of residue within the strip-tillage process. Differing philosophies are briefly presented as background information, as this general knowledge was used both in the development of the Alpha Prototype row-cleaner configuration, described in greater detail in following chapters, and to understand different methods of achieving similar seedbed formation results.

A survey of current manufacturers' strip-tillage products yielded two main philosophies that are used to manage residue in the strip tillage process. The first involves mixing the residue into the newly-formed seedbed and the second involves removing the residue to allow a seedbed constructed predominantly of tilled soil.

A couple of companies (Environmental Tillage Systems Inc., Faribault, MN; Brillion Farm Equipment, Brillion, WI) employ a system to cut and pulverize the residue and mix it into the seedbed while also tilling the strips of soil. In most cases, this process is accomplished using a configuration of wavy, fluted or notched coulters mounted parallel to the direction of motion of the machine. This method is used instead of or in combination with a fertilizer injection knife.

The alternative and more popular method of handling large amounts of residue is to remove as much as possible from the seedbed region just before the soil is tilled. In most cases this is accomplished using a system of toothed concave disks or coulters to "sweep" the residue off while minimizing the amount of soil removed from the seedbed region. The disks used have varying parameters: zero concavity to some degree of concavity (concavity defined in section 3.1); straight versus curved teeth; and shallow versus deep teeth. The disks may be mounted parallel to one another, meaning that, from a top view, the disk centres are located along the same line perpendicular to the direction of motion. They may also be staggered or offset from this line so that one is located ahead of the other. The disks may also be located forwards (Remlinger Manufacturing, Kalida, OH) or rearwards (Case IH, Racine, WI) of the leading coulter of the row unit.

1.3 Problem Statement

Issues pertaining to the performance of row cleaners have been identified as an area of interest for further study. In high-residue conditions, some configurations of row cleaners are unable to adequately clear the residue from the seedbed area creating a less-than-satisfactory residue distribution and opportunities for plugging the strip-till implement.

2.0 OBJECTIVES

The primary objective of this study was to conduct an experiment that compared the performance of row cleaners used on strip-tillage implements. The results from the experiment were then used to suggest the design and set parameters that should be used under certain operating conditions.

The experiment evaluated the effect of different levels of multiple factors on row cleaner performance. The response variable used to gauge performance was the change in residue distribution from before the strip-tillage operation to afterwards. The experimental factors were:

- row cleaner configuration (5 types)
    - Alpha Prototype
    - offset disk mount with 0.33-m (13-in.) diameter disk (Offset-13)
    - offset disk mount with 0.46-m (18-in.) diameter disk (Offset-18)
    - parallel disk mount with 0.33-m (13-in.) diameter disk (Parallel)
    - Case IH production mount with 0.33-m (13-in.) diameter disk - a parallel mount with different disk angles (Production)
- travel speed (2 levels)
    - 8 km/h (5 mph) (low speed)
    - 10.4 km/h (6.5 mph) in corn stubble & 11.2 km/h (7 mph) in wheat stubble (high speed)
- row unit orientation (2 types)
    - front position (front)
    - rear position (rear)

The co-factor of residue moisture content at time of operation was also measured for each trial. The 0.33-m (13-in.) diameter disks used in the row-cleaners are the same across all applicable configurations.

The experiment was conducted in two corn fields (heavy corn-on-corn residue, and medium residue) and one wheat field near Dumas, TX, February 10-12, 2009. Due to the nature of the data, there was a separate analysis for each type of crop.

3.0 LITERATURE REVIEW

What follows is a general review of topics pertinent to the proposed research. Because the row-cleaner configurations all incorporated concave disks in their design, the nomenclature used for their description and qualitative analysis is discussed. Various methods of measuring crop residue are then identified to provide insight on residue quantification techniques. These methods were researched to establish a methodology that could be used to effectively rate the performance of one row cleaner configuration against another.

Many studies have been conducted to determine whether or not there are benefits to incorporating strip tillage in a cropping system. However, there is very little work that has been published regarding the cleaning performance specific to row cleaning devices used on row-crop equipment and strip-tillage equipment. Kaspar and Erbach (1998), Raoufat and Matbooei (2007), and Fallahi and Raoufat (2008) have all conducted studies examining the effects of row cleaners as mounted on a planter. Even though the amount of residue after the operations was quantified, initial measurements were not employed, with the exception of Raoufat and Matbooei (2007), to provide a baseline for the amount of residue the row cleaner actually moved. It was also unclear whether there was residue left on the seedbed or not, and to what degree. A primary focus of these studies was to examine the agronomic results of using different types of row cleaners for planting, which when measured, could have substantially more variability than specifically examining the function which the row cleaners perform within the system.

3.1 Concave Disk Nomenclature

Three concave-disk parameters are defined to allow for easier identification during discussions in further sections. The terms are illustrated graphically in Figures 3.1 and 3.2. The disk angle, β (degrees, °), is defined as the angle between the circumferential plane of the disk with respect to the horizontal direction of motion (O'Dogherty et al., 1996). As the disk angle increases, the working width of the disk widens meaning it will move more material. The tilt angle, α (degrees, °), refers to the angle between the circumferential plane of the disk and the vertical plane, with positive & negative angles represented by the disk tilting backwards & forwards, respectively (O'Dogherty et al., 1996). A positive tilt angle provides the disk with more ability to scoop material and dig into the ground while a negative tilt angle provides more of a bull-

dozing or skimming effect making digging into the ground more difficult. The disk concavity, *c* (cm), is represented by the perpendicular distance between the circumferential plane of the disk to the centre of the front spherical surface (O'Dogherty et al., 1996).

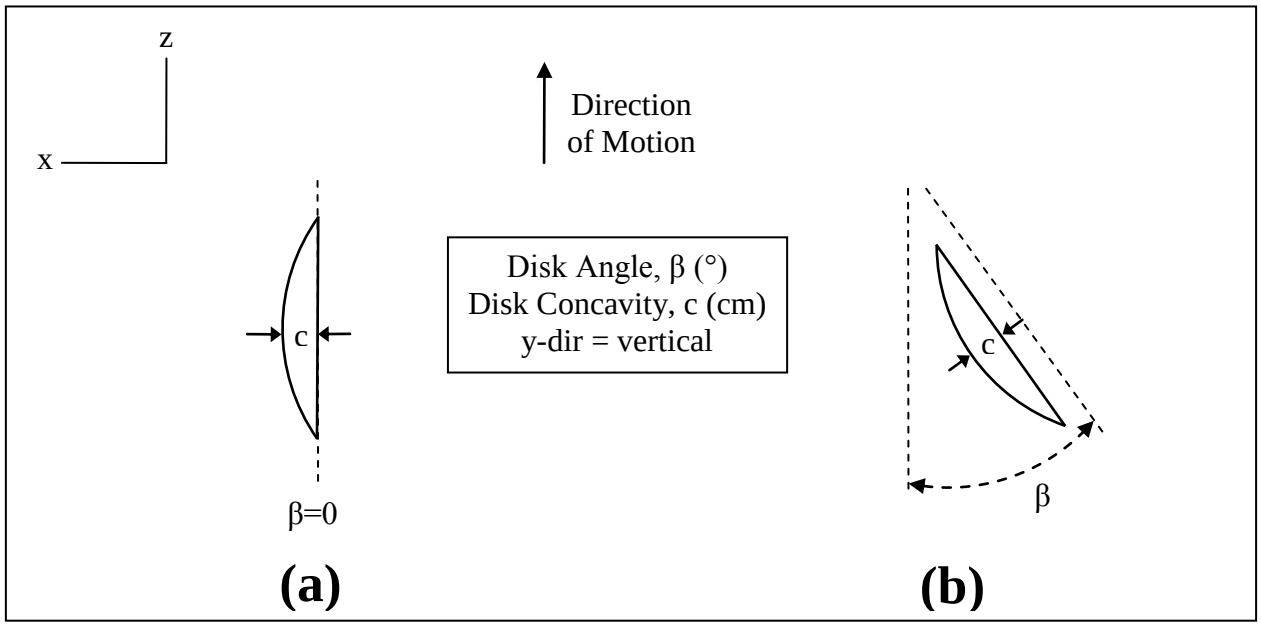

Figure 3.1. Top view of a concave disk element with (a) zero disk angle and (b) some positive disk angle β (°).

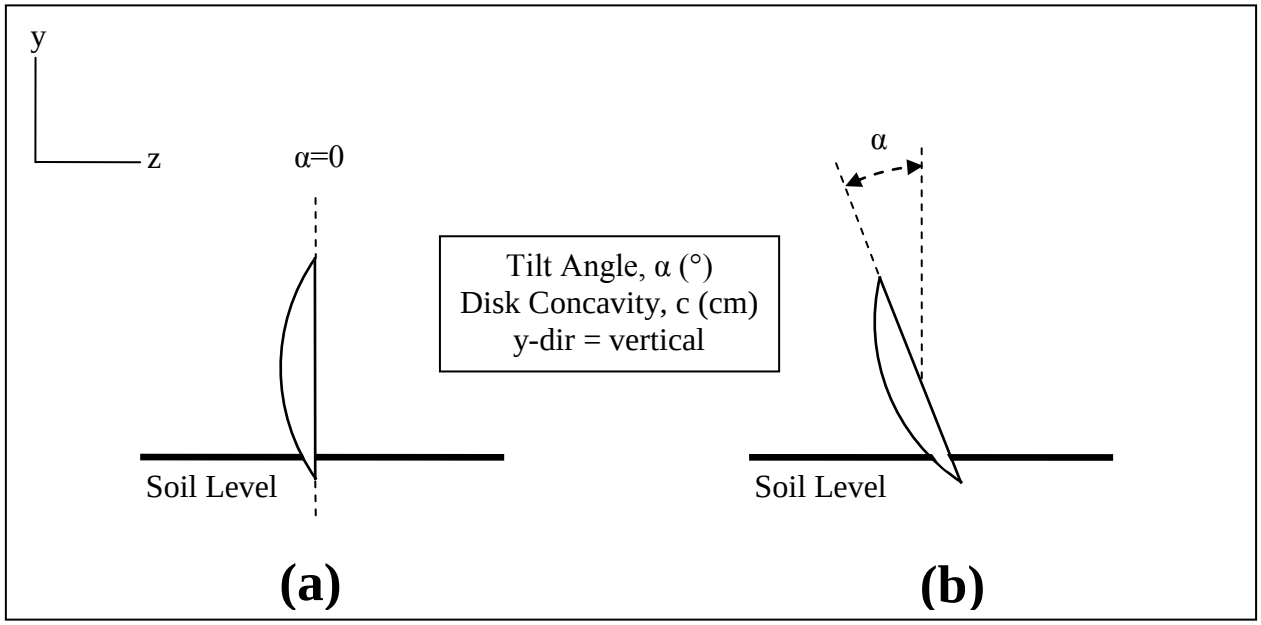

Figure 3.2. Side view of a concave disk element with (a) zero tilt angle and (b) some positive tilt angle α (°).

3.2 Quantifying Crop Residue in Field Situations

Being able to accurately quantify the amount of residue present in the field during the experiment is vital to effectively rate the cleaning performance of the various row cleaner configurations to obtain meaningful results. Residue is generally quantified by measuring the percent residue coverage, though there are exceptions. Percent residue coverage, or cover, can be defined as "the percentage of soil surface covered by pieces or fragments of plant material as seen by a nadir view" (Morrison et al., 1995). There are various methods by which residue cover can be quantified according to available literature. The two main categories of quantification methods are physical techniques and optical techniques. Physical techniques involve taking measurements *in situ* with little post-analysis required. Optical techniques often involve using digital imaging *in situ* followed by some form of post-analysis. These techniques are discussed in greater detail below.

3.2.1 Physical Techniques

Line-transect method

According to available literature, this was one of the first published methods developed to measure residue cover and is still widely used to the present day. The original method, defined by Sloneker and Moldenhauer (1977), involved setting a string down on the ground diagonally to the line of tillage with 50 beads (small hollow cylinders through which the string is threaded) attached at 0.15-m (6-in) intervals. Each bead in contact with a significant piece of residue was then counted towards the percent cover value. Newer versions of the line-transect method defined by Laflen et al. (1981) and Morrison et al. (1993) employed ropes with 100 beads installed so that each bead counted as a single percentage point.

Morrison et al. (1993) observed that there were two types of error that occurred when using this method. The first was the error due to operator bias where there was error between different operators taking measurements in a slightly different manner at each bead. The second source of error was the geometric patterns of residue distribution produced by various pieces of field equipment. To reduce the first error, they suggested using double beads with a small interstitial space at a single interval so a residue 'hit' would only be recorded if the residue was positioned

between the two beads. To reduce the effects of the geometric error they suggested randomizing the distance between beads using a range from 0.076 m (3 in) to 0.229 m (9 in) with a mean of 0.15 m (6 in). The number of required measurements depends on the precision that the user desires, however for most purposes, Laflen et al. (1981) recommended five measurements to come within 15% of the true mean value for the method.

This method has been widely used and accepted in several studies since it was first published. Examples of research conducted using the line-transect method include Brown et al. (1992), Azooz et al. (1995), Raper (2002), Vetsch and Randall (2002) and Fallahi and Raoufat (2008).

Meter-stick method

As described by Hartwig and Laflen (1978), this method involved placing a meter-stick on the field perpendicular to and between two adjacent crop rows, assuming the crop being measured was corn. Beginning with one row and moving towards the other, the total length of residue bordering one side of the meter-stick was measured. The percentage residue cover was then calculated by dividing the total length of residue bordering the meter-stick by the crop row-spacing. Though this method would work relatively well for small sampling areas, the precision may not be acceptable due to the large amount of variability. Hartwig and Laflen (1978) estimated that 12 sets of measurements would be required to obtain a 95% confidence interval and an estimated mean within 25% of the true value. Laflen et al. (1981) further estimated that 15 sets of measurements would be required to obtain a value within 15% of the true value, which would make it equivalent to five measurements of the line transect method. From the literature, it seems that although this method worked well for row crops, it would be difficult to implement in cereal crops with small diameter residue such as wheat stubble.

Standing-stubble hoop method

This method, described in Morrison et al. (1993), was developed to easily quantify the standing stubble in a field. The output of this method was not expressed as percent residue cover, but rather as tonnage per hectare. A hoop with a diameter of 0.72 m (28.26 in) was laid on the ground in a representative sample area. A stem count of the stems within the hoop was taken along with an average stem height. The stem count within the hoop was then converted to a stem

count per hectare. This was completed by using a conversion table to obtain a tonnage per hectare from the stem count, the area of the hoop and the average stubble height.

Residue wheel method

This measurement technique was based on the line-transect method, but rather than using a rope stretched across the ground, a land measurement wheel was employed. The wheel was equipped with spikes that were either evenly or randomly spaced around the circumference of the wheel. As the wheel rolled along, the spikes successively became adjacent to the ground. Each time a piece of residue was beneath a spike the operator recorded one count on the counting device. The counting device could be external or a data-logging system could be incorporated on the device. While the operator recorded the number of residue hits electronically, a magnetic reed switch sensed the total number of spikes that had passed over the ground. Experiments comparing various configurations of the line-transect method to the residue-wheel method concluded that the measuring techniques had the same level of precision. (Morrison et al., 1995)

Soil-core techniques for incorporated residue

Thus far, the quantification methods have all been used exclusively for surface residue. Allmaras et al. (1988) developed a method to measure residue incorporated in the soil, which obviously cannot be reported exclusively as percent surface-residue cover. They used two successive 0.3-m soil cores to collect a sample to a depth of 0.6 m. For every 1000 m^2 of field area, between eight and sixteen cores were taken. The cores were divided into 0.02-m depth increments and composited across the cores in a field area. This was completed so as to maintain at least two soil samples per reported mean for a particular 0.02-m depth increment. Following the sample collection, the soil samples were dried in low-light conditions to prevent decomposition and were sieved with a 0.5-mm sieve. At this point, the residue was then split as being greater than or less than 0.5-mm in size, depending upon whether or not it travelled through the sieve. The material in these two groups was then ground and analyzed to obtain the amount of organic carbon present in the soil. This was accomplished by measuring the total carbon content using a carbon analyzer and subtracting the amount of inorganic carbon present in the soil obtained through a carbon dilution technique. Allmaras et al. (1997) used this method to investigate the effects that conservation tillage had on the soil environment.

A much less in-depth approach was employed by Kaspar and Erbach (1998) and Raper (2002). Soil cores were collected for selected plot locations. The surface residue over the core was separated from the main mixture and washed, dried and weighed. The subsurface soil and residue mixtures were washed, separated, dried and weighed. Kaspar and Erbach (1998) represented surface and subsurface residue separately as mass per unit area and mass per unit volume of soil, respectively. Fallahi and Raoufat (2008) adapted Kaspar and Erbach's (1998) method to quantify wheat residue during a corn-planting field experiment. Raper (2002) was only interested in combining the subsurface residue with the total amount of residue and as such it was represented using a mass per unit area relationship.

Raper (2002) also measured flat and standing residue in four 0.25-m x 0.25-m areas in each experimental treatment, employing a square area rather than the circular area provided by the soil core. These values were also represented using a mass per unit area relationship. Raoufat and Matbooei (2007) used a quadrant of 0.5 m^2 to quantify wheat residue prior to and after tillage and planting operations and reported results as the amount of residue cleared and retained on a tonnage-per-hectare basis.

3.2.2 Optical Techniques

Even though the field work required to collect data for the optical techniques remains relatively unchanged since first developed, the methods by which the images are analyzed have changed dramatically with rapid advances in digital imaging and computer software. Much of the post-collection analyses associated with the photographic and video data have largely been replaced by user-friendly software such as PAX-it!™ (MIS Inc., Villa Park, IL).

Photographic method

The photographic method, like the line transect method, has also been used for a very long time. Various studies have used this technique as a comparison for the line-transect method to ensure residue cover results reported by either method were comparable (Sloneker and Moldenhauer, 1977; Corak et al., 1993; Laflen et al., 1981). Stationary photographs were taken of the residue

material viewing vertically (or nearly vertically) downward (Slonoker and Moldenbauer, 1977; Corak et al., 1993).

Once the film was developed, two different methods of post analysis could have been used. The first option was the use of a dot-grid overlay projected onto the photo as used by several studies (Slonoker and Moldenbauer, 1977; Hartwig and Laflen, 1978; Laflen et al., 1981; Lowery et al., 1984; Corak et al., 1993; and Raper, 2007). The dot-grid had either uniform or randomly positioned points, with the randomly positioned points being employed to reduce pattern bias (Corak et al., 1993; Lowery et al., 1984). The residue cover was the quotient of points over a significant piece of residue divided by the total number of points on the photograph. The second option was to use a densitometer to calculate the projected area of the residue digitally. A densitometer provided discrete values to various light intensities, which meant that residue could be identified from soil due to the light-to-dark contrast, respectively, exhibited by each material (Sloneker and Moldenbauer, 1977). By using different emulsion filters for red, blue and green light, Lowery et al. (1984) found that using a red filter provided the best contrast between the soil and residue reflectance values. They also compared the dot-grid overlay and densitometer post-analysis methods and found that the results of both methods were statistically equal.

There were several concerns identified with the photographic method. Like the meter-stick method, Laflen et al. (1981) found that 15 measurements using the photographic method were required to achieve the accuracy of five line-transect measurements. This large number of measurements could take a large amount of post-analysis time. It is also important to note that the photographic method would require relatively more expensive equipment and software to collect and analyze data, compared with physical techniques. It may also be difficult and time consuming to ensure the camera is set up at the exact same height and angle every time ensuring that representative images were acquired with equal spatial resolution. Equal resolution would be required to ensure consistency and comparable results.

Video image analysis/computer analysis method

This method was very similar to the photographic method, except that video cameras were used to capture images of crop residue. Post-analysis involved using software routines to distinguish

residue from soil. Morrison et al., (1993) and Corak et al. (1993) raised the issue that not enough contrast between soil and residue could cause deviations in residue cover measurements of up to 8% by using this method.

Residue meters

Residue meters incorporated sensors "to identify residue at a spot based on its reflective or fluorescent characteristics" (Morrison et al., 1993). The idea was to be able to evaluate whether or not residue was present at a small point on the ground opto-electronically, rather than visually by humans. The operator would walk along a transect line and take measurements at regular or random intervals as in the line-transect method, however with the human bias factor removed. (Morrison et al., 1993) This initial work with sensors for residue meters at the micro-scale has led to using spectral imaging for evaluating residue cover over wide areas of land. At this point, the topic of macro-scale spectral imaging leaves the scope of the thesis, however some physical and optical techniques were employed for sensor calibration as discussed in the section below.

3.2.3 Applications of Physical and Optical Techniques to Digital Residue Mapping

Shown in Table 3.1 is a list of academic studies conducted to develop methods for mapping residue using spectral imaging. This was researched to see how widely accepted the above methods are in regards to their use for obtaining model calibration data for large-scale spectral imaging of crop residue. Though this list is likely a small sample of spectral imaging research, it is interesting to note that only two methods of those listed above are employed.

Table 3.1. Calibration techniques used in previous crop residue spectral imaging research

Authors	Scale of Experiment	Calibration technique employed
Daughtry et al., 2006	Field scale	Line-transect method
Narayanan et al., 1992	Field scale	Line-transect method
Thoma et al., 2004	Field scale	Modified line-transect method
Bannari et al., 2006	Field scale	Photographic method
Biard and Baret, 1997	Field scale	Photographic method
Daughtry et al., 1997	Lab scale	Photographic method
Daughtry et al., 2004	Lab & field scale	Photographic method - dot-grid overlay
Haiping et al., 1994	Lab scale	Photographic method
Su et al., 1997	Field scale	Photographic method

3.3 Summary

A brief description of disk nomenclature was provided. The descriptions included definitions for disk angle, tilt angle, and disk concavity.

A variety of methods previously used to quantify surface-residue cover were presented, along with techniques for measuring incorporated residue. The two most common techniques were the line-transect method and the photographic method using a dot-grid overlay. Even though these methods worked on a small scale they would be difficult to set up on a micro-scale to fit the strip-tillage seed row. They would not account for differences in residue depth and would be subject to a large degree of operator bias that would be unable to be reconciled with enough multiple measurements in small plot areas. The photographic method also required additional equipment for pre- and post- analysis, as well as a significant amount of time for post-analysis of photographs. A mass measurement technique would virtually eliminate operator bias and could account for the depth of the residue, not only the percentage that covered the ground. A method, such as the one employed by Raoufat and Matbooei (2007) has the potential to be adapted for this field experiment. The background provided by these techniques were used to establish a suitable residue quantification method discussed in the methodology section.

4.0 MATERIALS AND METHODS

This section outlines the development of the experiment including the factors that were involved, any special data-collection procedures that were developed and the method of analysis used to obtain results from the experiment.

4.1 Experiment Design

The experiment was designed as a completely randomized block design. The response variable was cleaning performance of the row cleaners. The fixed factors were row-cleaner configuration, travel speed, and row-unit orientation and a co-factor of residue moisture content at the time the strip-tillage operation was conducted. Being a blocked design, there were also some random factors in the experiment, namely the field location, plot, and implement pass.

4.1.1 Machine Nomenclature

To allow the easy identification of row positions on the machine, the rows were numbered 1 through 16 from left to right as viewed from the rear of the machine, looking forward. Even though a 16-row machine was used in the experiment only row cleaners 1 through 8 (left side) of the machine were used in the experiment. The main reason for using half of the machine was to reduce the cost of parts required to perform the experiment.

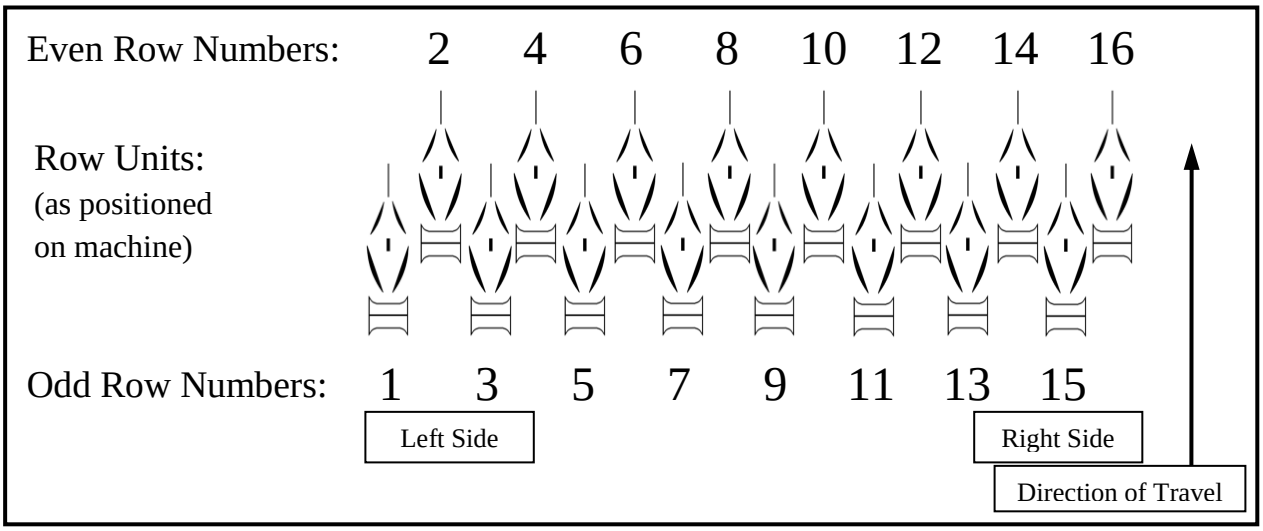

Figure 4.1. Schematic showing the numbering of the row units employed on the strip-till implement. The direction of travel points towards the front of the implement.

4.1.2 Response Variable – Cleaning Performance

From the comprehensive information provided in the literature review, it is apparent that many methods and variations thereof have been developed to quantify crop residue. There were certain criteria that had to be met in order for a method of quantification to be employed in the current study. It needed to be low cost, have a minimum of post-analysis time and operator bias, and it needed to be effective at a micro-scale within the seedbed area. Other important factors required that the process be accurate, easy to implement in a remote location using a minimum of materials and resources and it had to be able to account for a significant depth of material. Accounting for the depth of residue was important because even though the percentage residue cover may have been similar, there may have been areas with varying depths of residue where cleaning performance had to be compared. Because the row cleaners interact predominantly with the surface residue, a method of measuring subsurface residue was not required. Volume measurements were not used due to the compressibility and heterogeneity of the bulk residue material from pre- to post-operation and the high degree of error resulting from these measurements. After deliberating with the above requirements, a dry-matter mass measurement technique using a quadrat centred over the seedrow was used to quantify the residue. Cleaning performance was defined as the amount of material removed as compared to the initial material present calculated as:

$$Cleaning\ \ Performance = \frac{(initial\ \ mass - final\ \ mass)_{\ in\ sampling area}}{(initial\ \ mass)_{\ in\ sampling area}} \quad \textbf{(4.1)}$$

The mass sampling area

The residue mass measurements were recorded from a row unit (interval) sampling area that was 2 m in length and 0.25 m in width centred on the knife path of each row unit as shown in Figure 4.2. Figure 4.3 shows the positioning of the quadrat in the field used to collect residue mass data. A 2-m length was defined to allow a sufficient amount of material to provide a more accurate average for the interval sampling area. The 0.25-m width represented the maximum allowable berm width as advised by Jacky Payne (agronomist, CNH Goodfield). A quadrat was constructed from 38x89-mm wood studs with the above-noted inner dimensions with the addition of 4.76 mm tolerance to allow for the thickness of the cutting tool blades. Hand-operated clippers were used to cut any residue which resided along the perimeter line of the

interval sampling area. In the case where a piece of residue or a root ball was partially exposed or protruding from the ground AND was within the interval sampling area, it was pulled from the ground, had any attached soil physically removed, and included as a constituent within the mass measurement. Any residue covered entirely by soil was not included in the mass measurement. The mass of un-harvested ears of corn present in any samples was recorded and their locations noted. However their masses were not included in the analyses. After a preliminary analysis of the data, it was found that their presence could cause a significant influence in the data likely due to its large density. This would, in turn, severely reduce the calculated performance value. In reality however, the effect of an ear of corn on cleaning performance would have been very small due to its small volume relative to the large volume of the crop residue.

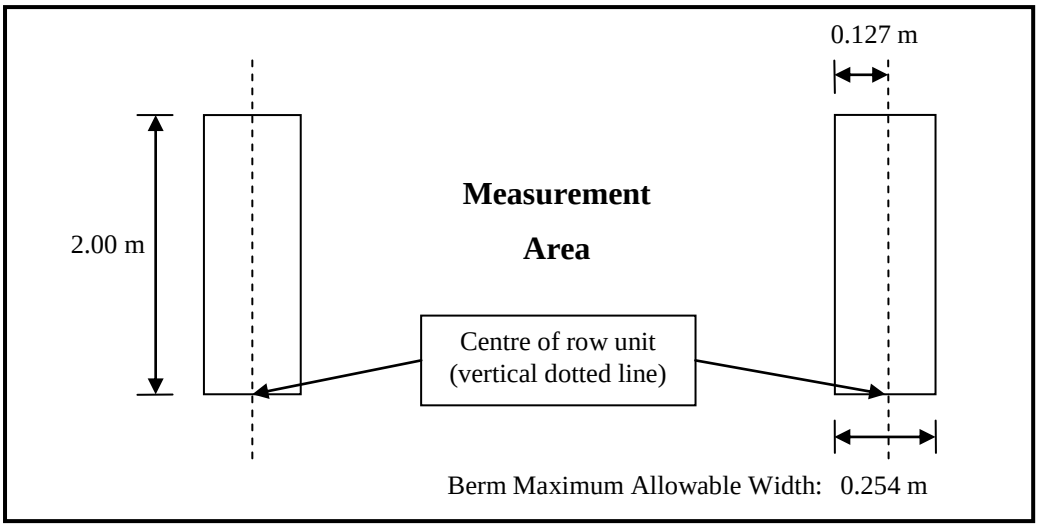

Figure 4.2. Measurement area for residue distribution.

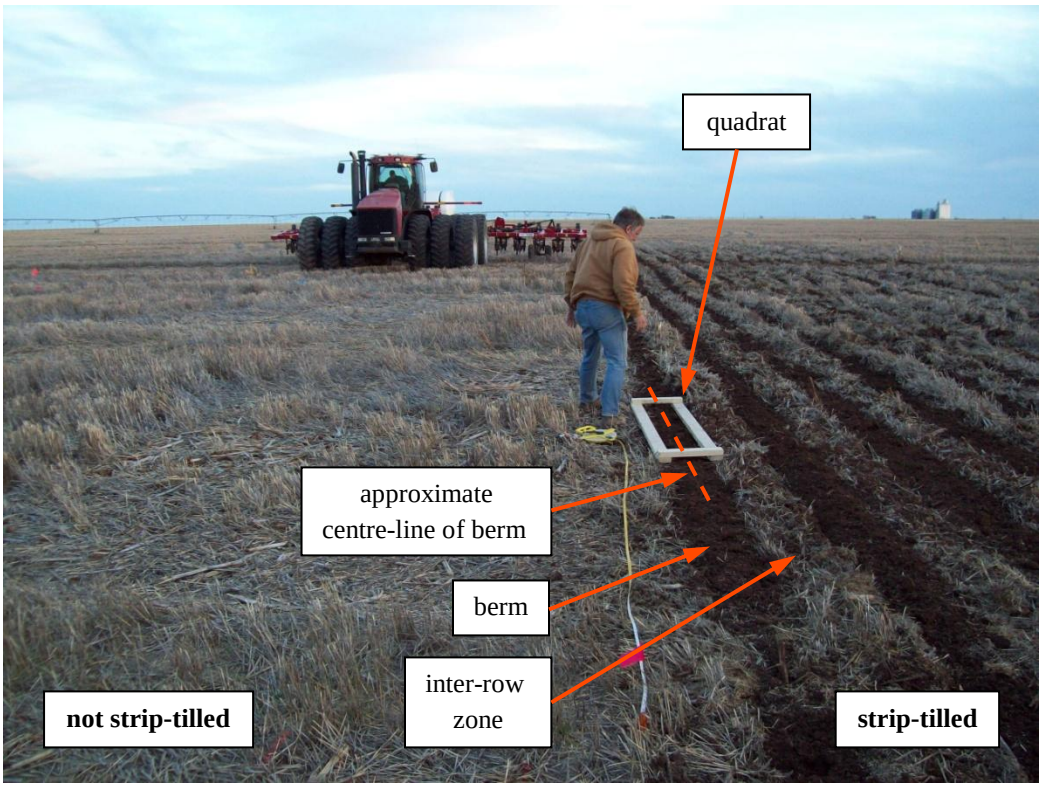

Figure 4.3. Jacky Payne (agronomist, CNH Goodfield) is shown positioning the sampling quadrat centred on a newly-constructed berm in a freshly-strip-tilled wheat field.

A five-step process was used to collect residue mass measurement data from a single interval sampling area. Each sampling area was randomly selected from those available in each plot. The following describes the process.

1. The location of the sampling area within the plot was located. The row location was identified by counting the number of corn rows from the center of the plot for the corn stubble and by measuring the distance from the center of the plot with a measuring tape in wheat stubble. The interval location was identified in both corn and wheat stubble by measuring the distance from one edge of the plot to the nearest edge of the sample quadrat as shown in Figure 4.4.

Figure 4.4. Photo of measurement quadrat *in situ* in a corn plot.

2. While standing on the quadrat to hold it firmly in place, the crop residue intersecting the quadrat perimeter was cut along the inner edge as shown in Figure 4.5. This allowed easy separation of residue contained within the quadrat from that which was externally located.

Figure 4.5. Ryan using grass clippers to cut the corn residue along the inner edge of the quadrat.

3. The crop residue within the quadrat was then collected and placed in a holding container as shown in Figure 4.6. A foam container and plastic totes were used for this purpose.

Figure 4.6. Jacky Payne (agronomist, CNH Goodfield) collects the residue in the quadrat and places it in a foam container.

4. The material was then weighed (Scout Pro SP2001, Ohaus, Pine Brook, NJ) with a resolution of ±0.1 g. Precautions had to be taken to shelter the balance from the wind. During the initial residue mass measurements the balance was kept within the cab of the field truck as shown in Figure 4.7. To reduce the time required to take final residue mass measurements (i.e. Walking back and forth from the truck) the balance was set on the lid of a clear plastic container on level ground. The container itself was then placed overtop to eliminate the wind's effect on the mass reading as shown in Figure 4.8.

Figure 4.7. A plastic container being weighed in the rear portion of the cab of the field truck.

Figure 4.8. Photo of the upside-down plastic container to collect final residue mass measurements.

5. The dry mass of the residue was then calculated using the moisture content determinations. During the initial and final residue mass measurements, residue moisture measurements were recorded at least once per hour. In cases where more than one plot was assessed within a single hour, residue moisture data were shared by multiple plots yielding one moisture content for the plot on which mass measurements were taken. If no residue sample was taken on a plot due to 'high productivity measurements' (i.e. taking measurements on 3 plots per hour), a weighted average of the two adjacent moisture contents was used as the moisture content for that particular plot. These data were used to calculate the dry matter content for the corresponding plots to ensure that a consistent comparison was made across plots and locations. The moisture measurements were completed according to ASABE Standard S358.2 (ASABE, 2008) utilizing a microwave oven as a drying method. The microwave oven used in this process is shown below in Figure 4.9 with a corn residue sample inside.

Figure 4.9. Microwave oven used to dry residue to obtain moisture content.

Plot organization

A sample diagram of one plot is shown below in Figure 4.10. The centre 12.19 m, or 16 row units, of each plot were used to obtain measurements. The blue regions indicate an interval where final residue mass measurements were taken and the yellow spaces indicate an interval where an initial mass measurement was taken. 'Pass 1' indicated a machine pass from the right to the left side of the plot as shown, while 'Pass 2' indicated a machine pass from the left to the right side of the plot as shown. Detailed schematics for the plot diagrams of locations I, II & III can be found in Appendix A.

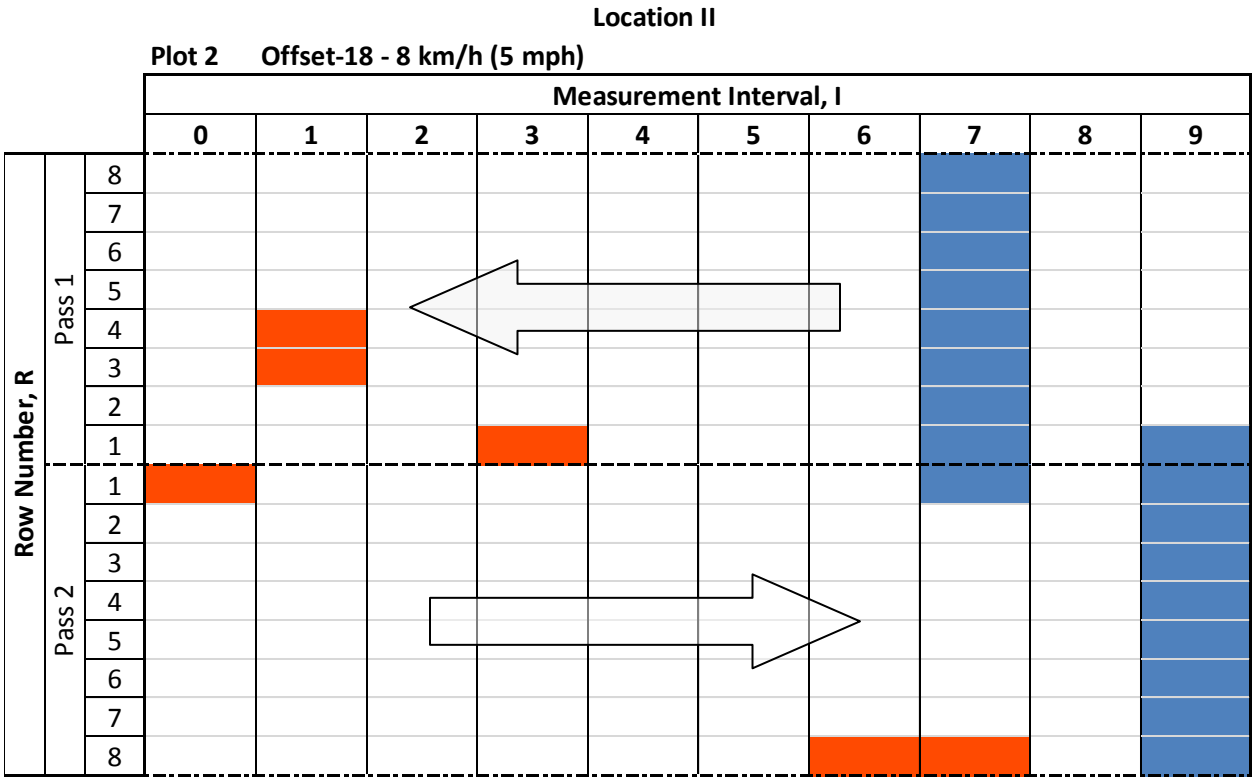

Figure 4.10. This is an example of a plot in the experiment. The orange blocks indicate a position where an initial residue measurement was taken while the blue regions indicate positions where final residue measurements were taken. 'Pass 1' and 'Pass 2' indicate machine travel directions from the right to the left sides of the plot, and from the left to the right sides of the plot, respectively, as shown by the large arrows.

Choosing initial and final sampling areas within the plot

Each plot was subdivided into a grid 16 machine row units in width (8 row units per pass with 2 passes) and 20 m (ten sample intervals of 2 m) in length. The locations of the initial and final sample measurements were randomly selected for each of the two passes. The final mass measurements were taken from the same interval for all row units of each pass to account for and minimize any interactive effects between row units. This ensured consistent residue conditions existed in the final sampling areas. It also maximized the number of sampling areas that could be randomly selected to characterize initial residue conditions. Subsequently, there were 3 initial residue measurement locations randomly chosen from each pass from all of the remaining sampling areas in the grid. There were controls instituted which ensured a minimum of 2 m between the final measurement intervals of the two passes, as well as 2 m and/or a one-row buffer between any given initial and final residue mass measurement. This was done to ensure that any final measurements could not be influenced by any of the initial measurements taken.

Special case – measuring cleaning performance for edge effects:

In this case, edge effects were described as the interaction of the outside row unit of the strip-tillage machine (row 1) with the area immediately adjacent to it, where the outside row unit of the former/following pass was hypothetically located. The neighboring area was either untouched field or had the strip-tillage operation conducted upon it. Measuring the edge effects identified whether or not residue was thrown over onto the operating path of the adjacent row unit of the neighboring pass.

For measuring the change in residue distribution for edge effects a specialized procedure of the general case was applied. A schematic is shown below in Figure 4.11. Descriptively the locations and times are:

1. The initial residue distribution was determined before any passes, as provided by the 'general case' scenario. This is indicated by position one in Figure 4.11.
2. A measurement was taken at position 2 in Figure 4.11 after the **first** pass of the machine at the location of the outside row unit of the **first** pass.
3. A measurement was taken at position 3 in Figure 4.11 after the **first** pass of the machine at the location of the outside row unit of the **second** pass (before second pass).

4. A measurement was taken at position 4 in Figure 4.11 after the **second** pass of the machine at the location of the outside row unit of the **first** pass.
5. A measurement was taken at position 5 in Figure 4.11 after the **second** pass of the machine at the location of the outside row unit of the **second** pass.

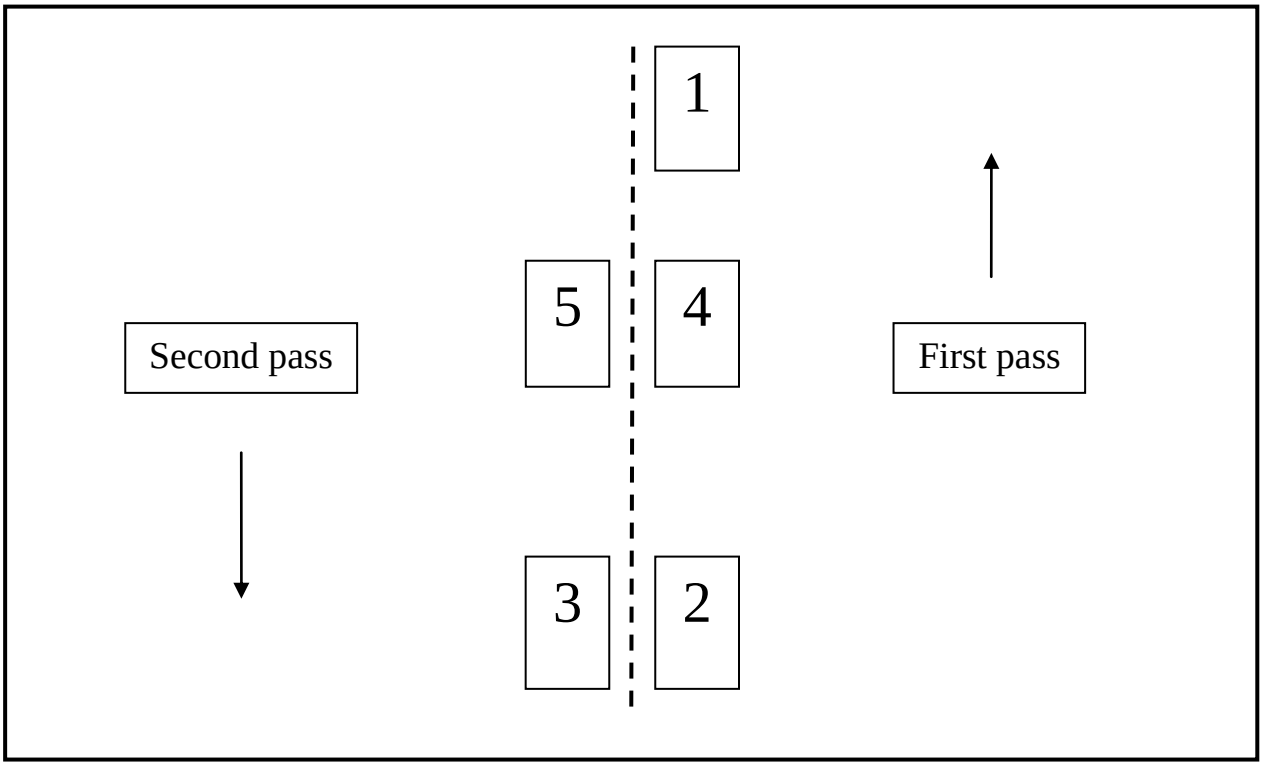

Figure 4.11. The measurement locations that were used for edge-type interaction. '1' was taken before any machine operation. '2' & '3' were taken after the first pass was conducted. '4' & '5' were taken after the second pass was conducted.

The measurement locations for positions 2 & 3 and 4 & 5 in Figure 4.11 were each taken at the same interval within the 20-m machine sampling area. Like in the general case, a difference of at least one sampling interval was maintained between the initial and final measurement locations. The sampling scheme for edge effects was already incorporated into the plot design shown above in Figure 4.10 as indicated by the four sampling areas of row 1 in both passes.

Order of measuring selected sample areas

Before the machine passed through the field, initial residue measurements for each pass were taken from 3 of the 8 rows selected at random from one of the seven available 2-m intervals,

yielding six initial mass measurements per plot. The average dry matter mass of these six measurements was recorded as the initial mass measurement for the plot. After the first pass of the machine, the sampling areas of row 1 in passes 1 & 2 were taken from the corresponding interval of pass one. These two measurements were taken at this time because they had to be completed between the first and second passes of the machine to obtain measurements for edge effects as per the procedure outlined above. After the completion of both machine passes, final mass measurements from all remaining rows of interest were taken from their respective intervals.

Videos for material flow

A camera system (Dakota Micro Inc., Cayuga, ND) was used to record video footage of each pass made for the trials. The videos of rows 4 and 5 of the machine were recorded with front and side views focused on the row cleaners, knife and berm building disks of each unit as shown in Figure 4.12. The videos were to be used to provide a qualitative means of explaining the results of the data analysis if there were any anomalies or significant findings.

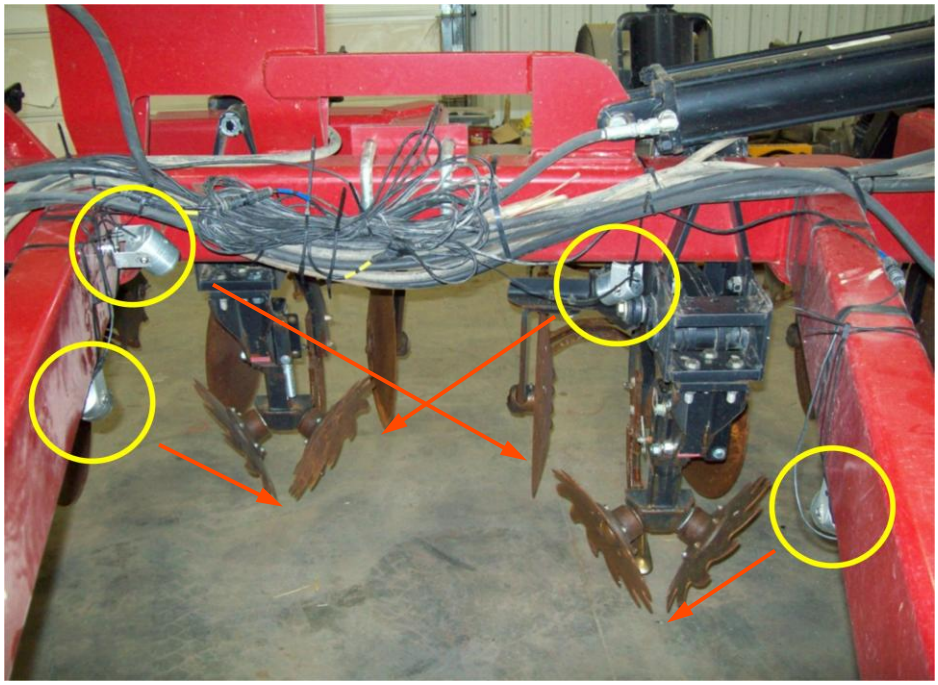

Figure 4.12. Rearward facing view showing mounting points for video cameras for rows 4 (right) and 5 (left). The yellow circles indicate the areas where the individual cameras were installed while the orange areas indicate the direction where each camera was pointed.

4.1.3 Fixed Factors

There were four fixed factors in the experiment. They were row cleaner configuration, machine travel speed, row cleaner orientation and residue moisture content at the time of operation. The first three were controlled throughout the experiment while the latter was only observed.

Row cleaner configuration

There were five different configurations used in the experiment:

1. Alpha Prototype
2. Offset with 0.33-m (13-in) diameter disk (Offset-13)
3. Offset with 0.46-m (18-in) diameter disk (Offset-18)
4. Parallel with 0.33-m (13-in) diameter disk (Parallel)
5. Case IH production with 0.33-m (13-in) diameter disk (Production)

In all of these configurations the row-cleaning disks were able to move vertically independent of the other row unit components and the implement frame. This then meant that the down-force of the row cleaner acting on the ground was predominantly a function of the weight of the row cleaner itself.

The alpha prototype is shown below in Figure 4.13 and Figure 4.14. It consisted of two Offset-18 row cleaners mounted directly behind the front cutting coulter with a flat bar residue roller in the inter-row space used to compress the residue and to control its trajectory. The author developed the original concept and worked with collaborators from CNH to finalize modifications.

The focus of typical row cleaners is to eject material from the berm-forming area. Beyond the acceleration and ejection of the residue into the inter-row region, there is no means of definitively controlling the end-portion of the residue's trajectory. By adding the residue roller, the focus changes from ejecting material from the seedrow to collecting unwanted residue in a windrow in the inter-row zone. This function meets the primary objective of controlling the residue's trajectory. As a secondary objective, the residue roller would also compress the residue to reduce its volume and cause plastic failure at several locations along the length of a stalk to increase the likelihood of microbial infection and decomposition.

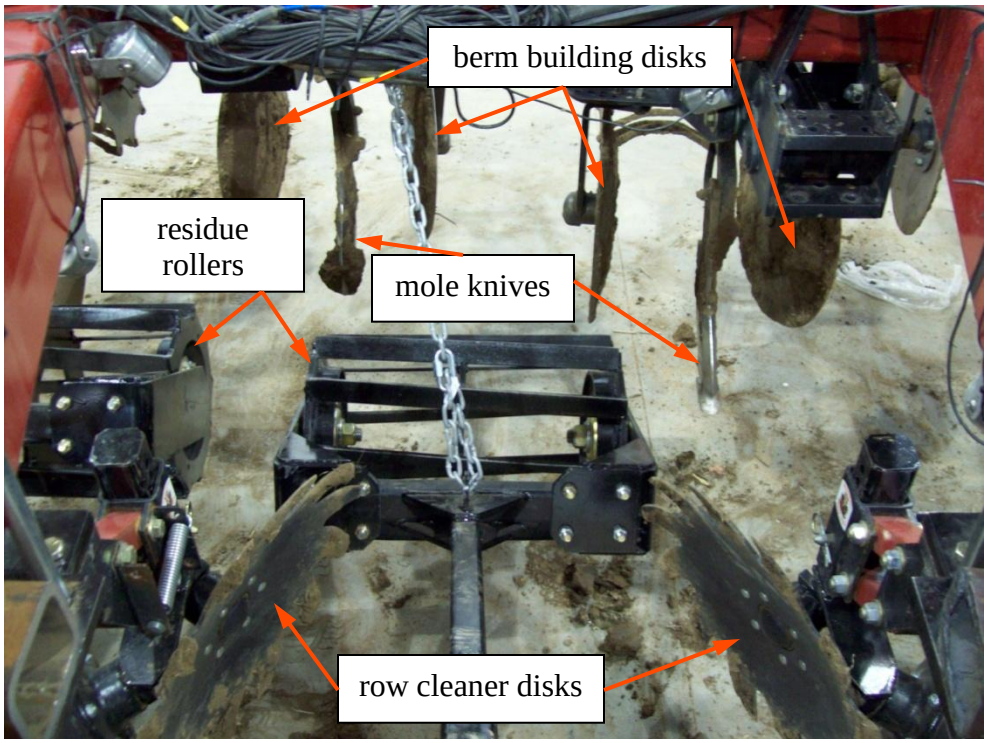

Figure 4.13. Rearward facing view of Alpha Prototype as built.

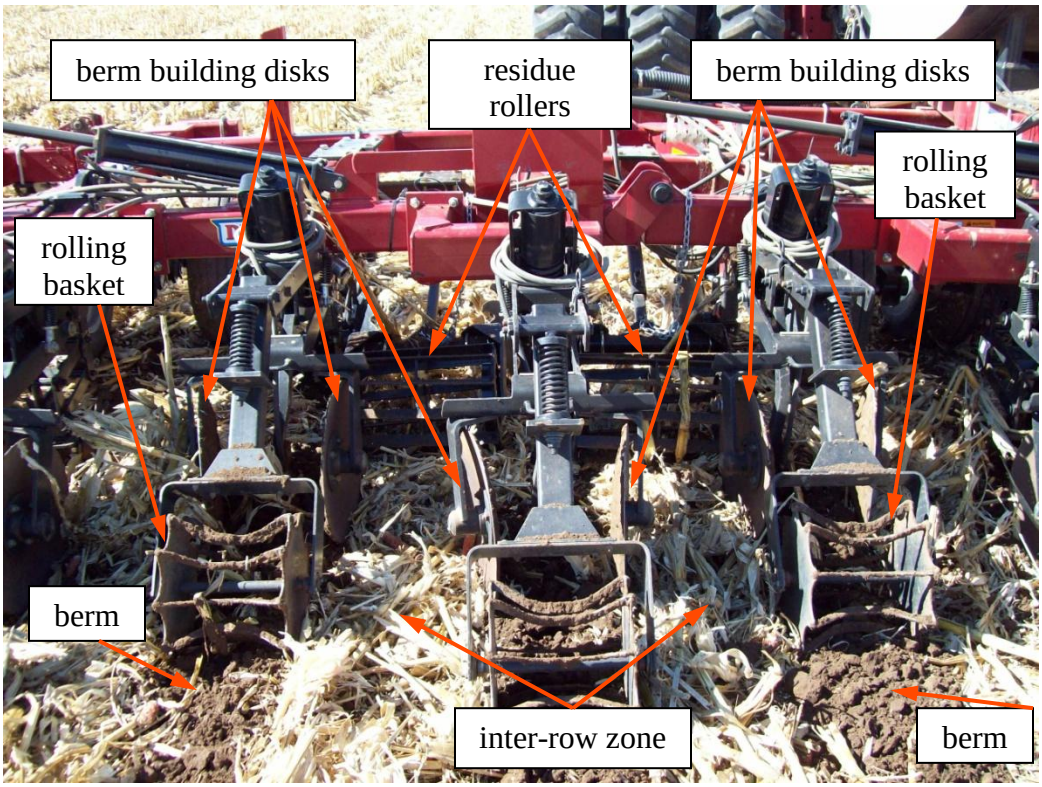

Figure 4.14. Forward-facing view of Alpha Prototype in a corn field.

The offset row cleaner mount is shown in Figure 4.15 below. As can be seen, there were two types – one where the left disk was in front (L) and one where the right disk was in front (R). The row cleaners were mounted in an alternating fashion. Due to the proximity between the implement wheels and the adjacent row units (rows 2 & 6) only one pattern was possible (ie. R-L-R-L-R-L-R for rows 1 through 7, respectively). An offset mount could not be mounted on row 8 because the disks interfered with the movement of the wheel rockshaft for raising/lowering the implement. The offset mount was used with two different sizes of disk – 0.33-m (13-in.) and 0.46-m (18-in.) diameter, as shown in Figure 4.16.

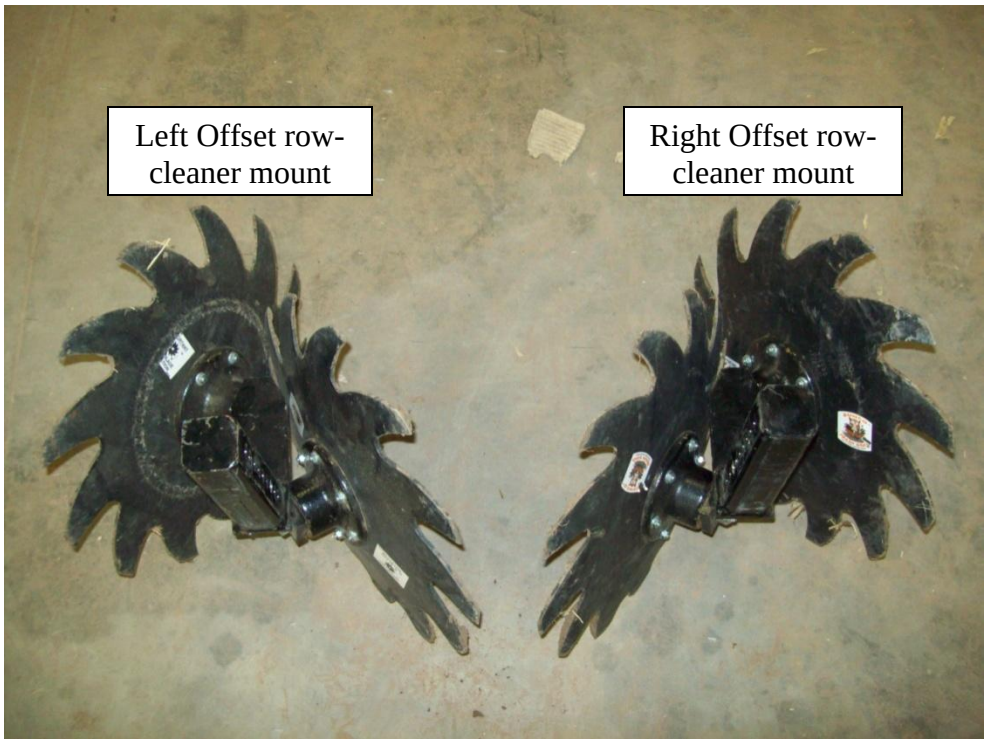

Figure 4.15. Top-rear view of Offset row cleaner mounts shown with 0.33-m (13-in) disks.

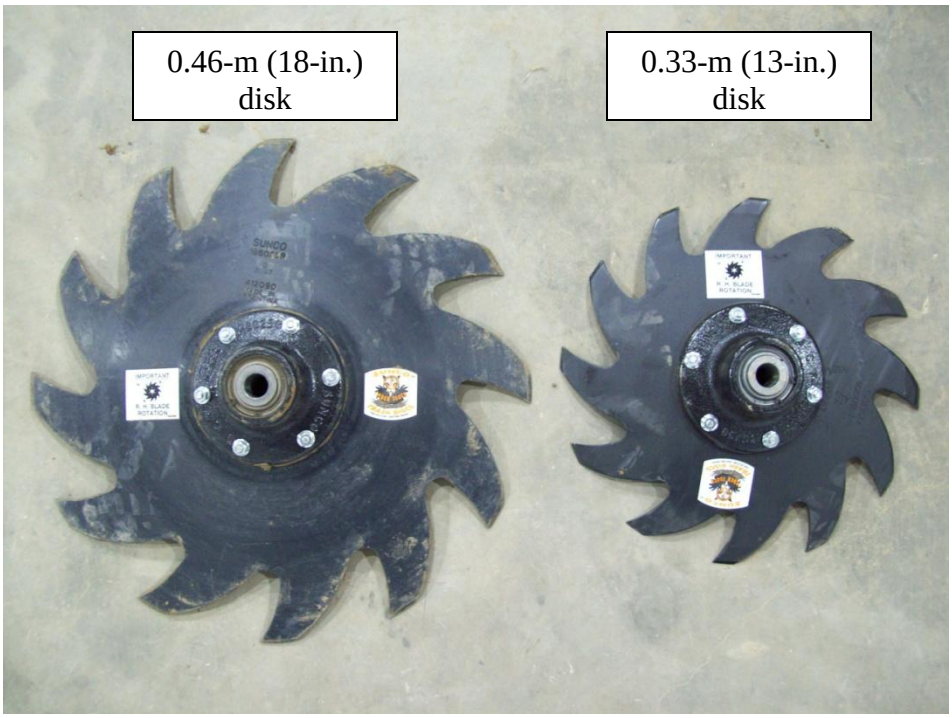

Figure 4.16. Rear view of 0.46-m (18-in) and 0.33-m (13-in) disks (left and right, respectively).

The Parallel mount is shown below in Figure 4.17. The axes of rotation for these disks were located in the same vertical plane, which was perpendicular to the direction of motion. This mount could only be used with the smaller disk because the larger disks physically interfered with one another at the leading edge due to the mounting angles of the disks.

Figure 4.17. Rearward facing view of Parallel row cleaner mount.

The Case IH production mount (Production) is shown below in Figure 4.18. It was quite similar to the Parallel row cleaner, with two exceptions. The first was that the axes of rotation of the disks were more horizontal, which made the disks interact with the residue more aggressively. The second exception was that the disks were mounted further away from each other so as to provide greater separation at the leading edge of the row cleaner. As in the Parallel configuration, a line connecting the disks' centres of rotation was perpendicular to the direction of motion. Because the large disks caused a physical interference with one another, they were unable to be installed on this configuration.

Figure 4.18. Rearward-facing view of the Production row cleaner unit.

Travel speed

Two levels of travel speed were used in the experiment. In corn stubble the speeds were 8 km/h (5 mph) and 10.4 km/h (6.5 mph). The high-speed target was 11.2 km/h (7 mph) in corn residue, but the tractor lacked sufficient power to reach and maintain this target given the field conditions encountered. In wheat stubble, the slower and faster speeds were 8 km/h (5 mph) and 11.2 km/h (7 mph), respectively. The Case IH STX 450 tractor's speedometer was used to gauge travel speed.

Row cleaner orientation

There were two different orientations of the row units - front-mounted and rear-mounted. Including row-cleaner orientation was not a specific objective of the experiment, but rather it arose as a result of the configuration of the machine used in the experiment. For the performance measurement of a given row unit to be valid, it had to be bounded by row units of the opposite orientation. In addition, the adjacent row units had to be equipped with the same row-cleaner configuration as the focal row unit. It was assumed that the performance data of row cleaners

separated by a minimum of 1.52 m (in this case, one separating row unit) would be independent of one another. With this in mind, rows 2, 4, and 6 were considered to be in the "front" and rows 3 and 5 were considered to be at the "rear" as shown in Figure 4.19. Examples of the two orientations are shown in Figure 4.20. One restriction of this experiment was that for the Alpha Prototype configuration, only one row unit (row 5) was able to be measured for economic reasons. Four row cleaner configurations, which excluded the Alpha Prototype, could be mounted in the front orientation on the implement. All configurations could be mounted in the rear orientation. Thus, 8 of the 10 possible configuration×speed combinations could be tested in the front row. All 10 combinations were evaluated in the rear row. For the front orientation, there were six replicates per plot for the four configurations excluding the Alpha Prototype. For the rear orientation, there were two replicates per plot for the Alpha Prototype and four replicates per plot for the remaining 8 treatments. It should be noted that this created an unbalanced dataset, because there was a different number of replicates for various treatments and plots.

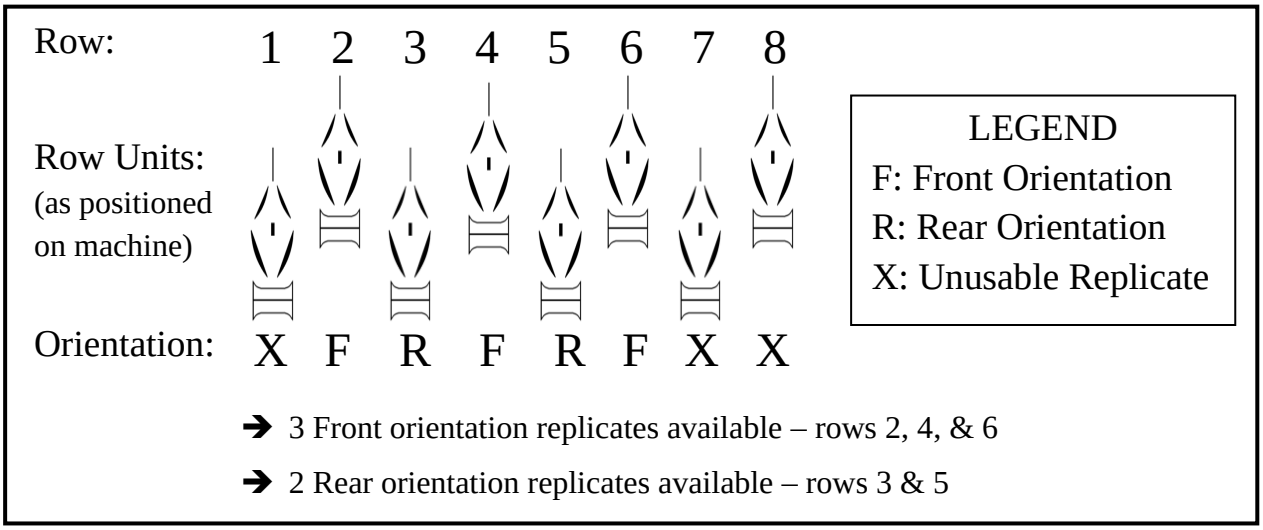

Figure 4.19. Diagram identifying machine location of front and rear orientations by row number, as well as the number of replicates available per machine pass.

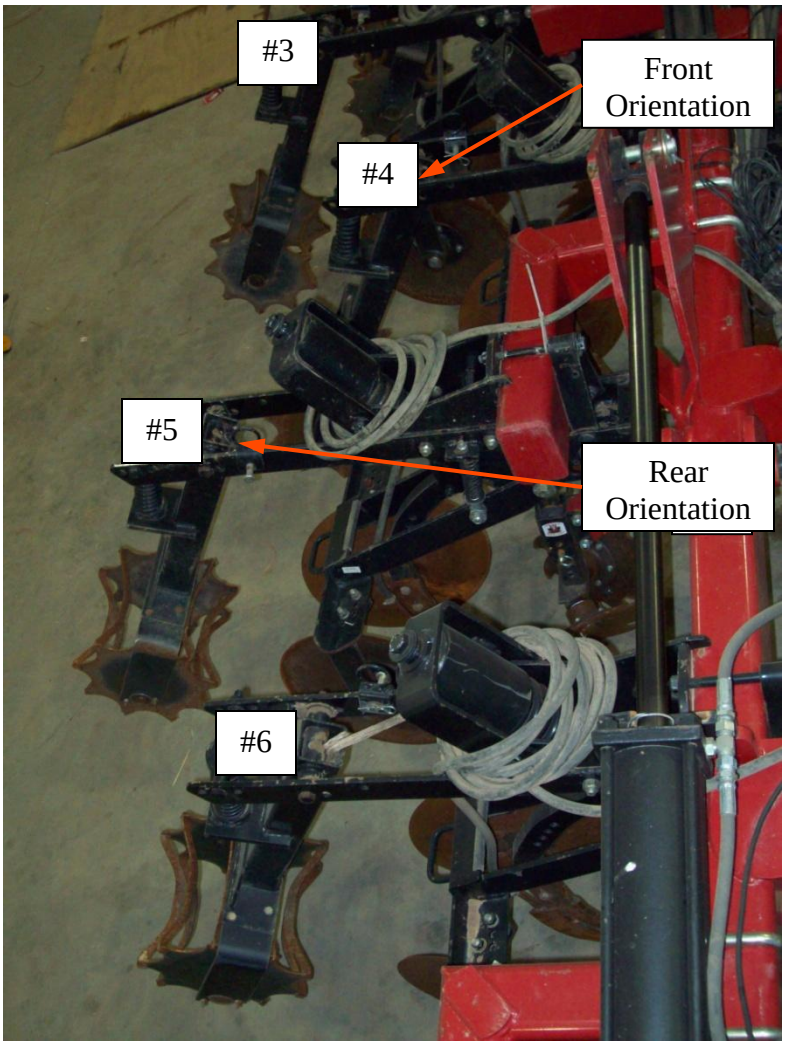

Figure 4.20. Top leftward rearward-facing view of a front orientation (row unit 4 bounded by 3 & 5 and 6 bounded by 5 & 7) and a rear orientation (row unit 3 bounded by 2 & 4 and 5 bounded by 4 & 6).

Residue moisture content at time of operation

The residue moisture content at the time of operation was a covariate in the experiment as it was measured but could not be carefully controlled. At the time of operation a residue sample was collected to obtain the moisture content. The value was typically shared between two plots per location (tests completed using the same row-cleaner configuration). The procedure to determine the residue moisture content is described above in section 4.1.2 *Response Variable - Cleaning Performance* under the sub-section titled *The mass sampling area*.

4.1.4 Random Factors

Due to the blocking in the experiment, there were random factors included that need to be discussed. A random factor can be associated with spatial or time considerations (Crawley, 2008). In this case, the random factors were solely associated with spatial dependencies. From the top level to the bottom level of nesting these were the field location, the plot, and the pass.

Location

The level of greatest influence was location. There were three field locations that were used in this experiment located near Dumas, TX. They were named Location I, Location II and Location III. Location I was a field with heavy corn residue that was a mixture of old and new residue. The reason for the presence of older residue was likely due to the use of newer pest-resistant varieties of corn. With the newer varieties, in combination with the drier climate in Texas the decomposition rate was likely slower. Corn had been grown on this field for three previous seasons prior to the strip tillage tests with no intensive tillage since 2006. Figure 4.21 and Figure 4.22 show a sample of the old and new residue present at the site, respectively. Figure 4.23 shows the field after the strip-till operation.

Figure 4.21. Old residue present at Location I.

Figure 4.22. New residue present at Location I.

Figure 4.23. Location I after the strip tillage operation.

Location II was a corn field with less residue than Location I. During the previous two seasons prior to the strip tillage tests, cotton and corn were grown in the field in 2007 and 2008, respectively. There was no heavy tillage completed in this location since 2007. It is depicted in Figure 4.24 after the strip tillage operation.

Figure 4.24. Location II after the strip tillage operation.

Location III was a field with wheat stubble from the previous season shown in its original state in Figure 4.25 and after strip-tillage in Figure 4.26. It had been plowed prior to seeding the wheat crop, therefore there was very little corn residue remaining from previous years. There was some volunteer corn throughout the field and within the experimental region. A control was thereby instituted that any volunteer corn within the experimental region was removed to ensure uniform conditions across the plots for the wheat stubble. Due to the traveling path of the combine there were also narrow swaths of area where there were large accumulations of chaff. The mass measurements that were taken where there was a large accumulation of chaff was noted in each instance.

Figure 4.25. Location III prior to the strip tillage operation.

Figure 4.26. Location III after the strip tillage operation.

Plot

The second highest level of influence was plot. There were 10 plots per location in a single line numbered consecutively from west to east at locations I & III, and south to north at location II. At this level, the ten different main treatments (5 configurations x 2 speeds) were randomly assigned to a given plot. The plot layout for locations I & II are shown in Figure 4.27 and Figure 4.28.

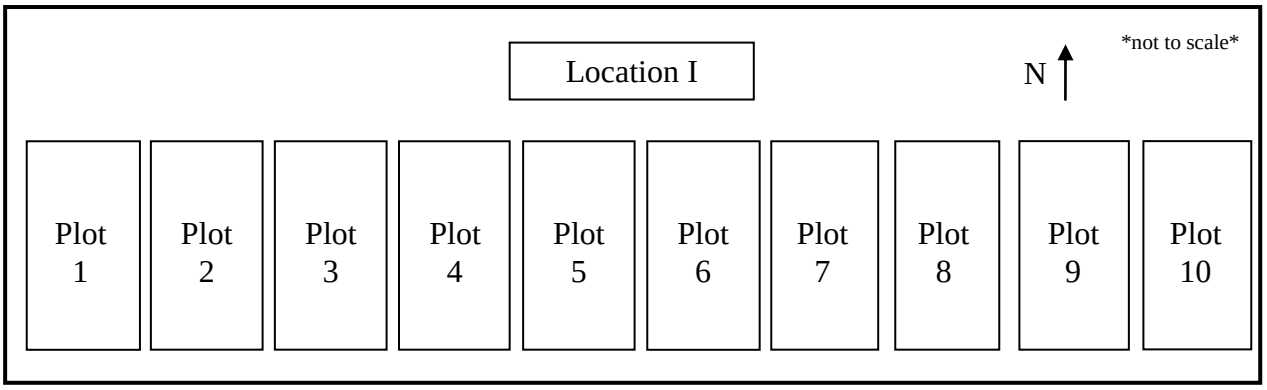

Figure 4.27. Plot schematic for Location I.

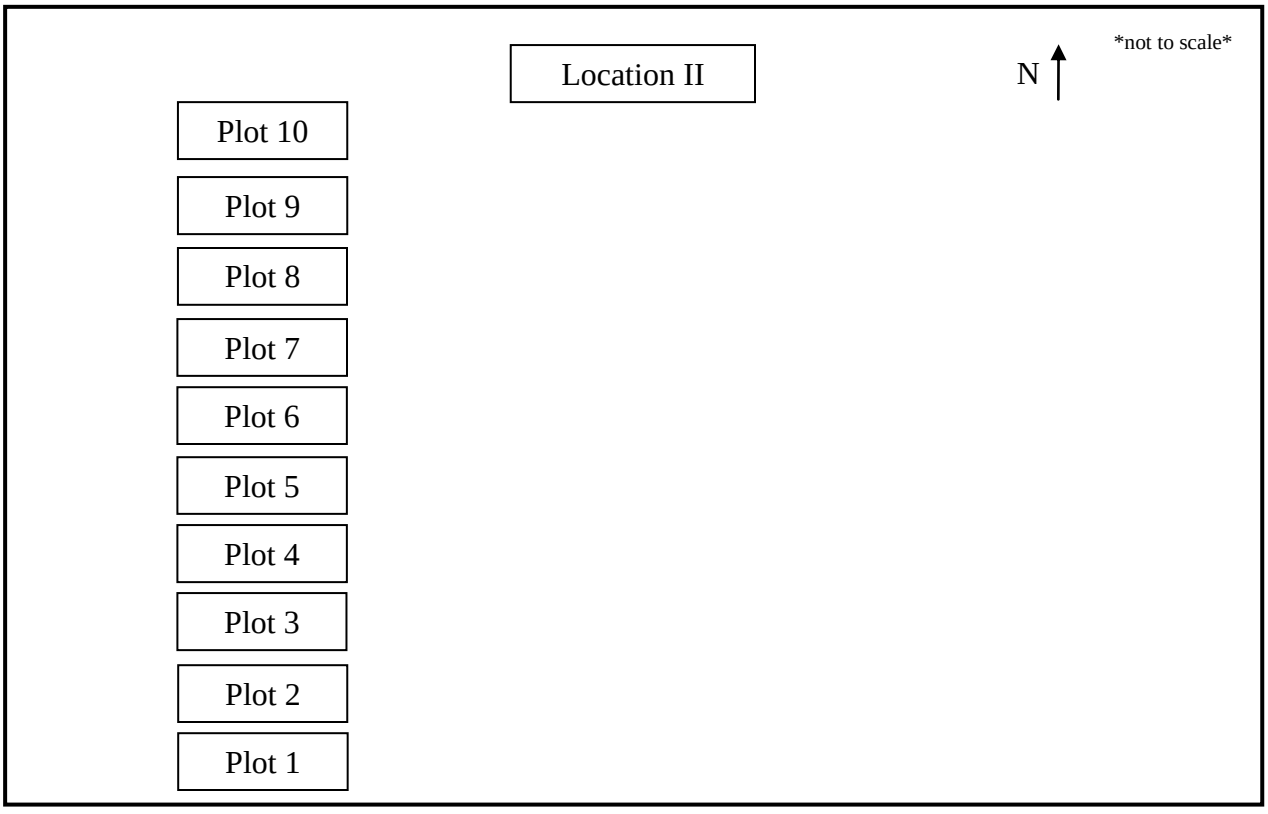

Figure 4.28. Plot schematic for Location II.

At Locations I & II, the plots were aligned to run parallel to the previous year's corn rows; the strip tillage units operated between the rows of the previous crop. The plots were placed as close together as possible given the restriction that irrigation pivot tracks were not allowed to be in the machine sampling area. As a result of this restriction, there was a spacing between adjacent plots

ranging between 0 and 26 rows. A frequency chart with this information is shown in Figure 4.29.

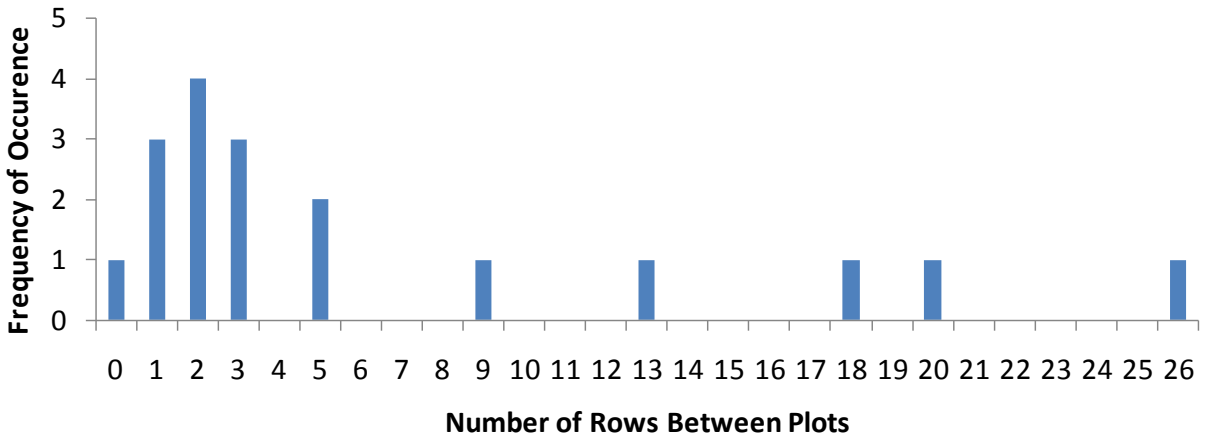

Figure 4.29. Frequency chart showing the spacing between plots for Locations I & II combined.

At location III, the plots were arranged circumferentially between the tracks of the second and third towers of the irrigation pivot in an effort to minimize the separation distance required between plots as shown in Figure 4.30. The average space between plots was approximately 0.91 m at the inner radius and 3.66 m at the outer radius. They were numbered consecutively in a clockwise direction, approximately west to east.

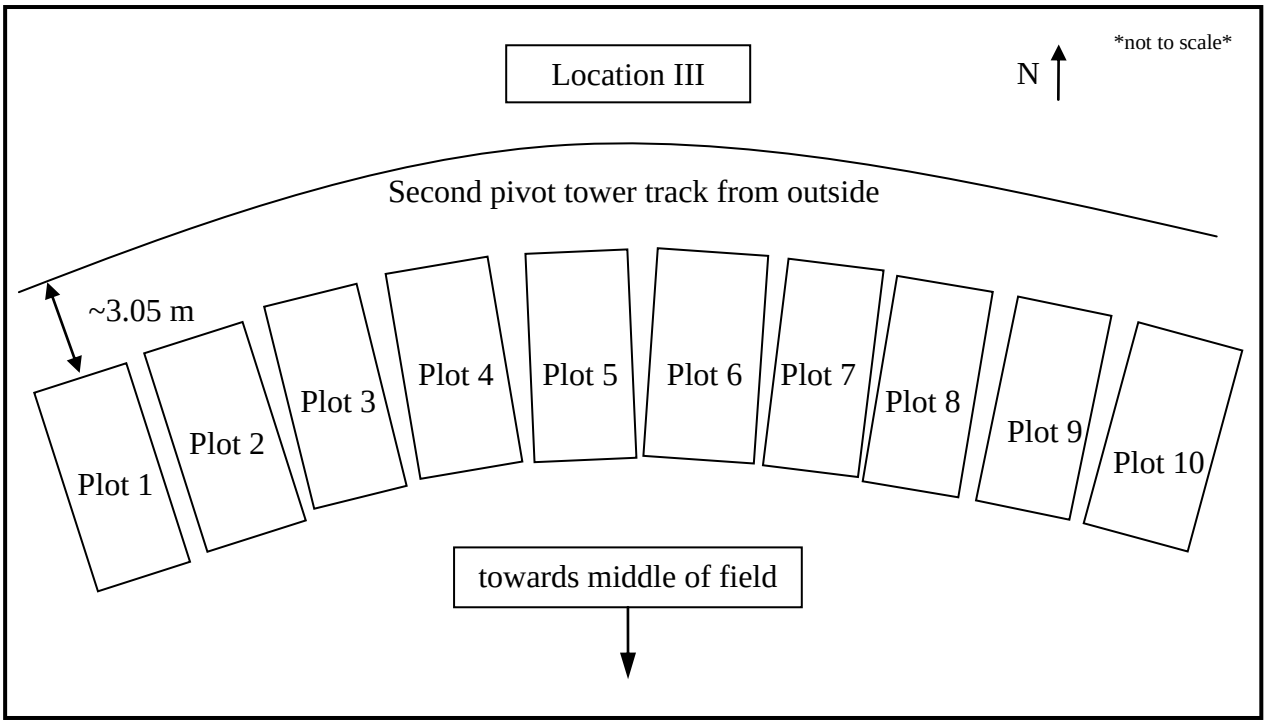

Figure 4.30. Plot schematic for Location III.

Pass

Each plot consisted of two passes which traveled in opposite directions. The first pass within a plot was performed by travelling southward on the west side of the plot at locations I and III and by travelling easterly on the south side of plots at location II.

4.1.5 Background Measurements

Soil Moisture Content

Soil moisture content measurements were recorded twice per day; once in the morning and once in the afternoon. These results are shown in Table 4.1. The first two days of test runs were completed in the afternoon time period. The last day's trials took place in the morning. The soil samples were collected immediately after the operation of the machine from two rows in a random plot per location per testing session. They were dried using a microwave oven according to ASTM Standard D4643-08 (ASTM, 2008). The soil moisture content was calculated using the following:

$$Soil\ Moisture\ Content = \left(1 - \frac{Soil\ Dry\ Mass\ (g)}{Soil\ Wet\ Mass\ (g)}\right). \quad \textbf{(4.2)}$$

Table 4.1. Soil moisture data at time of operation

Location	Date	Plot where sample taken	Time of Sample	Wet Mass (g)	Dry Mass (g)	Moisture Content (dry basis) (kg kg^{-1})
I	Feb. 10	10	4:47 PM	682.7	555.7	0.186
	Feb. 11	5	2:05 PM	969.7	755.7	0.221
	Feb. 12	3	10:08 AM	849.0	682.3	0.196
II	Feb. 10	5	3:10 PM	628.9	539.7	0.142
	Feb. 11	7	1:22 PM	879.2	733.8	0.165
	Feb. 12	8	9:33 AM	878.1	742.1	0.155
III	Feb. 10	1	6:18 PM	550.1	453.0	0.177
	Feb. 11	7	3:30 PM	995.2	849.5	0.146
	Feb. 12	10	11:05 AM	824.1	700.6	0.150

Soil Texture

An analysis of the soil texture at each location was completed using a composite soil sample from those collected for soil moisture content. Soil texture results were provided by a commercial lab (MTVL Laboratories Inc., New Ulm, MN) and are shown in Table 4.2.

Table 4.2. Soil property lab test results (MTVL Laboratories Inc., New Ulm, MN)

Property	**Location I**	**Location II**	**Location III**
Bulk density, loose (g cm^{-3})	1.02	1.11	1.10
Bulk density, packed (g cm^{-3})	1.21	1.29	1.28
Sand (%)	35.0	20.0	47.5
Silt (%)	32.5	65.0	32.5
Clay (%)	32.5	15.0	20.0
Soil Texture	Clay loam	Silt loam	Sandy loam

Other Parameters

For the purposes of this experiment, several factors were held constant. The operating depth and configuration of the implement were not changed from how the cooperating farmer normally used it. This included the depth of the front cutting coulter and the mole knife. The knife depth was approximately 0.23-0.254 m (9-10 in). The machine was equipped with 0.46-m (18-in) diameter wavy coulters, 0.46-m (18-in) diameter berm-building disks mounted in convex fashion and the production rolling baskets. These components are shown in Figure 4.31, Figure 4.32, and Figure 4.33.

Figure 4.31. Wavy coulter mounted at the front of the machine.

Figure 4.32. Front view of the mole knife and standard berm-building disks mounted in a convex fashion. The rolling basket is visible in the rear of the photo.

Figure 4.33. Rear view of the standard rolling basket mounted at aft end of row unit.

4.2 Method of Analysis

Due to the different operating conditions and their resulting differing scales of cleaning performance, a separate analysis for each type of crop residue was used. Thus, two locations were used in the corn analysis and a single location was used for wheat. The following is a discussion of the data used in the analysis and the procedure for identifying statistically significant differences in mean cleaning performance, the procedure used to quantify each configuration's consistency of cleaning performance, and the method employed to determine if edge effects were significant in the machine's operation.

Unless otherwise indicated, all residue mass measurements have been presented in dry-mass basis. They were converted using the various moisture measurements taken throughout the duration of the field trials as appropriate. The formula used was,

$$m_{dry} = (1-u)m_{wet}, \quad \textbf{(4.3)}$$

where: m_{dry} = dry matter residue mass (g),

u = calculated residue moisture content g of water per g of wet residue expressed as a decimal fraction (g g^{-1}) and,

m_{wet} = wet mass of residue as measured in situ (g).

4.2.1 Method of analysis to determine a difference in mean cleaning performance values

A linear mixed-effects model was used to identify potential differences between the mean performance values for the various configurations, travel speeds, orientations, and moisture contents at the time of operation. The mixed-effects model included both the fixed and random factors in its analysis and adjusted the degrees of freedom appropriately for each level of spatial blocking and/or nesting. By adjusting the degrees of freedom, this model effectively dealt with the unbalanced dataset of field data that was collected. It should be noted that even though the mixed-effects model provided coefficients for each term to be used in an empirical model, this was not the goal. The goal was to use the model selection process and the p-values of each fixed factor to determine which fixed factors had a statistically significant effect on cleaning

performance. The statistical tests were conducted using three different subgroups of the data for each crop-type:

1. the front orientation only with four configurations
2. the rear orientation only with all five configurations (including the alpha prototype)
3. the front and rear orientations together with four configurations

The decision to perform a separate analysis for the front and rear orientations arose from two issues. First, there were zero measurements for the Alpha Prototype in the front orientation which meant that the statistical equations were unsolvable for the front orientation. Secondly, because any row cleaner mounted in the front row is immediately adjacent to two row cleaners in the rear row and vice versa, they are not completely independent of one another. Combining both orientations (test 3 in the above list) was completed only if there were no significant factors in the tests for each individual orientation. The code implemented in R© to perform the mixed-model analysis is located in Appendix B.

4.2.2 Method of analysis to quantify the consistency of performance for each configuration

Quantitatively, consistency was defined as how close each configuration operated to the mean performance value. The indicator used to quantify consistency was the range of the performance data excluding any outliers in the distribution. The *boxplot.stats()* function in R© (R Development Team, 2009) was used to extract the appropriate data points from each distribution. The full set of code implemented in R© can be found in part B.2 of Appendix B. The formula used to calculate consistency was,

$$Consistency(\%) = 100 * (1 - Range), \quad \textbf{(4.4)}$$

where: $$Range = P_{\max} - P_{\min}, \quad \textbf{(4.5)}$$

P_{max} = maximum cleaning performance value (excluding outliers) and

P_{min} = minimum cleaning performance value (excluding outliers).

A higher consistency was more desirable with a value of 100% meaning that the performance data for a particular configuration were the same value. The consistency calculation yielded only a single number from a distribution of cleaning performance for a particular configuration and thus no statistical comparison analysis was performed.

A graphical representation of a box plot is shown in Figure 4.34 with the main elements labeled. P_{max} and P_{min} were the outermost data points above and below the median, respectively that were within 1.5 inter-quartile ranges of the median value. The value of 1.5 was the default value incorporated into the R© code.

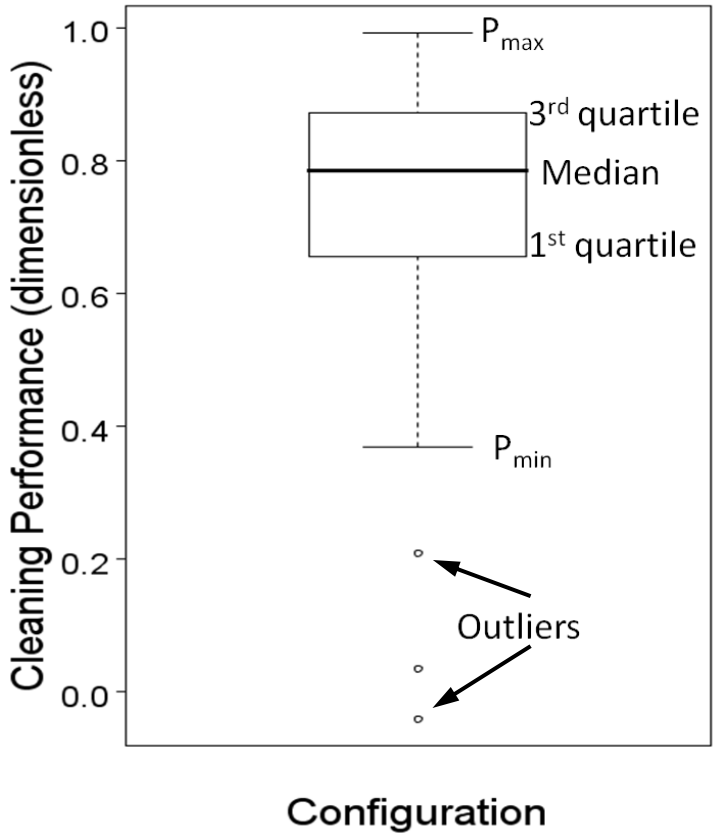

Figure 4.34. Box-and-whisker plot demonstrating the values used in the consistency equation

4.2.3 Method of analysis to determine whether edge effects affect row cleaner performance

A three-step process was used to evaluate whether edge effects affected the cleaning performance of row 1 and the area immediately adjacent to row 1 on the neighboring pass for a particular plot. First, the mean and sample standard deviation of the six initial residue mass measurements were calculated. Secondly, these parameters were then used to calculate a 95%

confidence interval. Finally, the residue mass measurement from the neighboring pass (position 3 from Figure 4.11) was compared to the confidence interval. If the residue mass measurement was within the upper and lower bounds it was considered to be the same as the initial mass measurement. In this case, no throw-over occurred onto the neighboring pass. If however, the residue mass measurement was larger than the upper bound of the 95% confidence interval, it was deemed that throw-over occurred. If the residue mass measurement was smaller than the lower bound, the result was noted, however given the physics of the strip tillage implement, it was physically impossible for the machine to "suck in" material from an area beyond its outer limits. With the data collected, an analysis for throw-over from pass 2 into pass 1 after the completion of pass 2, was unable to be conducted.

5.0 RESULTS AND DISCUSSION

The five row-cleaner configurations all performed very well at both lower and higher speeds. Plugging of the implement was generally not an issue with the exception of the first pass of plot 8 in Location II due to operator error. During the time the machine was in the plot, the machine had veered across one row and then returned to its proper position. This caused the machine to plug with residue a distance after the end of the plot. However, the error occurred in such a manner that the collection of accurate cleaning performance measurements was not hampered.

The videos collected during the trials were of good quality to analyze and qualitatively compare the performance of the various row cleaner configurations. Example snapshots from the corn residue and wheat stubble videos emphasizing the flow of residue through the implement are shown in Figures 5.1 and 5.2, respectively. The row cleaners operated as intended in that the residue was parted by the row-cleaner blades and was ejected to the inter-row zones on each side of the row units. This remained valid for the operating condition where the implement was operated with the row units aligned in-between the previous crop's seed rows. All configurations threw aside much more soil in the wheat residue as compared to the corn residue. As such, more counter-balancing of the row cleaner may have to be employed to reduce this undesirable effect. It was noted that one of the disks of the Offset-18 configuration row unit 3 (not directly filmed) occasionally quit rotating on pass 2 of plots 2 & 4 at Location II. This was likely due to a combination of wet clay-silt soil binding the two disks together in the narrow gap of separation and a possible slight error in the manufacture of the bracket controlling the disk-angle. The residue rollers employed in the Alpha Prototype configuration received the residue ejected from the Offset-18 row cleaners (used as a component of the Alpha Prototype configuration) mounted immediately in front of them and proceeded to flatten the corn residue as observed in the videos. This effectively controlled the residues' trajectory as intended. However, in heavy residue conditions, as observed in the field after the passage of the machine, it appeared as though the corn residue was distributed laterally during the final portion of the flattening process. This would be undesirable as it would move the residue towards the berms that were created – possibly reducing their size. Should the residue rollers be used in additional trials, the surface could be modified to be concave – similar to the initial design to examine

whether or not the lateral movement of residue is reduced or eliminated. Because the 5 row-cleaner configurations generally operated as intended, no further detailed analysis of the recorded videos will be completed.

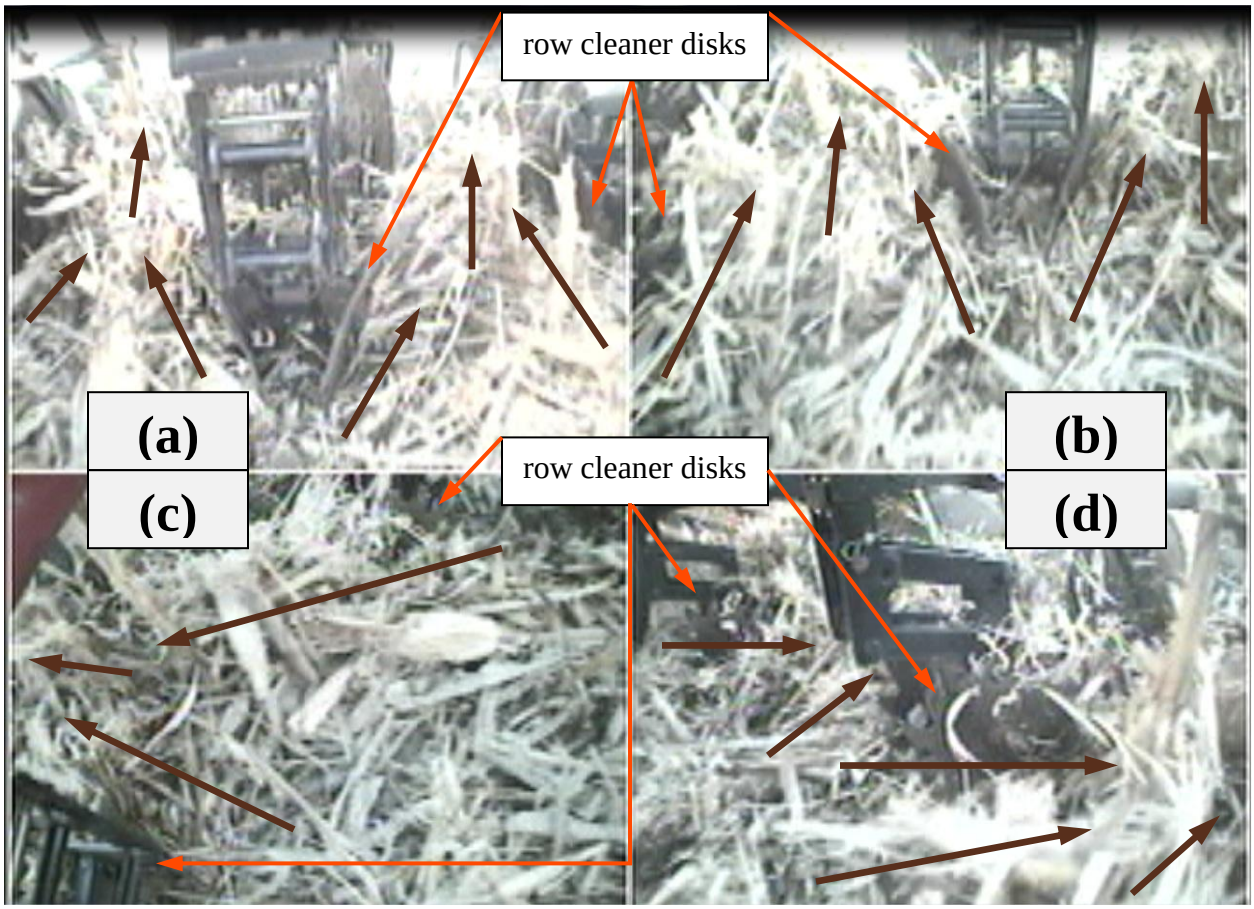

Figure 5.1. Video snapshot of Location I, plot 8, pass 2 at time of 28 s utilizing the production configuration operating at high speed. (a) is a top-front view of row 4. (b) is a top-front view of row 5. (c) is a top-diagonal view of the inter-row zone between rows 4 & 5 with row 4 near the top and row 5 visible in the bottom left corner. (d) is a top-diagonal view of row 5 with row 6 visible in the background and the inter-row zone between rows 4 & 5 visible in the bottom-right corner. The brown arrows indicate the direction of residue flow through the implement via the row cleaner disks.

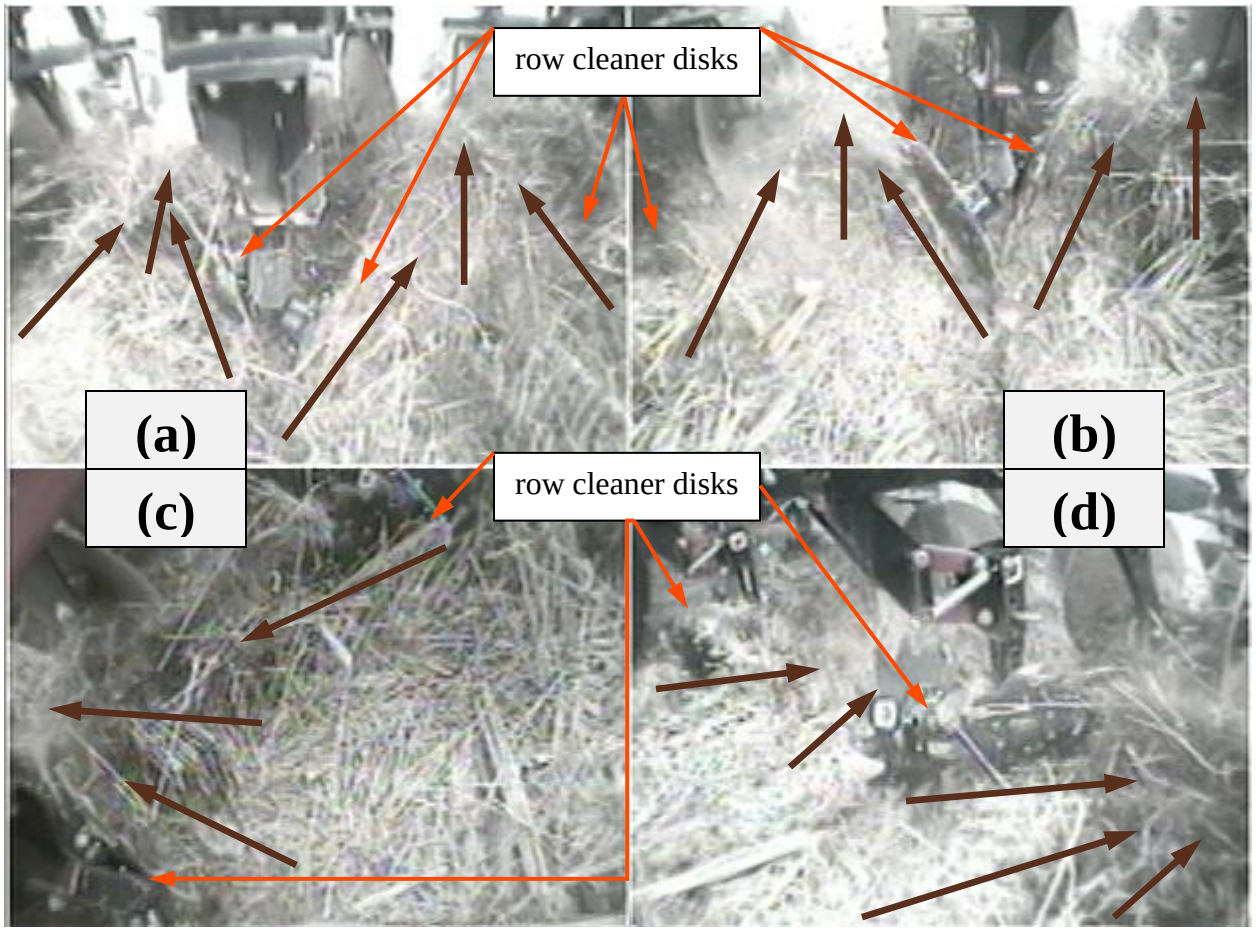

Figure 5.2. Video snapshot of Location III, plot 10, pass 1 at time of 9 s utilizing the Offset-13 configuration operating at high speed. (a) is a top-front view of row 4. (b) is a top-front view of row 5. (c) is a top-diagonal view of the inter-row zone between rows 4 & 5 with row 4 near the top and row 5 visible in the bottom left corner. (d) is a top-diagonal view of row 5 with row 6 visible in the background and the inter-row zone between rows 4 & 5 visible in the bottom-right corner. The brown arrows indicate the direction of residue flow through the implement via the row cleaner disks.

5.1 Presentation of Data

The data were summarized in 'box-and-whisker' plots. The black dot represented the median, the lower line of the box was the 25th percentile and the upper line of the box was the 75th percentile. The dashed line (or 'whiskers') represented the smaller value of 1: the maximum (minimum) value or 2: 1.5 times the inter-quartile range of the data (~2 standard deviations).

The points outside the box-and-whisker plots were outliers and were therefore plotted individually. (Crawley, 2007)

5.1.1 Categorized experimental data for corn

The cleaning performance for the front orientation for Locations I & II is shown in Figure 5.3. Figure 5.3a represents data collected at low speed (8 km/h) while Figure 5.3b represents the high-speed (10.4 km/h) data. They illustrate little difference between the median performance, with different amounts of data variation for each configuration. The Alpha Prototype was unable to fit on the front orientation of the machine and was therefore not tested.

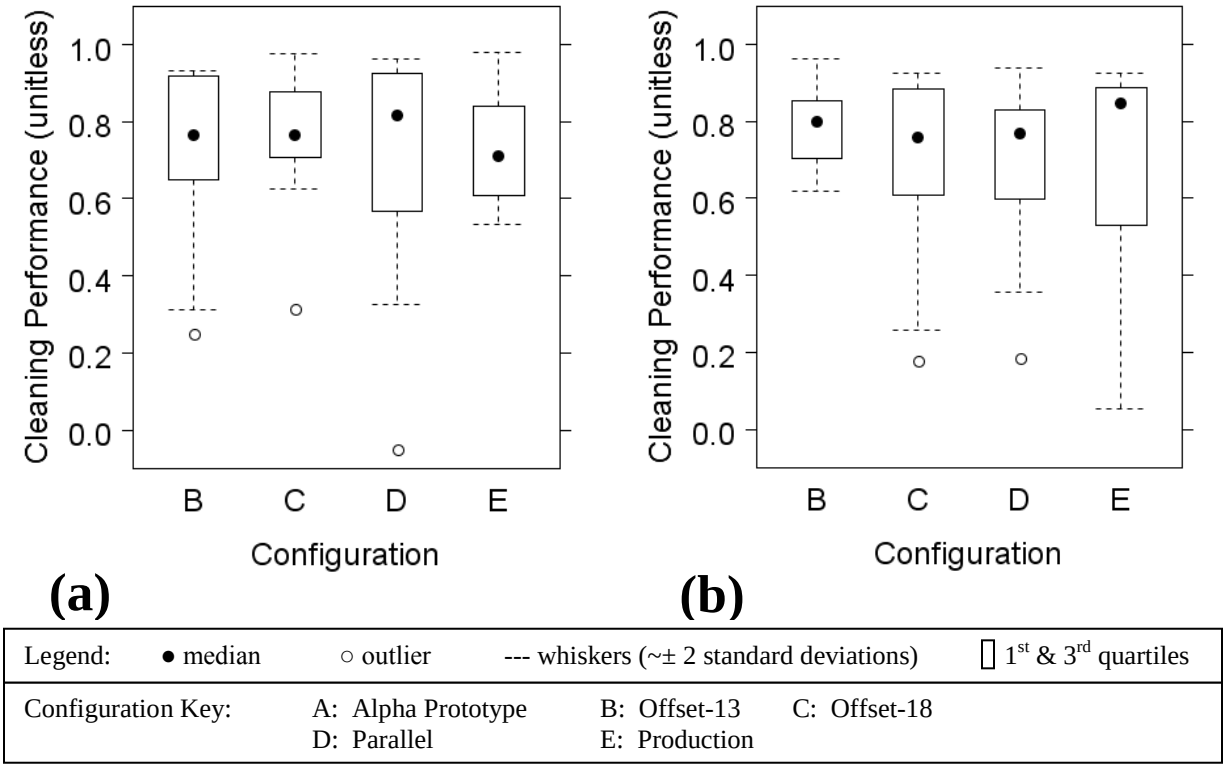

Figure 5.3. Cleaning performance versus configuration for the front orientation in corn residue. (a) represents low speed (8 km/h) and (b) represents high speed (10.4 km/h). Configuration A was unable to fit on the front orientation of the machine and was therefore not tested.

The cleaning performance for the rear orientation for locations I & II is shown in Figure 5.4. Figure 5.4a represents data collected at low speed (8 km/hr) while Figure 5.4b represents the

high-speed (10.4 km/hr) data. As shown in Figure 5.3, there was little difference between the median performance, with the exception of the Production configuration at low speed. There was a large degree of variation amongst the data and plenty of overlap in the cleaning performance values between the five configurations.

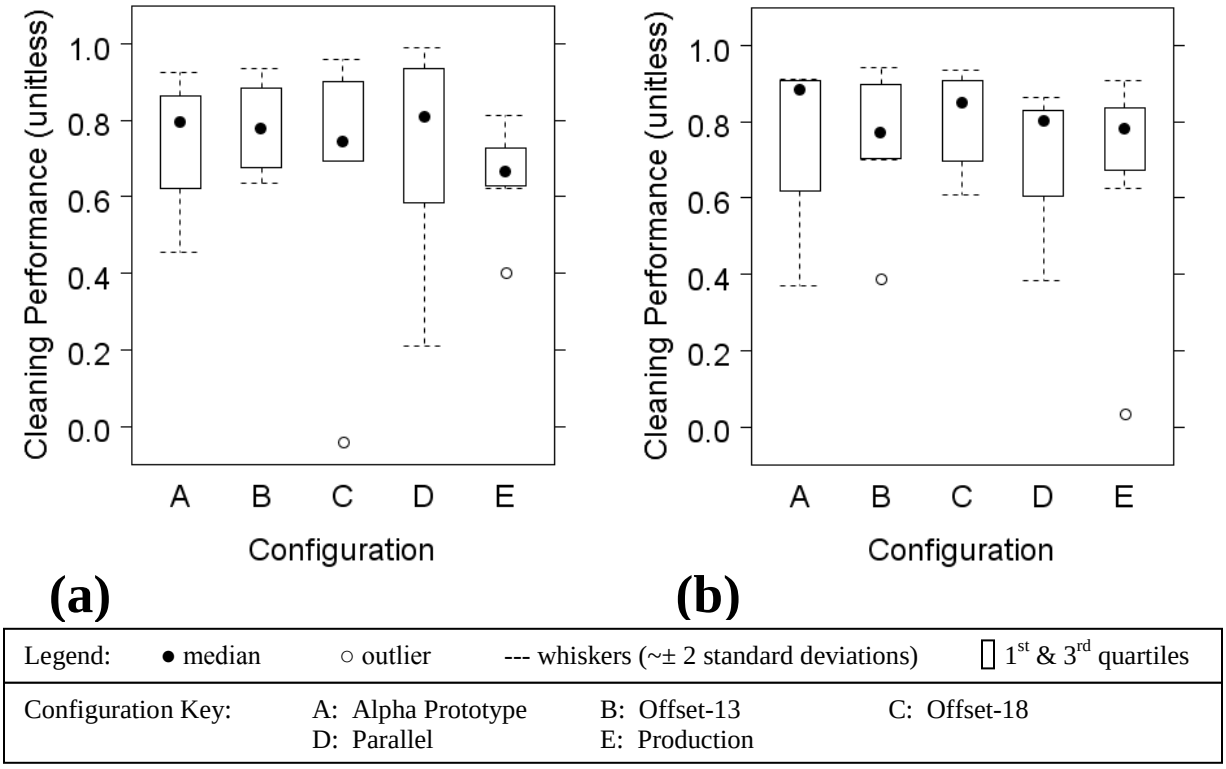

Figure 5.4. Cleaning performance versus configuration for the rear orientation in corn residue. (a) represents low speed (8 km/h) and (b) represents high speed (10.4 km/h).

5.1.2 Categorized experimental data for wheat

Figures 5.5 and 5.6 show the full-scale plots of cleaning performance versus row-cleaner configuration for wheat residue at location III for the front and rear orientations, respectively. Each of Figures 5.5a and 5.6a represents the low-speed (8 km/h) results while Figures 5.5b and 5.6b represent the high-speed (11.2 km/h) results. The median cleaning performance values were larger than those observed in the corn residue, but were similar between the row-cleaner configurations. However, there was much less variation in the performance values of the wheat residue than those of the corn residue. With the exception of one outlier in Figure 5.5b for the Offset-13 configuration, there were no cleaning performance values less than 0.60.

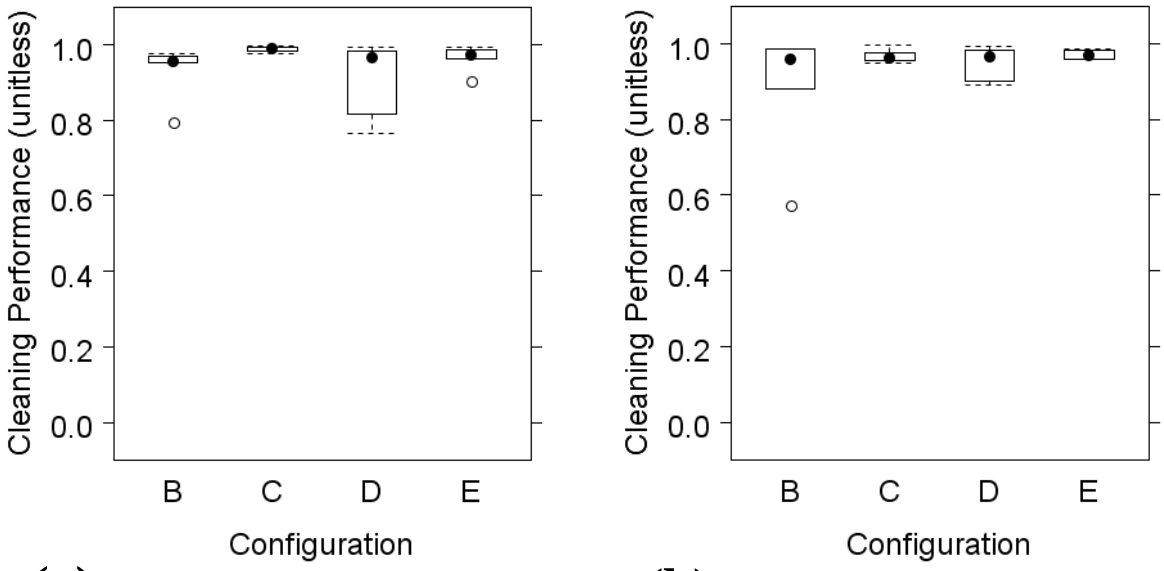

Legend:	● median	○ outlier	--- whiskers (~± 2 standard deviations)	▯ 1st & 3rd quartiles
Configuration Key:	A: Alpha Prototype	B: Offset-13	C: Offset-18	
	D: Parallel	E: Production		

Figure 5.5. Cleaning performance versus configuration for the front orientation in wheat residue. (a) represents low speed (8 km/h) and (b) represents high speed (11.2 km/h). Configuration A was unable to fit on the front orientation of the machine and was therefore not tested.

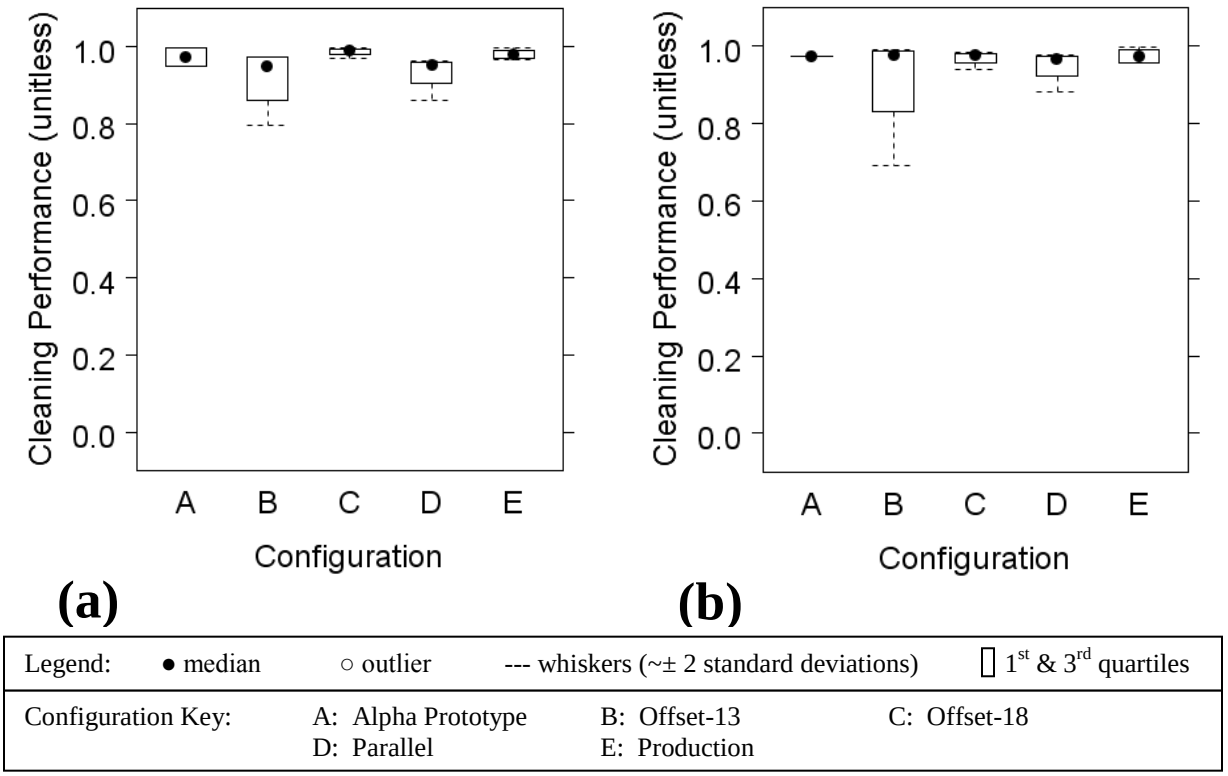

Figure 5.6. Cleaning performance versus configuration for the rear orientation in wheat residue. (a) represents low speed (8 km/h) and (b) represents high speed (11.2 km/h).

Figures 5.5 and 5.6 provided a good basis for an initial investigation of the wheat residue data and to directly compare to those figures portraying data for corn residue. However, to compare the various configurations within the wheat residue trials it was necessary to focus more closely on the data. As such, Figures 5.7 and 5.8 were created using minimum and maximum cleaning performance values of 0.6 and 1.0, respectively. Upon closer examination, the median values in all four cases were still very similar, however the variation between the configurations was much more apparent. In all four cases, the Offset-18 and Production configurations had less variation than other configurations. For the front orientation shown in Figure 5.7, the Parallel configuration at low speed displayed more variation than the other three configurations tested. It had a range of 0.76-0.99 versus ranges between 0.95-0.99 for the other three configurations. For the rear orientation shown in Figure 5.8, the Offset-13 configuration had more variation than the other four configurations tested. It had low and high-speed ranges of 0.80-0.97 and 0.69-0.99, respectively, as compared to ranges between 0.86-1.00 and 0.88-1.00 for low and high-speed, respectively, of the remaining four configurations. One source of variation in the performance

measurements could have been the regions of the plots where excessive chaff had been distributed by the combine during the harvest of the previous year. The locations where this condition occurred were duly recorded. The outlier shown for configuration B in Figure 5.5b is excluded in Figure 5.7b as its presence would have automatically expanded the range of cleaning performance shown on the y-axis of the plot. Another note should be made about the Alpha Prototype configuration in Figure 5.8b, in that the box appears as a single line. For wheat residue, the Alpha Prototype had only two measurements per speed and the exact same measurement was observed in both cases.

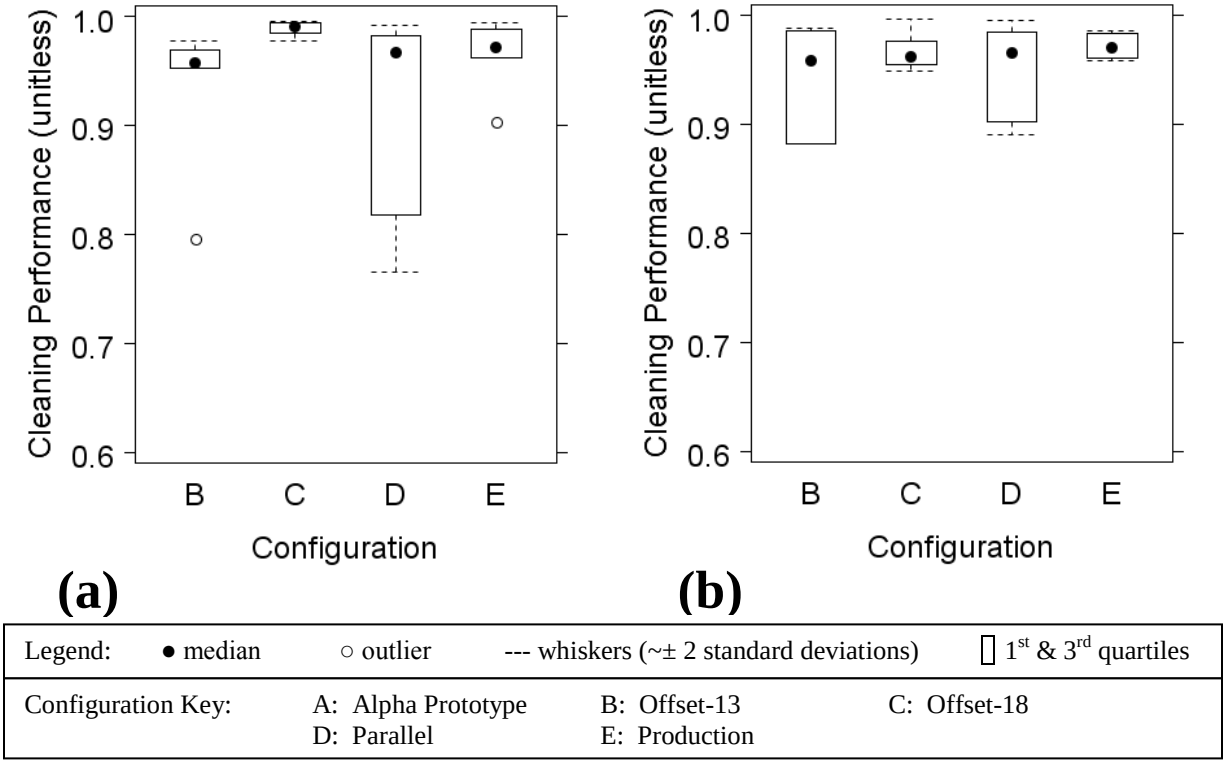

Figure 5.7. Enlarged and focused view of cleaning performance versus configuration for the front orientation in wheat residue. (a) represents low speed (8 km/h) and (b) represents high speed (11.2 km/h). Configuration A was unable to fit on the front orientation of the machine and was therefore not tested.

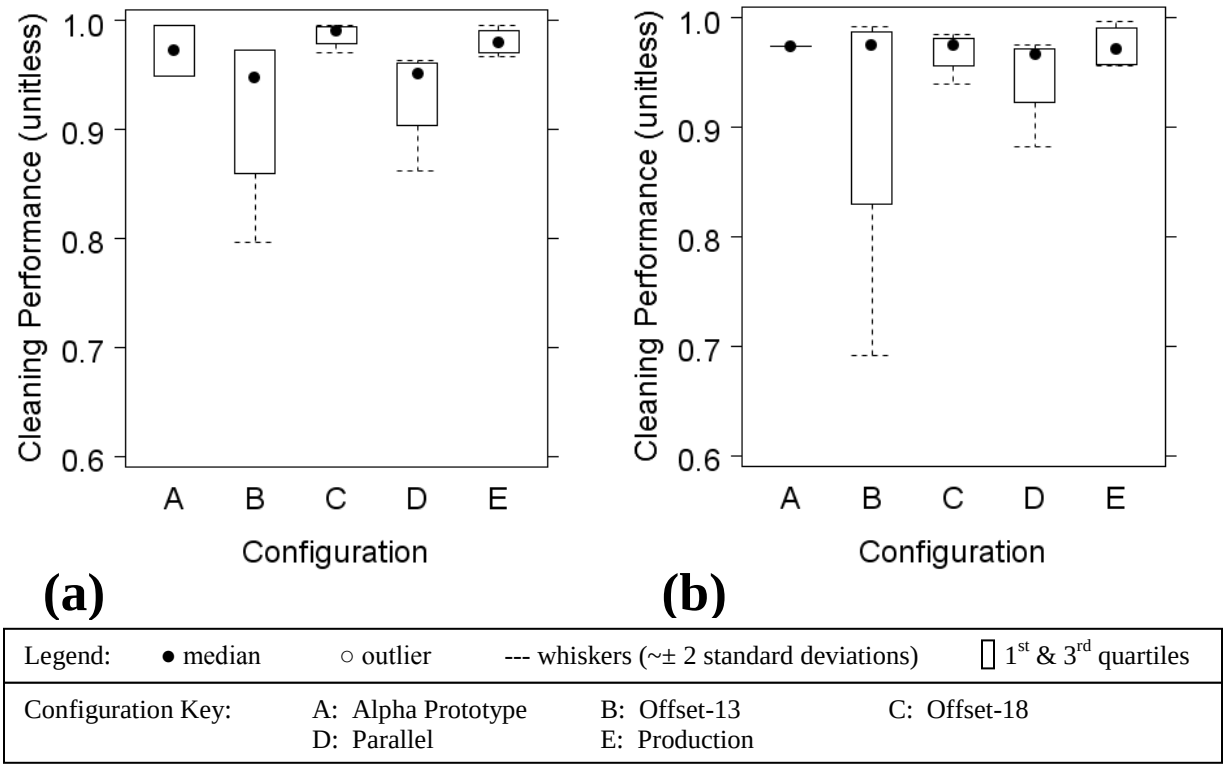

Figure 5.8. Enlarged and focused view of cleaning performance versus configuration for the rear orientation in wheat residue. (a) represents low speed (8 km/h) and (b) represents high speed (11.2 km/h).

5.2 Differences in Mean Performance

Before the data were analyzed using R©, they were reviewed to ensure the statistical tests would yield usable results. This included checking for goodness of fit to the normal distribution.

5.2.1 Using a natural logarithmic transform for cleaning performance data

Before the data were analyzed using the mixed-effects model, they were reviewed to ensure the data followed a normal distribution. This was accomplished using a normal quantile-quantile plot. On this type of plot, a solid line is shown representing where the data should lie if it follows a perfect normal distribution. The data are represented by individual points on the plot. One can compare the data and various transformations thereof to visually determine whether a certain data transformation provides a better or worse fit to a normal distribution. Figure 5.9 shows the raw cleaning performance data for all three field locations plotted on a quantile-quantile plot. As can be seen, the data in the middle portion follows the normal distribution line

quite well, but at the lower and upper ends, the data fall well below the normal distribution line. A logarithmic transform was then applied to the data as follows,

$$invlogPerform = \ln(1-(Cleaning\ \ Performance)). \quad \textbf{(5.1)}$$

A difference conversion was incorporated to accommodate the two negative performance values observed during the experiment. The transformed data are shown in Figure 5.10. In this case the data at the lower and upper ends of the plot were much closer to the normal distribution line. Because the transformed data more closely represented a normal distribution, they were used in all statistical tests in place of the raw data.

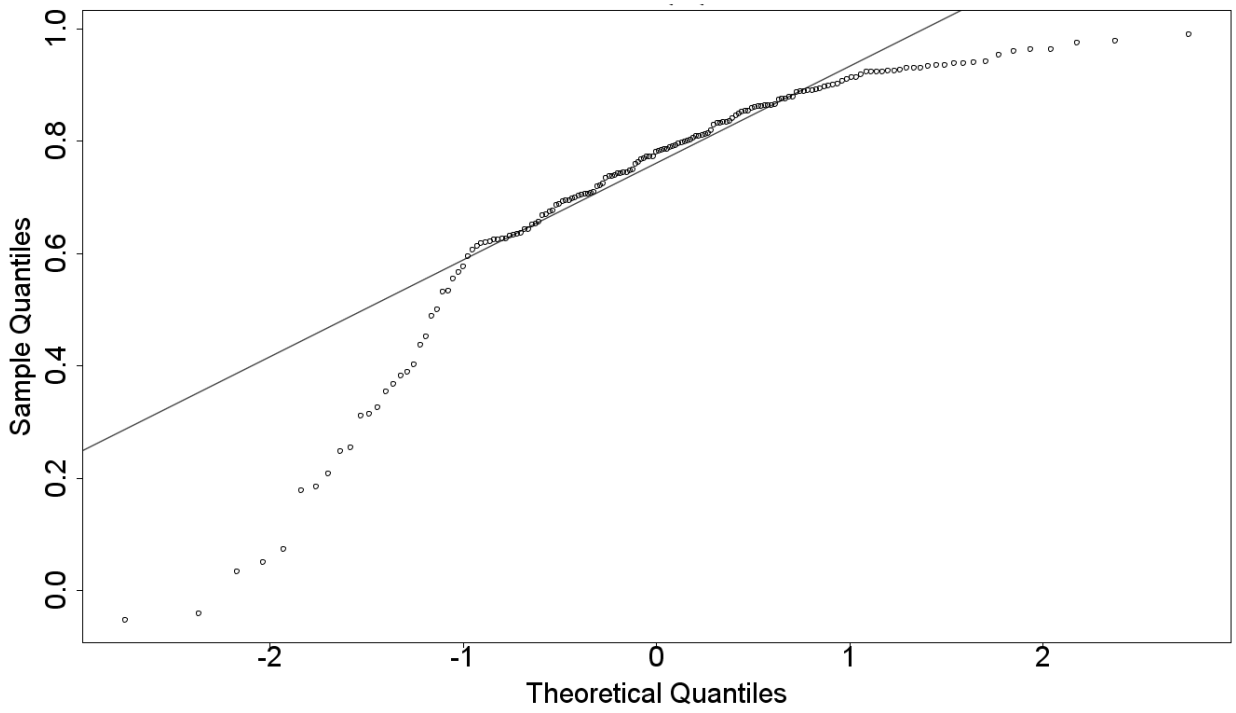

Figure 5.9. Normal quantile-quantile plot of raw performance data for all three field locations.

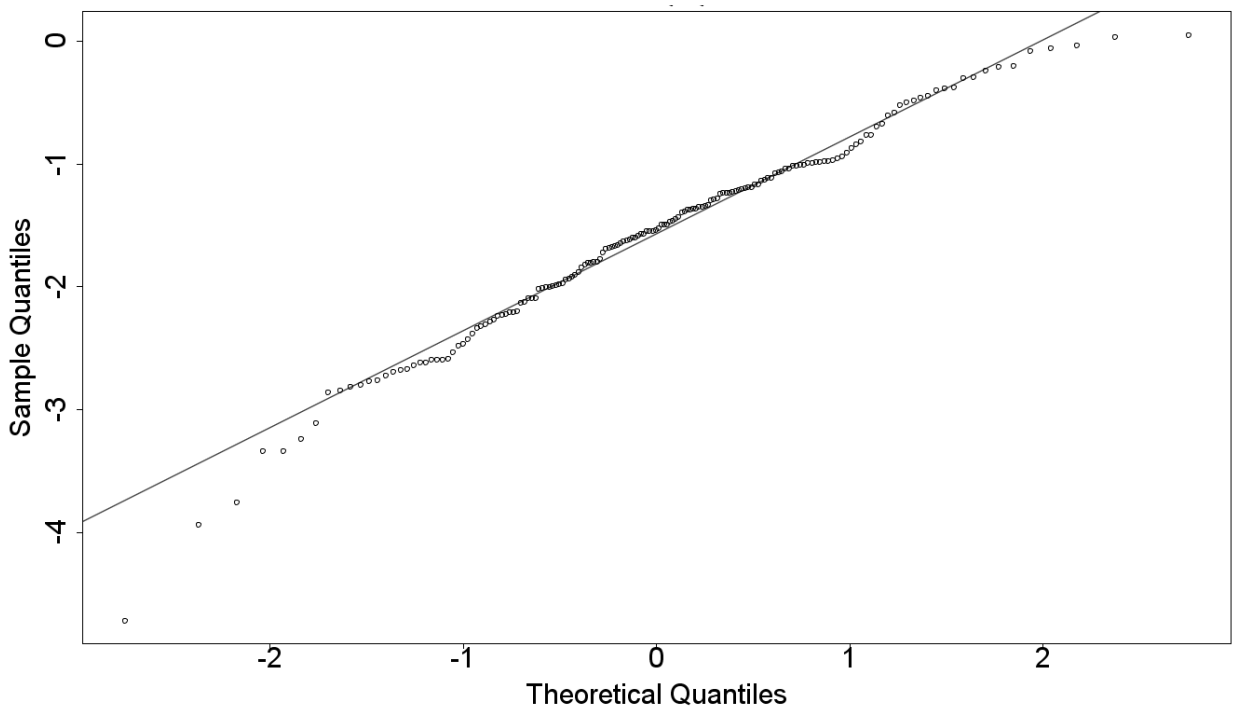

Figure 5.10. Normal quantile-quantile plot of natural-logarithmic transformed data for all three field locations.

5.2.2 Omitting "Row" from the list of random factors

A few diagnostic tests were examined before a true analysis was performed to see whether or not the row unit number of the implement should have been included as a fourth level of nesting within the level of 'pass.' After conducting statistical tests with and without the random factor 'row,' a decision was made to omit it from the linear mixed-effects model for the reasons given below.

The first test examined was a plot of standardized residuals versus fitted values. Plots were generated for each case of including and excluding row as a random factor, examples of which are shown in Figures 5.11 and 5.12, respectively. In Figure 5.11, a distinct linear pattern was observed as the fitted data increased in value. Alternatively, in Figure 5.12, a relatively even spread of residuals above and below the y=0 axis was presented. Because a normal distribution of residuals was preferable, the model that generated Figure 5.12 would be considered to be superior. Therefore with respect to this diagnostic, it was preferable for 'row' to be excluded from the random factor list.

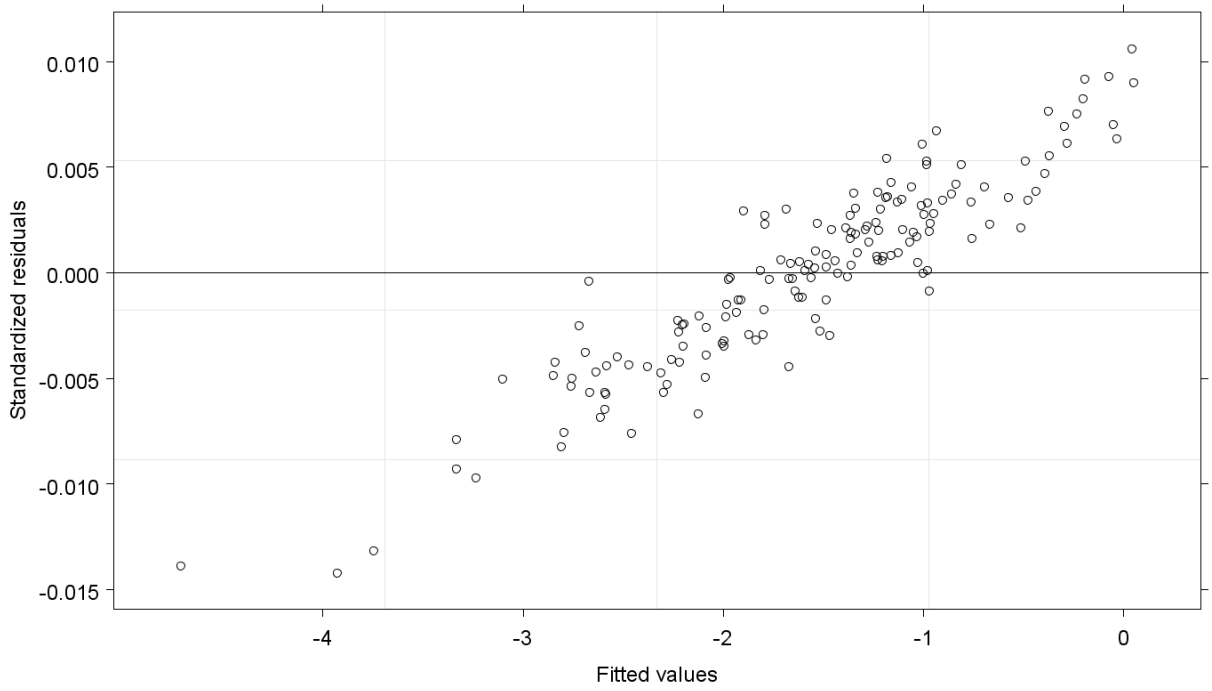

Figure 5.11. Standardized residuals versus fitted values diagnostic plot for corn including "Row" in the random factor list.

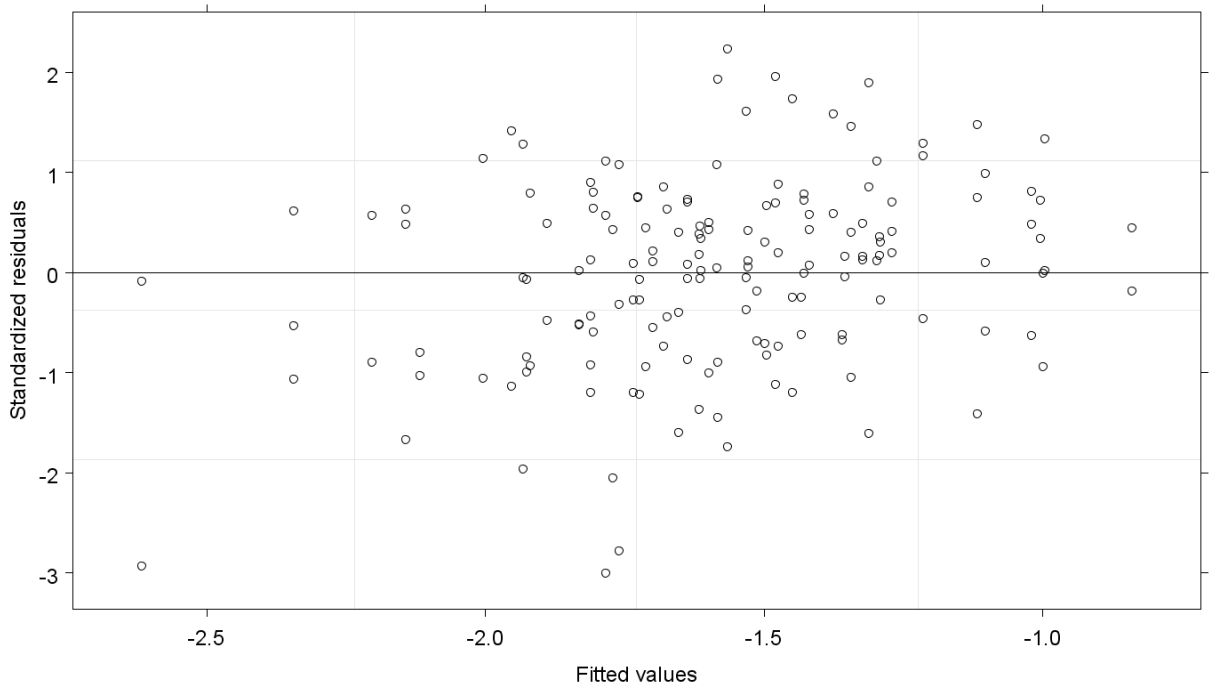

Figure 5.12. Standardized residuals versus fitted values diagnostic plot for corn excluding "Row" in the random factor list.

The second diagnostic examined was a plot of the response variable (logarithmic transformed cleaning performance or *invlogPerform*) versus the fitted values of the model in question. Plots were generated for each case of including and excluding row as a random factor, examples of which are shown in Figures 5.13 and 5.14, respectively. One would expect that these plots should display an approximate 1:1 line indicating a high level of goodness-of-fit, as both figures do. However, the problem lies in the fact that the data displayed in Figure 5.13 follow an exact 1:1 line and is suspicious, while in Figure 5.14 an underlying 1:1 trend is present with a degree of variation. The cause of the trend shown in Figure 5.13 was likely due to the presence of only one unique data point for each incidence of a given row number in the nesting sequence of the random factors. For 'row' to be included, it is preferable to have at least 2-3 data points for each incidence of a given row number within a nesting sequence in order for 'row' to be included as a random factor in the model. Therefore with respect to this diagnostic as well, it was preferable for 'row' to be excluded from the random factor list.

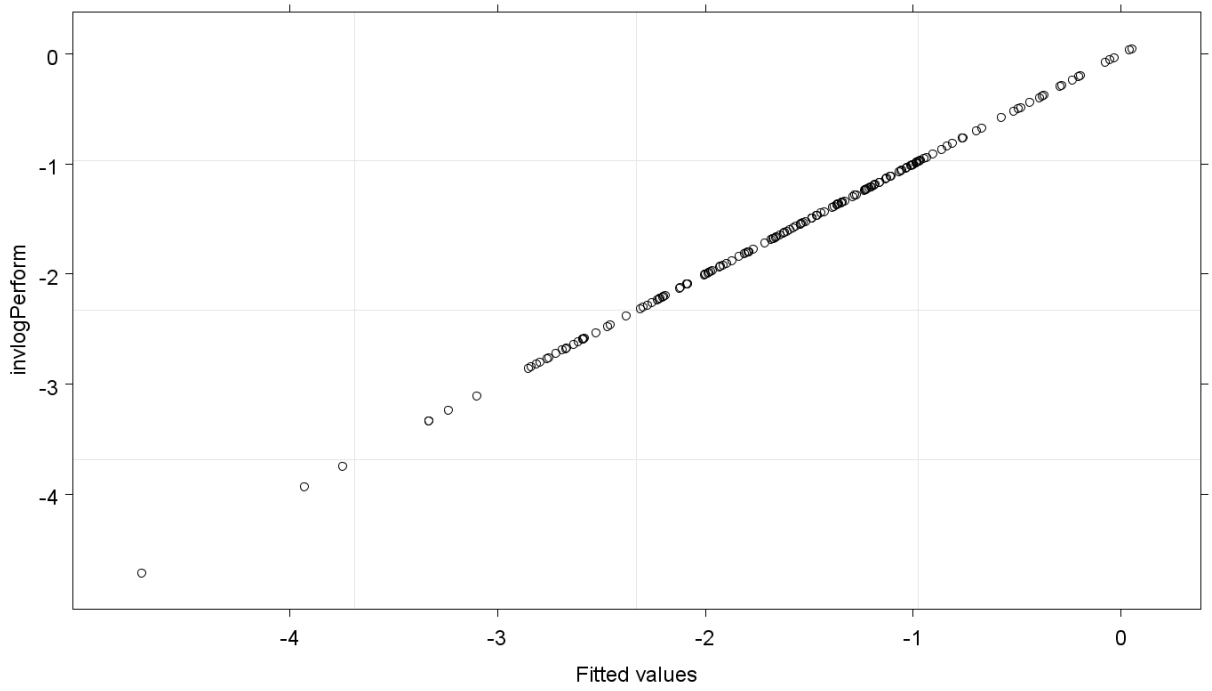

Figure 5.13. Response variable versus fitted values for corn including “Row" in the random factor list.

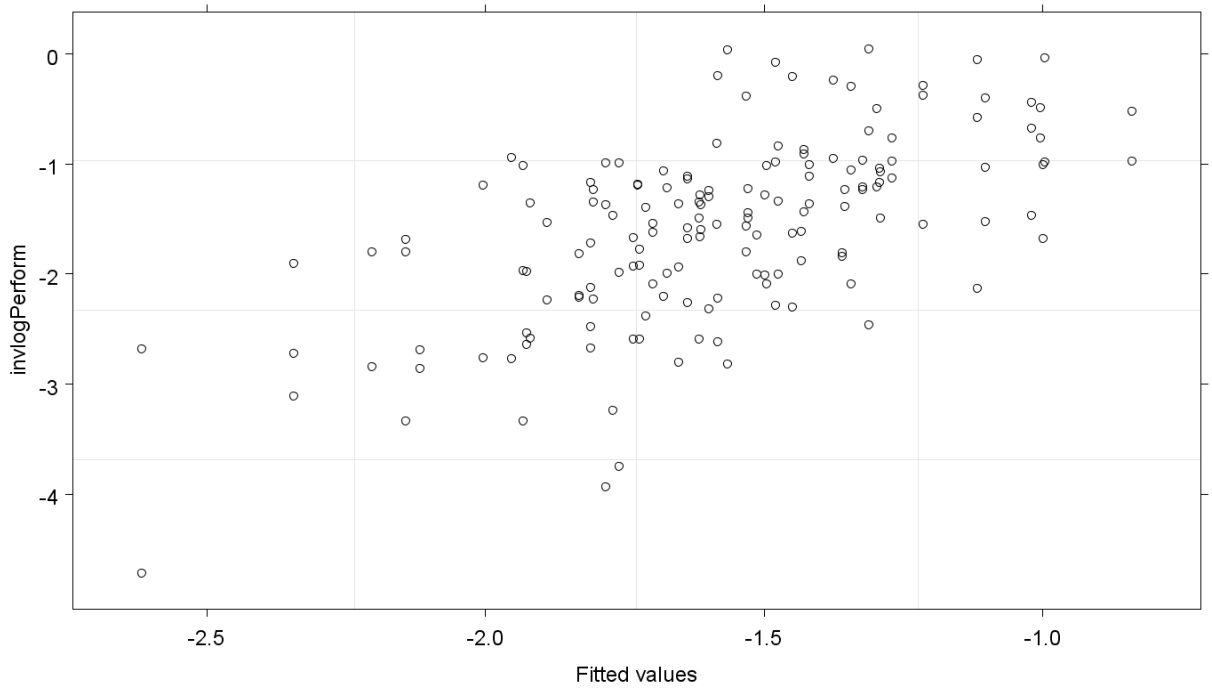

Figure 5.14. Response variable versus fitted values for corn excluding "Row" in the random factor list.

5.2.3 Corn Stubble Results

The maximal mixed-effects model for corn stubble was constructed using main effects for configuration, speed and the residue moisture content at the time of the trial, as well as an interaction effect between configuration and speed. An interaction effect for moisture content at time of operation could not be included as singularities in the solving process could not yield a solution. A detailed explanation of tables and results is shown below for the statistical test of the front orientation, while detailed tables for the rear orientation and both orientations combined can be found in Appendix C.

Front orientation only (four configurations)

Model simplification was used to reduce the maximal model to the minimally adequate model. This was accomplished by removing one fixed-effect model parameter at a time, evaluated by choosing the parameter with the largest p-value (continuous variable) or set of p-values (discrete value with several levels). The p-values that were evaluated are highlighted in Table 5.1. The

interaction effects were removed first followed by the main effects, if any. This process continued until there were no p-values left that were greater than 0.05 or until the null model was reached. The maximal model summary from R© is shown below in Table 5.1, while the minimally adequate model summary (null model) is shown in Table 5.2. The standard deviation (denoted by *StdDev*) associated with each random factor is shown under the random effects section. The *(Intercept)* notation under the fixed effects heading refers to a default set of model parameters chosen as a baseline value for the response variable. In this case the *(Intercept)* notation represents main and interactive effects for the Offset-13 row cleaner configuration operating at 8 km/h with a residue moisture content of 0%. It should be noted that factors with discrete levels (such as configuration and speed) introduce a discrete change in the response variable as indicated under the column *value*. Continuous variables (such as moisture content at the time of the trial) offer a varying amount of change in the response variable where the number under the column *value* must be multiplied by the desired residue moisture content to obtain a result. It should be noted that the correlation matrix was removed from each model summary table as it was large and uninformative for this situation.

Table 5.1. Maximal model summary for corn for the front orientation

Linear Mixed-effect model fit by maximum likelihood

Data: NULL

AIC	BIC	log likelihood
260.3055	293.642	-117.1528

Random Effects:

Formula: *~1 | Location*

(Intercept)

StdDev: 2.44E-05

Formula: *~1 | Plot in Location*

(Intercept)

StdDev: 6.89E-06

Formula: *~1 | Pass in Plot in Location*

	(Intercept)	Residual
StdDev:	0.1945217	0.7977561

Fixed Effects: **invlogPerform ~ Configuration * facSpeed + Oper.MC**

	Value	Std.Error	DF	t-value	p-value
(Intercept)	-0.915798	1.123038	64	-0.81546	0.4178
Configurationoffset18	-0.326944	0.54217	6	-0.60303	0.5686
Configurationparallel	-0.262325	0.473205	6	-0.55436	0.5994
Configurationproduction	-0.155353	0.488244	6	-0.31819	0.7611
facSpeed11.2	-0.107604	0.371374	6	-0.28975	0.7818
Oper.MC	-3.449207	5.556849	6	-0.62071	0.5576
Configurationoffset18:facSpeed11.2	0.260049	0.525967	6	0.49442	0.6386
Configurationparallel:facSpeed11.2	0.367829	0.525202	6	0.700357	0.5099
Configurationproduction:facSpeed11.2	0.118139	0.525202	6	0.224941	0.8295

Standardized Within-Group Residuals:

Min	Q1	Med	Q3	Max
-2.8521282	-0.7089884	0.0895918	0.6439797	2.15702

Number of Observations: 96

Number of Groups:

Location	Plot in Location	Pass in Plot in Location
2	16	32

Table 5.2. Minimally adequate model summary for corn for the front orientation

Linear Mixed-effect model fit by maximum likelihood

Data: NULL

AIC	BIC	log likelihood
245.7812	258.6029	-117.8906

Random Effects:

Formula: *~1 | Location*

	(Intercept)
StdDev:	0.03731743

Formula: *~1 | Plot in Location*

	(Intercept)
StdDev:	4.40E-05

Formula: *~1 | Pass in Plot in Location*

	(Intercept)	Residual
StdDev:	0.2197652	0.797756

Fixed Effects: **invlogPerform ~ 1**

	Value	Std.Error	DF	t-value	p-value
(Intercept)	-1.582071	0.09448749	64	-16.7437	0

Standardized Within-Group Residuals:

Min	Q1	Med	Q3	Max
-2.81354919	-0.6757066	0.04670678	0.62824714	1.929394

Number of Observations: 96

Number of Groups:

Location	Plot in Location	Pass in Plot in Location
2	16	32

Tables 5.3 and 5.4 display a compact summary of the detailed results shown above in Tables 5.1 and 5.2 using generalized p-values for each factor.

Table 5.3. Summary table for the maximal model for corn for the front orientation

MAXIMAL MODEL	Numerator DF	Denominator DF	F-value	p-value
(Intercept)	1	64	290.3688	< 0.0001
Configuration	3	6	0.06803	0.9749
facSpeed	1	6	0.20126	0.6695
Oper.MC	1	6	0.40598	0.5475
Configuration:facSpeed	3	6	0.18782	0.9009

Table 5.4. Summary table for the null model for corn for the front orientation

NULL MODEL	Numerator DF	Denominator DF	F-value	p-value
(Intercept)	1	64	280.3518	< 0.0001

A comparison between the maximal and minimally adequate (null) models is shown in Table 5.5. The p-value on the right hand side was much greater than 0.05 which meant that there was no statistically significant difference in the results between the two models. The null model could therefore be used to predict cleaning performance with very little difference from the maximal model with much greater simplicity. This meant that none of the fixed factors used in the experiment had a statistically significant impact on the mean cleaning performance of the various row cleaner configurations.

Table 5.5. Comparison table between the maximal model and the null model for corn for the front orientation

Model		Degrees of					L.	p-
Type	Number	Freedom	AIC	BIC	logLik	Test	Ratio	value
maximal	1	13	260.306	293.642	-117.15			
null	2	5	245.781	258.603	-117.89	1 vs 2	1.47567	0.9931

Rear orientation only (all five configurations)

There were no statistically significant differences within each the five configurations, and the two travel speeds. In addition there were no statistically significant differences between the

factors of configuration, travel speed and moisture content at time of operation. The mean cleaning performance for the rear orientation for corn residue could therefore be considered to be equal regardless of the configuration or travel speed chosen within the statistical bounds of this experiment.

Both front and rear orientations (four configurations)

Because there were no significant differences within the datasets for each orientation, the two datasets were combined and tested as a single dataset. When completed, there were no statistically significant differences in mean cleaning performance.

5.2.4 Wheat Stubble Results

The maximal mixed-effects model for wheat stubble was constructed using main effects for configuration, and speed. An interaction effect for configuration and speed as well as main and interactive effects for moisture content at time of operation could not be included as singularities in the solving process could not yield any solutions. Because a detailed explanation example of tables and results was shown for corn and because the same analysis was used for wheat stubble, the detailed tables of statistical results can be found in Appendix C. Generally, the smaller range of data values for wheat stubble led to smaller p-values as compared to corn, however not to the point where there was a statistically significant difference ($p \leq 0.05$). In all three statistical tests, using datasets for the front orientation only (four configurations), the rear orientation only (five configurations), and both orientations combined, respectively, similar results to the corn stubble were obtained. In all three cases there were no statistically significant differences within each of the five configurations and the two travel speeds. This meant that the mean cleaning performance for the front and rear orientations could be considered to be equal regardless of the configuration or travel speed chosen within the statistical bounds of the experiment.

5.3 Differences in Consistency of Cleaning Performance

Because the statistical tests for mean cleaning performance yielded no significant differences between configurations and speeds and the median cleaning performances are relatively large, a weighted method was not used to account for different skewness in the data distributions. A weighted method could have involved giving data points with higher cleaning performance

values a larger score than those values which were smaller. This would have meant that even though the 95% confidence interval range of performance values for two configurations were equal, one would receive a higher score than the other if its data were negatively skewed while the former had positive skew. A weighted method such as this would have also caused issues between rating the Alpha Prototype against the other four configurations as it would achieve a much lower score due to the smaller number of samples.

A note should be made as to the significance of rating the Alpha Prototype directly against the other four configurations as there was a limited number of samples relative to the other four configurations. This fact might have influenced the Alpha Prototype to appear much more (much less) consistent than it really was relative to the other configurations.

Generally, the row cleaners were much more consistent in wheat than in corn, possibly due in part to the larger volume of corn residue that was required to be moved, even though the masses of residue measured for each crop-type were similar.

5.3.1 Corn

The overall consistency of cleaning performance by configuration is shown in Figure 5.15. The Offset-13 and Offset-18 configurations had the best consistency while the Parallel configuration had noticeably lower consistency compared to the other four configurations. The general trend shown in Figure 5.15 was similar for all orientations (front or rear) and speeds (low or high) shown in Figures 5.16 and 5.17, respectively. One exception to this trend was the low consistency of the Offset-13 configuration operating at low speed versus high speed shown in Figure 5.17. One possible reason for its poorer consistency at low speed could be that with the smaller disk angle of the Offset-13, the disks were not able to provide enough momentum to laterally accelerate the residue towards the inter-row zone leaving more residue at the outer edge of the berm, inside the perimeter of the measuring quadrat. This inability to laterally accelerate the residue could also be applied to the Parallel configuration as the tilt angle of the disks was more negative than the other configurations. This would cause a bull-dozing effect whereby more energy would be expended by pushing the residue forward against the ground rather than simply translating it from the location of the berm to the inter-row zone.

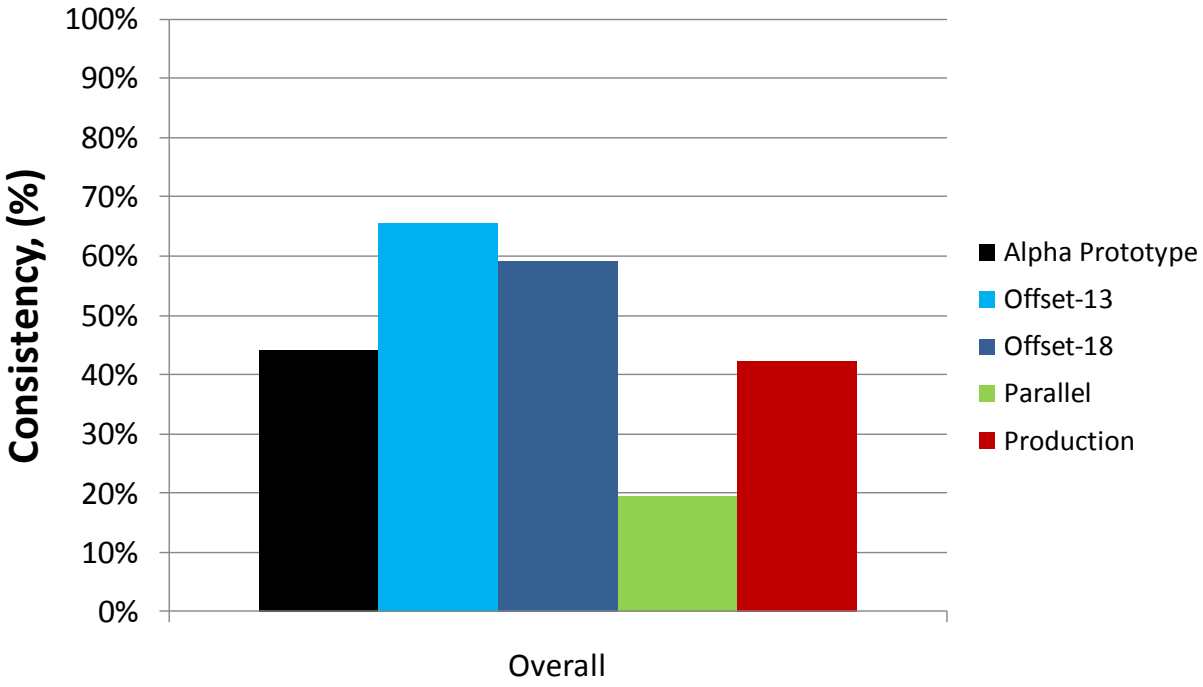

Figure 5.15. Overall consistency of cleaning performance for corn stubble.

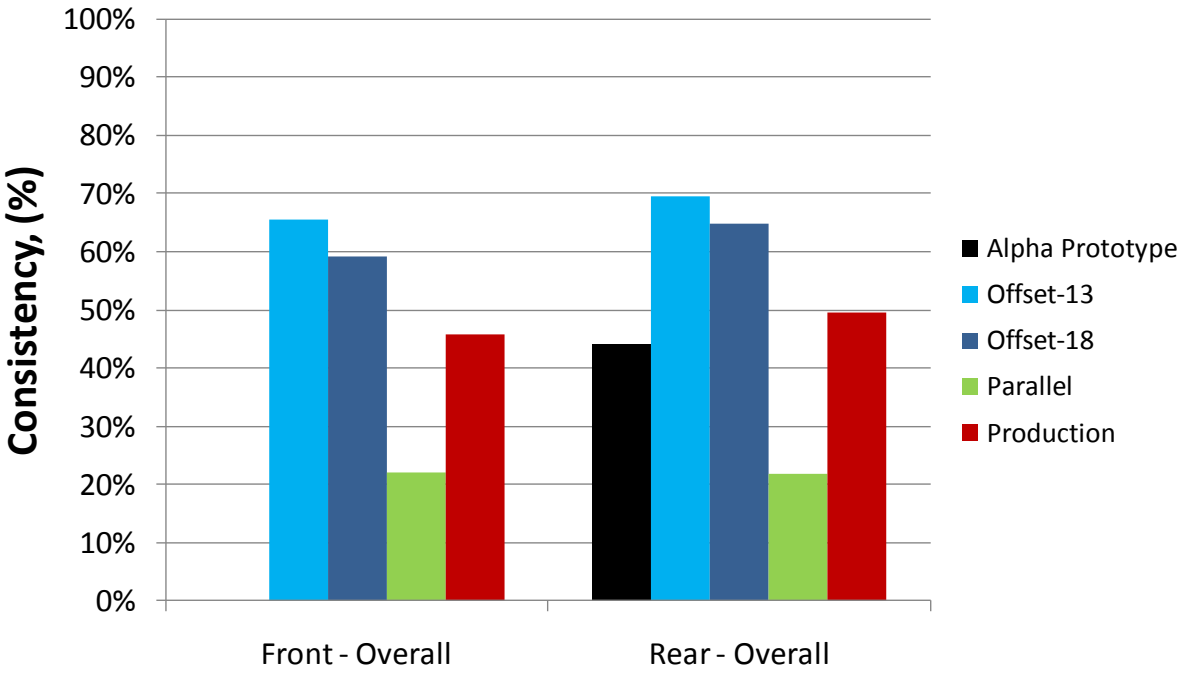

Figure 5.16. Consistency of cleaning performance for corn stubble categorized by orientation.

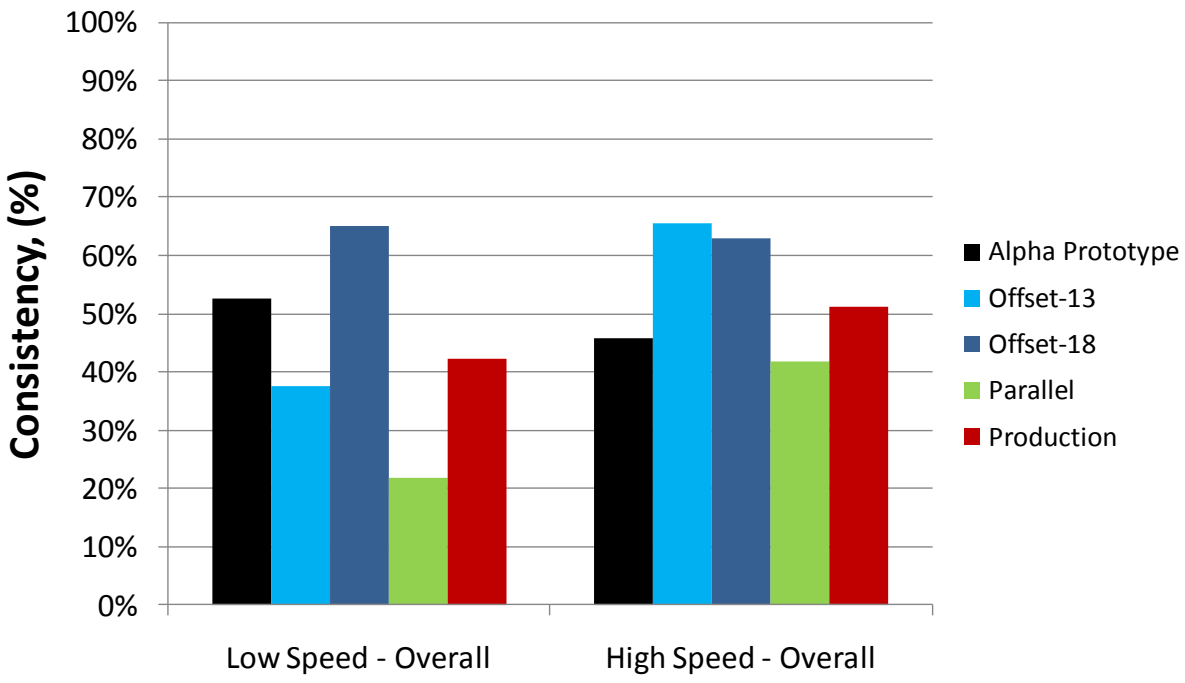

Figure 5.17. Consistency of cleaning performance for corn stubble categorized by speed.

5.3.2 Wheat

All five configurations performed with a high level of consistency in wheat stubble as shown in Figure 5.18. As such it was impossible to choose one configuration over another due to the fact that their consistency values were within 12-15% of one another. A slightly poorer consistency was observed for the rear orientation of the Offset-13 configuration in the rear orientation and the Parallel configuration at low speed, shown Figure 5.19 Figure 5.20, respectively. Barring these slight differences the general trend was followed regardless of orientation (front or rear) and speed (low or high).

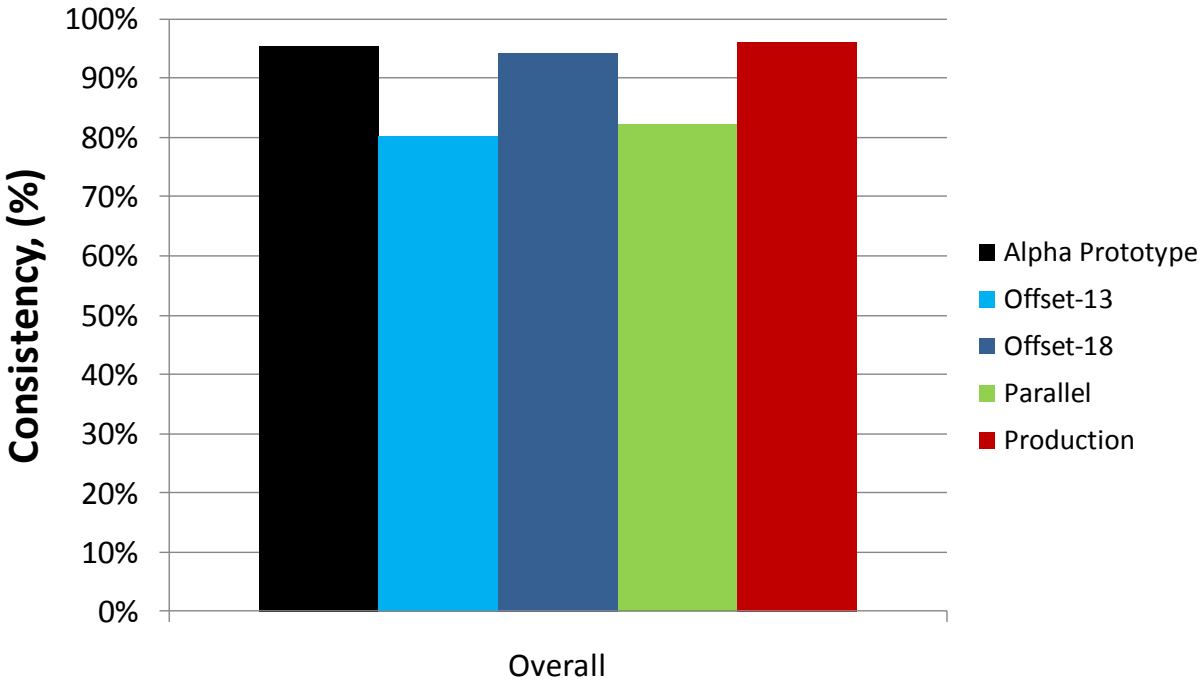

Figure 5.18. Overall consistency of cleaning performance for wheat stubble.

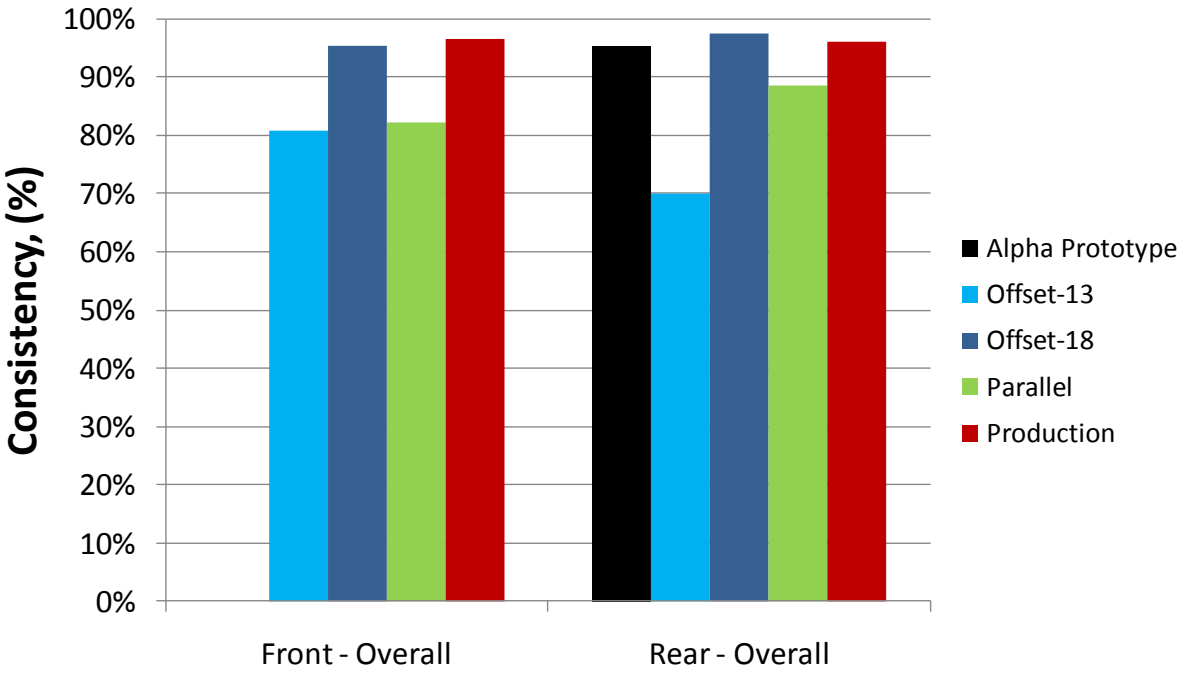

Figure 5.19. Consistency of cleaning performance for wheat stubble categorized by orientation.

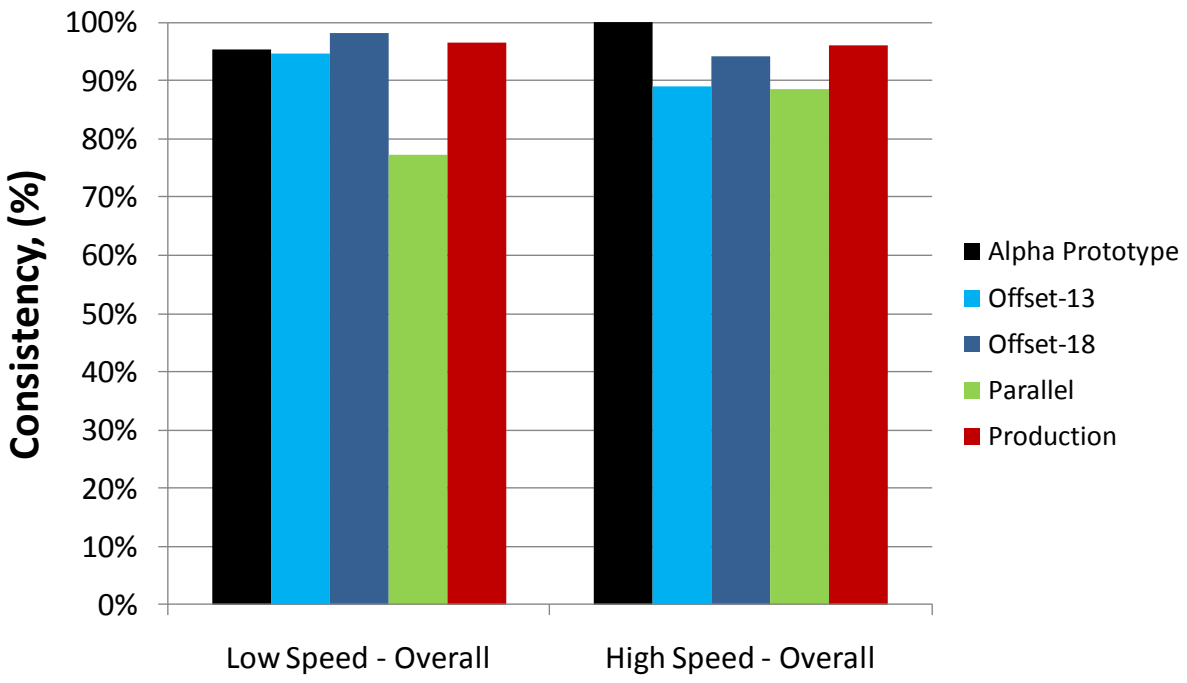

Figure 5.20. Consistency of cleaning performance for wheat stubble categorized by speed.

5.4 Evaluation of Edge Effects

The results for edge effects of the strip-tillage implement are shown in Table 5.6. At all three field locations there was generally no statistical difference between the initial residue distribution in the plots and the residue mass in the area immediately adjacent to the first machine pass. One exception in Location II was the Production configuration at high speed (10.4 km/h), however the reason for this was likely due to an abnormally low initial residue mass measurement. The second exception was in Location III using the Offset-13 configuration at high speed (11.2 km/h). One reason for this anomaly was likely due to an abnormally large outside-row residue mass measurement in a region where excessive chaff was deposited on the ground during the wheat's harvest. The detailed results tables displaying mass values can be found in Appendix D. These results indicate that the effects of residue thrown onto the area immediately adjacent to that on which the machine was operating was largely negligible. One field condition in corn stubble that prevented residue throw-over at the edge of the machine was the remaining standing stubble which provided a physical barrier for any residue ejected by the row cleaners. In wheat stubble, very little mass of residue may have been ejected into the area adjacent to the machine

due to the small particle size. This would then cause an insignificant change of material mass collected from this area. It should also be noted that these results for edge effects do not take into account any soil ejected by the row cleaners as noted in the comments relevant to the videos at the beginning of this chapter.

Table 5.6. Edge-effects results summary table for all locations

Configuration	Speed	Outside the 95% Confidence Interval?		
	km/h (mph)	Location I	Location II	Location III
Offset-13	**Low**	No difference	No difference	No difference
	High	No difference	No difference	HIGH
Offset-18	**Low**	No difference	No difference	No difference
	High	No difference	No difference	No difference
Parallel	**Low**	No difference	No difference	No difference
	High	No difference	No difference	No difference
Production	**Low**	No difference	No difference	No difference
	high	No difference	HIGH	No difference

5.5 Observations from the field tests

The following is a qualitative discussion hypothesizing what the effects were of various parameters on the cleaning performance of the row cleaners. This discussion was based on observations during the field trials and from the videos collected at that time. The issues discussed may be topics worthy of further scientific study to quantify their effects on cleaning performance but were outside the scope of the current study.

5.5.1 Effect of Parallel Versus Offset Mounting of Disks

The parallel and offset mounting of disks were the two key disk-mounting styles employed in the row-cleaner configurations. The parallel mounting fostered more of a competitive nature between the two disks where the disks would compete for the same piece of residue. This competition occurred because the disks were given equal opportunity to move the same piece of residue. On the other hand, the offset mounting removed competition for pieces of residue between the two disks by giving priority to the forward-mounted disk to move residue just before the rear-mounted disk. This virtually eliminated the possibility that the same piece of residue would be grabbed by both disks simultaneously, preventing a disruption in the flow of residue to the inter-row zones on either side of the row-cleaner. One possible method by which to test this

hypothesis would be to collect and analyze high-speed video of the machine in the field or a soil bin.

5.5.2 Effect of Disk Size

The two disk-sizes were only able to be mounted using an offset or staggered disk-mounting style. From analysis of the videos it appeared as though residue was moved in a similar fashion. In this case, with the disk geometry used and the environmental conditions during the field trials, the main difference between the two disk sizes was the amount of soil that was thrown. The large disk appeared to throw much more soil than the small disk. The best explanation for this observation would be that because the row-cleaners float over the ground, the weight of the additional steel in the large disk may have provided more down force of the row-cleaner against the ground. The additional force then permitted the large disks to penetrate into the ground to a larger degree than the small disk, meaning more soil would be moved. Further comment on soil throwing is also provided in a sub-section below.

5.5.3 Effect of Disk Separation

The Parallel configuration had a very small amount of disk separation at the leading edge of the row cleaner, while the Production configuration had substantially more separation. This difference seemed to have little effect on the configurations performance in these field tests. More separation would reduce the competitive tendencies of the disks as described above in the effect of an offset versus a parallel mounting style. It would also however tend to leave small pieces of residue in the berm-building region which could be considered less desirable for berm formation. It could be counter-argued that the small residue pieces would introduce a minimal amount of volume to the berm and could decompose rather rapidly, having a minimal effect on the agronomic aspects of the berm.

5.5.4 Effect of Disk Angle

The disk angle affected the degree of lateral acceleration and therefore the lateral velocity of the residue. A small disk angle, such as that employed in the offset disk-mounting style, tended to have less lateral acceleration than a larger disk angle, such as that used in the parallel disk-mounting style. From the videos it was observed that the offset disk-mounting style configurations had better, smoother residue flow at higher speeds because the residue was not

overthrown into the berm area of the neighboring row as was observed to a small degree in the parallel disk-mounting style configurations. At slower speeds the parallel disk-mounting style configurations had smoother residue flow than offset disk-mounting styles because they were able to accelerate the residue enough to eject it out of the berm-formation area. The offset disk-mounting style configurations were still able to eject material out of the berm-formation area at the low speed (8 km/h) in these tests, but it was expected that this would become even more pronounced at lower speeds.

5.5.5 Effect of Disk Tilt Angle

The Parallel configuration had a pronounced negative tilt angle while the Production configuration had very little tilt angle. The Parallel configuration likely had a negative tilt angle to reduce the digging effect of the disk on the soil so it skimmed over the soil rather than digging in slightly as did the Production configuration. This skimming, however, introduces the bulldozing effect of the residue as it translates along the ground rather than being lifted and translated as was more pronounced in the Production configuration. The bulldozing effect could cause problems in high residue conditions as it would slow or impede residue flow to the inter-row zones. A positive tilt angle would be undesirable for row cleaners because the disk would begin digging into the ground and moving a substantial amount of soil along with the residue, leaving less soil available for berm construction.

5.5.6 General Observations which may have affected Performance throughout the Trials

Most of the disks employed on the various configurations were either slightly used, but had rust on the surface from sitting dormant over the course of a year, or were brand-new and painted. The paint caused some issues pertaining to clay soil build-up on the disks especially in the two corn field locations. If the disks were polished steel it was assumed that this build-up may not occur. Any soil build-up on the disks, if any, was removed before each plot to reduce its effect. It was expected that soil build-up would impede the disk to perform its residue-clearing function as designed.

In a couple cases, it was also observed on the video that the rear disk on the Offset-18 would stop turning due to a combination of soil build-up and clearance issues between the front and rear disks. This appeared to have a minimal effect on performance most likely because the front disk moves a large portion of the residue from the berm-building region.

Throughout the videos for all the tests it was very apparent that there were residue recirculation issues with the disks. This would reduce the ability of the disk to continually grab and transfer new residue with each rotation. Changing the disk parameters or the disk edge-design may be able to reduce this effect.

All of the configurations tested also threw varying amounts of soil. This could also be an area for potential study. This phenomenon was much more apparent in the wheat residue as opposed to the corn residue, most likely due to the wheat residue's smaller volume relative to the corn residue. To reduce this effect, changing disk parameters or the disk edge-design may be employed, as well as potentially limiting or regulating the down-pressure of the row cleaners when performing strip-till operations in certain crops.

Berm formation appeared to be good throughout the experiment using the farmer's normal implement settings. It was not expected that a chosen row-cleaner configuration would have a large impact on berm formation as this was mostly a function of the soil type and moisture content as well as the settings employed by the berm-building disks and the rolling basket.

5.6 Selecting a Single Configuration for Both Crops

Based on the results of this experiment and examining how the row cleaners work in 'real-time' in the field, the author chose the Offset-13 configuration as the best configuration. The main reason this configuration was chosen to be superior was because it had one of the best overall consistency of cleaning performance of the configurations, especially at the higher speed in corn (10.4 km/h). Because it performed well at higher speeds, the field capacity of the machine was higher which led to higher productivity without sacrificing the quality of the field operation. From the video examination it was also one of the configurations which appeared to throw less soil. This meant that more soil would be available for berm construction rather than being

ejected into the inter-row region, creating a better environment in which to grow a crop. The choice for this decision was made primarily employing the operating results from corn considering all of the row cleaner configurations performed well in wheat stubble.

6.0 CONCLUSIONS AND RECOMMENDATIONS

A field experiment was conducted with a strip-tillage implement that evaluated the cleaning performance of five different row-cleaner configurations at two travel speeds and two row-unit mounting orientations. The experiment was conducted utilizing two corn-field locations and one wheat-field location, with separate analyses being conducted for each type of stubble. The conclusions drawn from the study are as follows:

1. The median cleaning performance values were relatively large and similar over all test conditions. The statistical results also indicated that there was no difference in mean cleaning performance between the five configurations and both travel speeds.

2. Consistency of cleaning performance provided a good indicator by which to evaluate the row cleaners even though a statistical analysis could not be completed. The consistency of cleaning performance in corn residue was approximately the same for each configuration with the exception of the Parallel configuration. Cleaning performance consistency for wheat residue was very high and relatively equal for all five configurations. Due to the higher degree of variability of cleaning performance in corn residue, further studies should focus upon large, thick amounts of low density residue as opposed to more friable residue such as wheat stubble, where the cleaning performance observed was excellent. By focusing only on heavy amounts of trash it may prove easier to distinguish clear differences in cleaning performance between different configurations.

3. In the future, if a statistical analysis of cleaning performance consistency is required, it would be recommended to obtain consistency numbers from several (three or more) field experiments in different locations to be able to perform a statistical analysis. As this type of experiment was very labor intensive it would require serious considerations of economic constraints before proceeding.

4. Edge effects of the implement could be neglected in further experiments as they yielded no significant findings in this experiment. As a result, more resources could therefore be allocated to a different aspect of future field trials.

5. As the residue moisture content at the time of operation was only measured in this experiment, it may be warranted to complete trials at 2-3 different residue moisture contents to see if any identifiable relationship is present.

6. Given the amount of soil ejected by the row-cleaner disks, as viewed on the videos, it may be worthwhile to develop a method by which to quantify the 'soil spatter' by the disks and subsequently carry out field tests with different disk designs and operating parameters.

7.0 REFERENCES

Al-Kaisi, M.M., X. Yin, and M.A. Licht. 2005. Soil carbon and nitrogen changes as affected by tillage system and crop biomass in a corn-soybean rotation. *Applied Soil Ecology* 30(1-2): 174-191.

Allmaras, R.R., J.L. Pikul, J.M. Kraft, and D.E. Wilkins. 1988. A method for measuring incorporated crop residue and associated soil properties. *Soil Science Society of America Journal* 52: 1128-1133.

Allmaras, R.R., S.M. Copeland, and D.E. Wilkins. 1997. Tillage tool control over crop residue placement: Conservation impacts. ASAE Paper no. 971090. St. Joseph, MI: ASABE.

ASABE Standards. 2008. *ASAE S358.2 DEC 1988 (R2008) – Moisture Measurement – Forages.* Obtained November 2008 from members only area of <www.asabe.org>.

ASTM International. 2008. *D4643-08 - Standard test method for determination of water (moisture content of soil by microwave oven heating.* Obtained from ASTM website through University of Saskatchewan Library website <https://library.usask.ca/astmdlreferral?time=1245365236>.

Azooz, R.H., B. Lowery, and T.C. Daniel. 1995. Tillage and residue management influence on corn growth. *Soil & Tillage Research* 33: 215-227.

Baird, F., and F. Baret. 1997. Crop residue estimation using multiband reflectance. *Remote Sensing of Environment* 59: 530-536.

Bannari, A., A. Pacheco, K. Staenz, H. McNairn, and K. Omari. 2006. Estimating and mapping crop residues cover on agricultural lands using hyperspectral and IKONOS data. *Remote Sensing of Environment* 104: 447-459.

Brown, L.C., R.K. Wood, and J.M. Smith. 1992. Residue management demonstration and evaluation. *Appliced Engineering in Agriculture* 8(3): 333-339.

CNH. 2010. *Case IH Web Press Room - Image Library - Fertilizer Placement Equipment*. Retrieved on August 29, 2010 from < http://pressroom.caseih.com/index.cfm?fuseaction=imagelibrary.DisplayImageLibrary&productid=113>.

Corak, S.J., T.C. Kaspar, and D.W. Meek. 1993. Evaluating methods for measuring residue cover. *Journal of Soil & Water Conservation* 48(1): 70-74.

Crawley, M.J. 2007. *The R Book*. John Wiley and Sons: West Sussex, England.

Daughtry, C.S.T., P.C. Doraiswamy, E.R. Hunt Jr., A.J. Stern, JE. McMurtrey III, and J.H. Prueger. 2006. Remote sensing of crop residue cover and soil tillage intensity. *Soil & Tillage Research* 91: 101-108.

Daughtry, C.S.T., E.R. Hunt Jr., and J.E. McMurtrey III. 2004. Assessing crop residue cover using shortwave infrared reflectance. *Remote Sensing of Environment* 90: 126-134.

Daughtry, C.S.T., J.E. McMurtrey III, M.S. Kim, and E.W. Chappelle. 1997. Estimating crop residue cover by blue fluorescence imaging. *Remote Sensing of Environment* 60(1): 14-21.

Fallahi, S., Raoufat, M.H. 2008. Row-crop planter attachements in a conservation tillage system – a comparative study. *Soil & Tillage Research.* 98: 27-34.

Haiping, S., M.D. Ransom, E.T. Kanemasu, and T.H. Demetriades-Shah. 1994. Second-derivative spectra for estimating crop residue cover. *Agronomy Journal* 86: 349-354.

Hartwig, R.O., and J.M. Laflen. 1978. A meterstick method for measuring crop residue cover. *Journal of Soil and Water Conservation* 33: 90-91.

Kaspar, T.C., and D.C. Erbach. 1998. Improving stand establishment in no-till with residue-clearing planter attachments. *Transactions of the ASABE* 41(2): 301-306.

Laflen, J.M., M. Amemiya, and E.A. Hintz. 1981. Measuring crop residue cover. *Journal of Soil & Water Conservation* 36(6): 341-343.

Licht, M.A., and M.A. Al-Kaisi. 2005. Strip-tillage effect on seedbed soil temperature and other soil physical properties. *Soil & Tillage Research* 80(1-2): 233-249.

Lowery, B., T.M. Lillesand, D.H. Mueller, P. Weiler, F.L. Scarpace, and T.C. Daniel. 1984. Determination of crop residue cover using scanning microdensitometry. *Journal of Soil and Water Conservation* 39(6): 402-403.

Morrison, J.E. Jr. 2002. Strip tillage for "no-till" row crop production. *Applied Engineering in Agriculture* 18(3): 277-284.

Morrison, J.E. Jr., J. Lemunyon, H.C. Bogusch Jr. 1995. Sources of variation and performance of nine devices when measuring percent residue cover. *Transactions of the ASABE* 38(2): 521-529.

Morrison, J.E. Jr., C. Huang, D.T. Lightle, and C.S.T. Daughtry. 1993. Residue measurement techniques. *Journal of Soil & Water Conservation* 48(6): 478-483.

Narayanan, R.M., L.N. Mielke, J.P. Dalton. 1992. Crop residue cover estimation using radar techniques. *Applied Engineering in Agriculture* 8(6): 863-869.

O'Dogherty, M.J., R.J. Godwin, M.J. Hann, and A.A. Al Ghazal. 1996. A Geometrical Analysis of Inclined and Tilted Spherical Plough Discs. *Journal of Agricultural Engineering Research* 63: 205-218.

R Development Team. 2009. *R: A Language and environment for statistical computing.* R Foundation for Statistical Computing, Vienna, Austria. Accessed March 2009 from <http://www.r-project.org>.

Raoufat, M.H., Matbooei, A. 2007. Row cleaners enhance reduced tillage planting of corn in Iran. *Soil and Tillage Research.* 93: 152-161.

Raper, R.L. 2002. The influence of implement type, tillage depth, and tillage timing on residue burial. *Transactions of the ASABE* 45(5): 1281-1286.

Raper, R.L. 2007. In-row subsoilers that reduce soil compaction and residue disturbance. *Applied Engineering in Agriculture* 23(3): 253-258.

Sloneker, L.L., and W.C. Moldenhauer. 1977. Measuring the amounts of crop residue remaining after tillage. *Journal of Soil & Water Conservation* 32(5): 231-236.

Su, H., M.D. Ransom, and E.T. Kanemasu. 1997. Simulating wheat crop residue reflectance with the SAIL model. *International Journal of Remote Sensing* 18(10): 2261-2267.

Swan, J.B., T.C. Kaspar, and D.C. Erbach. 1996. Seed-row residue management for corn establishment in the northern US corn belt. *Soil & Tillage Research* 40: 55-72.

Thoma, D.P., S.C. Gupta, and M.E. Bauer. 2004. Evaluation of optical remote sensing models for crop residue cover assessment. *Journal of Soil and Water Conservation* 59(5): 224-233.

Vetch, J.A., and G.W. Randall. 2002. Corn production as affected by tillage system and starter fertilizer. *Agronomy Journal* 94: 532-540.

Wolkowski, R.P. 2000. Row-placed fertilizer for maize grown with an in-row crop residue management (I-RRM) system in Southern Wisconsin. *Soil & Tillage Research* 54(1): 55-62.

APPENDIX A – PLOT DIAGRAMS AND COLLECTED DATA

This appendix contains information about the experiment design and the data collected during the experiment. All of the plots from locations I, II, and III are depicted in Figures A.1-A.10, Figures A.11-A.20, and Figures A.21-A.30, respectively. Within each plot, the appropriate initial and final residue sampling areas are shown in orange and blue, respectively. The mass of residue (g) collected in each sampling area is indicated by the number written in each cell. The 'initial' residue moisture content was used to convert the initial mass measurements to dry mass (g). The 'final' residue moisture measurements were used to convert most of the final mass measurements (solid-blue-colored) to dry mass (g). The final measurements from the blue-speckled regions were collected at the time of the field operation, thus the 'operating' residue moisture content was used in its conversion.

Location I

Plot 1 Offset-18 - 8 km/h (5 mph)

Row Number, R			Measurement Interval, I									
			0	1	2	3	4	5	6	7	8	9
	Pass 1	8					208					
		7					116					
		6					616					
		5					251					685
		4					188					
		3					121					
		2	775				149					
		1					56					108
	Pass 2	1					724					575
		2										247
		3		981								54
		4										261
		5								919		935
		6										89
		7										22
		8								746		352

Residue Moisture Content (dry basis): Initial = 6.3% Operating = 12.9% Final = 17.9%

Figure A.1. Plot schematic for Plot 1 at Location I showing the initial and final residue mass measurement locations in orange and blue, respectively. The initial, operating and final residue moisture contents were used to convert the wet mass measurements to dry mass of residue for the orange, blue-speckled, and solid blue sampling areas, respectively.

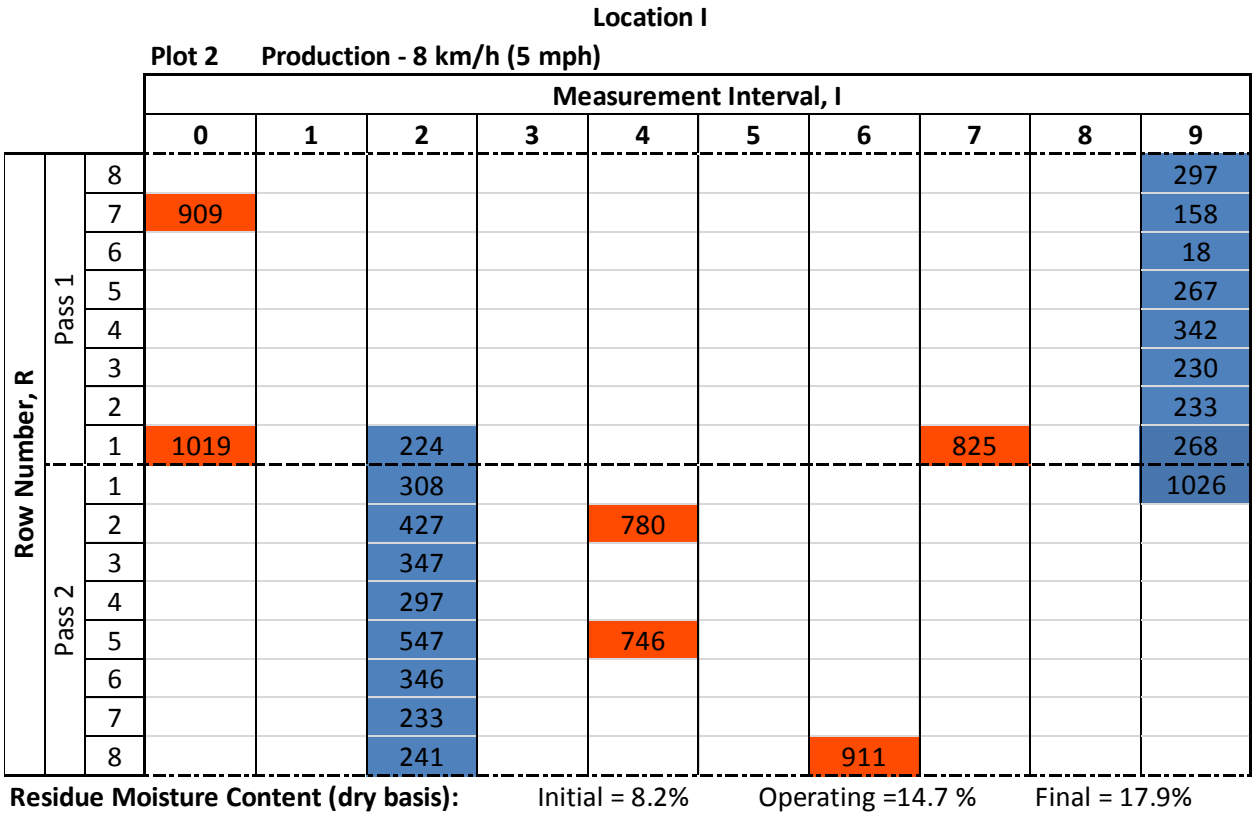

Figure A.2. Plot schematic for Plot 2 at Location I showing the initial and final residue mass measurement locations in orange and blue, respectively. The total wet mass of residue (g) measured in each sampling area is shown in its respective cell. The initial, operating and final residue moisture contents were used to convert the wet mass measurements to dry mass of residue for the orange, blue-speckled, and solid blue sampling areas, respectively.

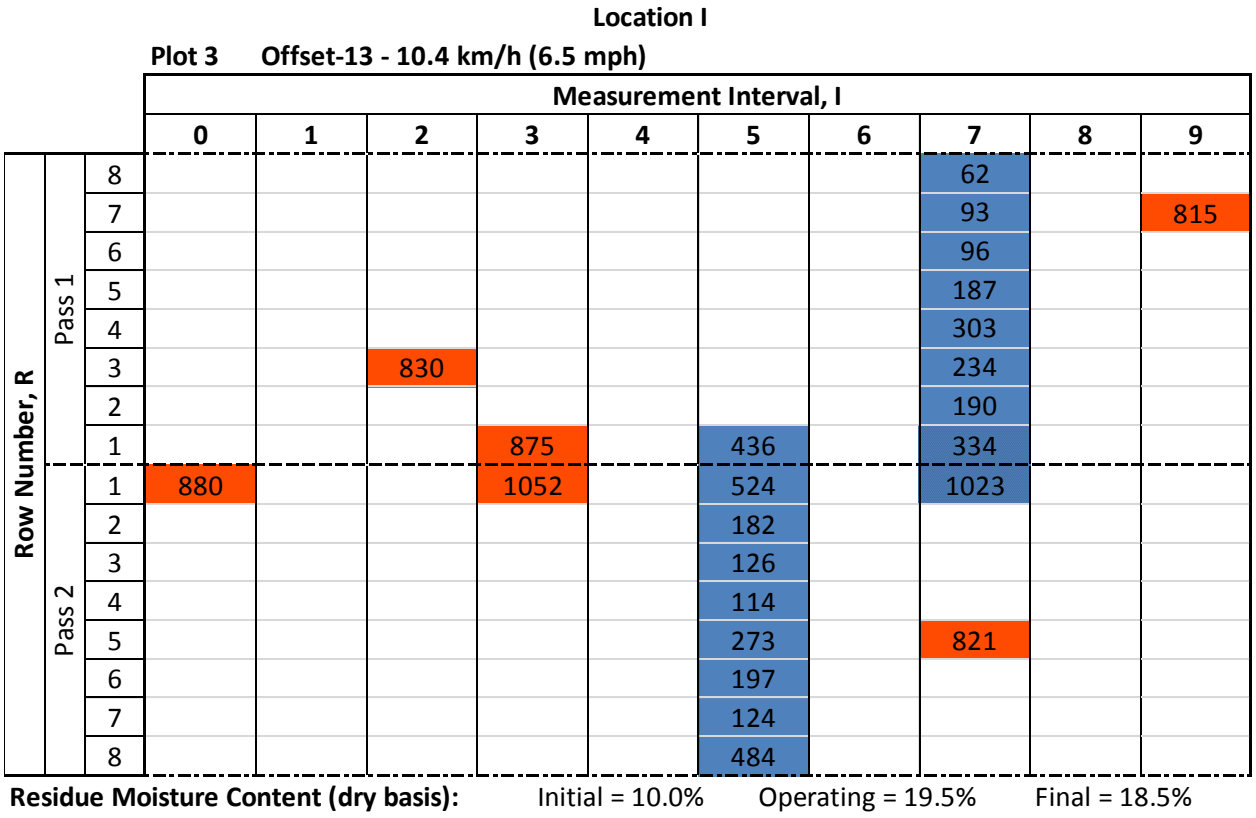

Figure A.3. Plot schematic for Plot 3 at Location I showing the initial and final residue mass measurement locations in orange and blue, respectively. The total wet mass of residue (g) measured in each sampling area is shown in its respective cell. The initial, operating and final residue moisture contents were used to convert the wet mass measurements to dry mass of residue for the orange, blue-speckled, and solid blue sampling areas, respectively.

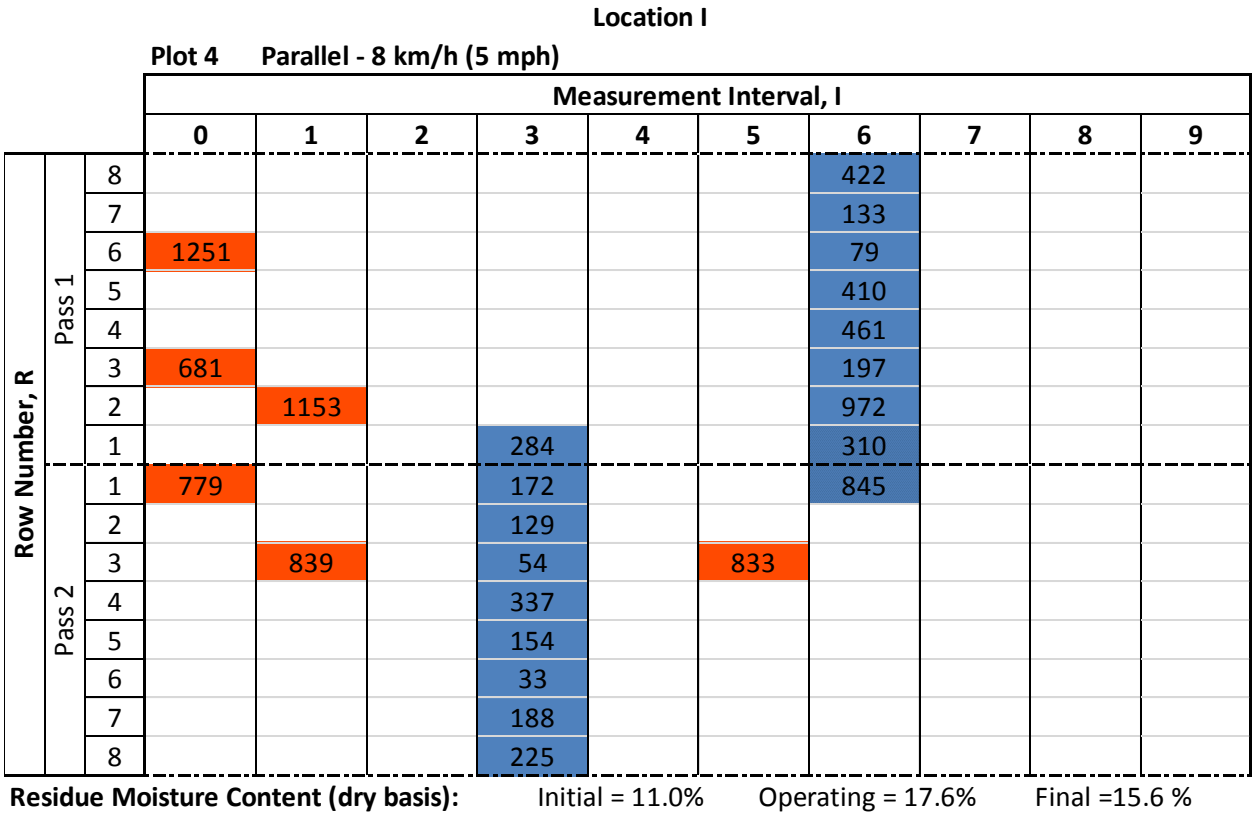

Figure A.4. Plot schematic for Plot 4 at Location I showing the initial and final residue mass measurement locations in orange and blue, respectively. The total wet mass of residue (g) measured in each sampling area is shown in its respective cell. The initial, operating and final residue moisture contents were used to convert the wet mass measurements to dry mass of residue for the orange, blue-speckled, and solid blue sampling areas, respectively.

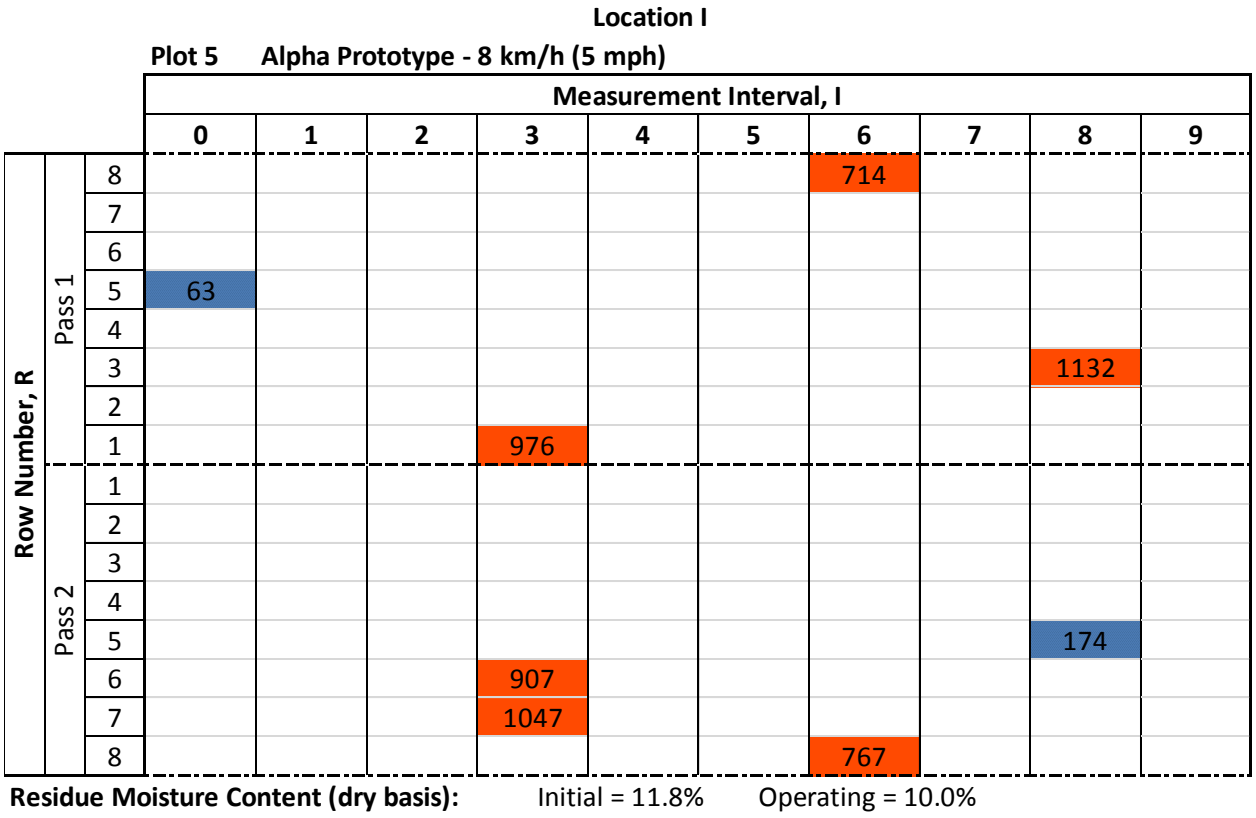

Figure A.5. Plot schematic for Plot 5 at Location I showing the initial and final residue mass measurement locations in orange and blue, respectively. The total wet mass of residue (g) measured in each sampling area is shown in its respective cell. The initial, operating and final residue moisture contents were used to convert the wet mass measurements to dry mass of residue for the orange, blue-speckled, and solid blue sampling areas, respectively.

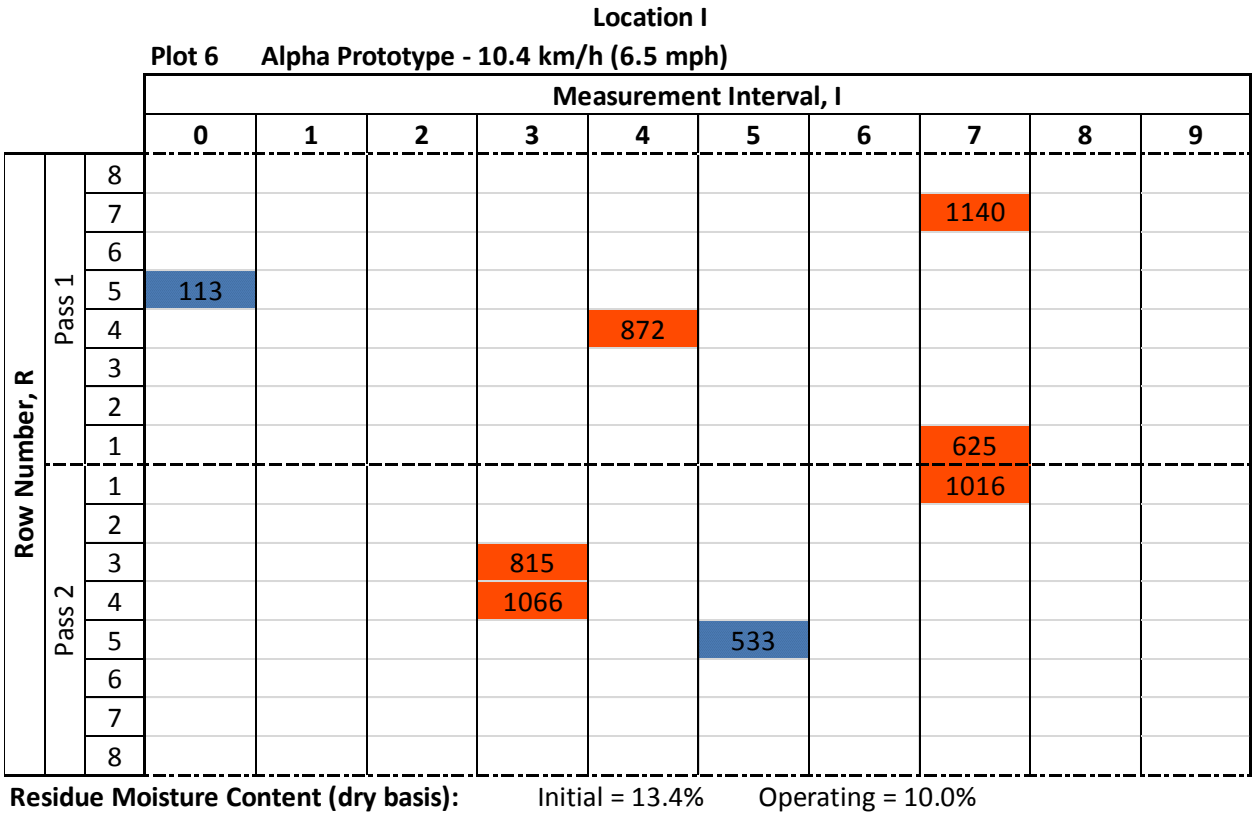

Figure A.6. Plot schematic for Plot 6 at Location I showing the initial and final residue mass measurement locations in orange and blue, respectively. The total wet mass of residue (g) measured in each sampling area is shown in its respective cell. The initial, operating and final residue moisture contents were used to convert the wet mass measurements to dry mass of residue for the orange, blue-speckled, and solid blue sampling areas, respectively.

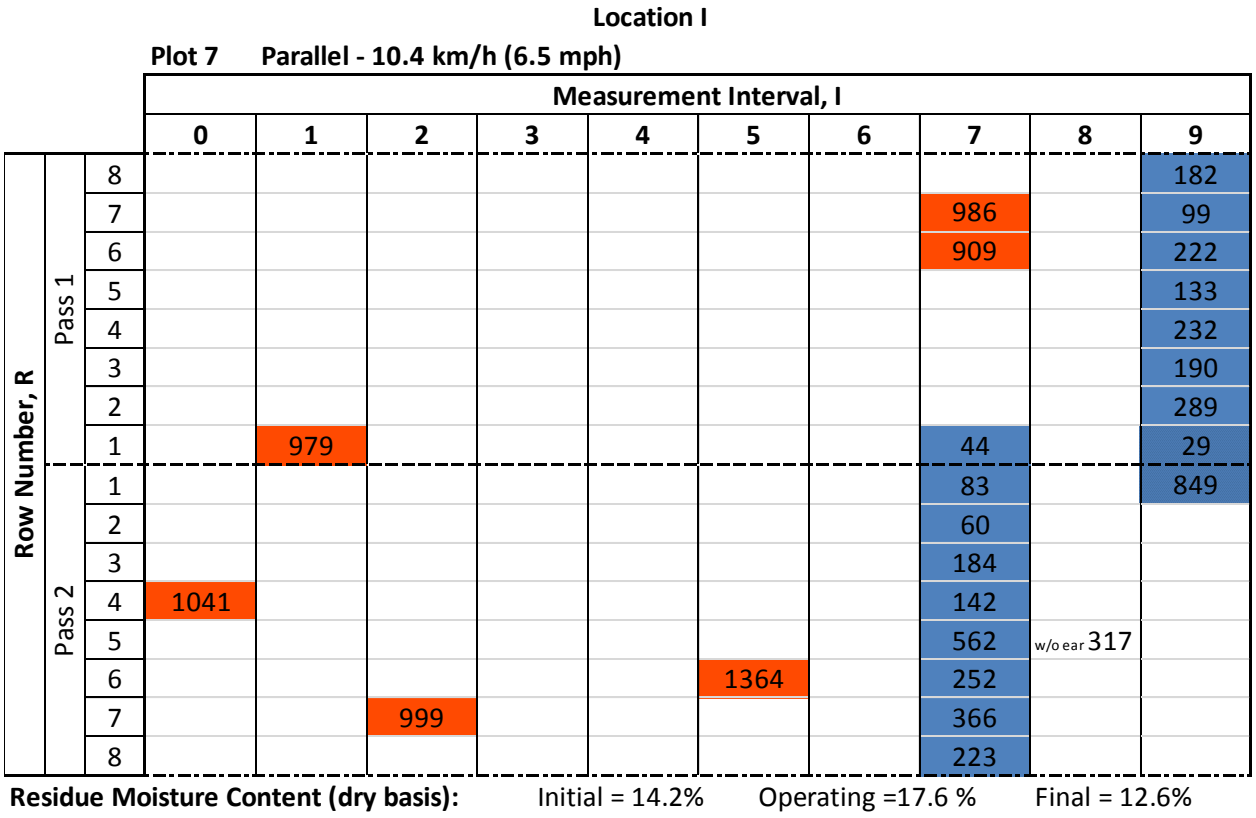

Figure A.7. Plot schematic for Plot 7 at Location I showing the initial and final residue mass measurement locations in orange and blue, respectively. The total wet mass of residue (g) measured in each sampling area is shown in its respective cell. The notation 'w/o ear' immediately adjacent to a measurement indicates the total mass of the residue excluding the ear present in the sample. The initial, operating and final residue moisture contents were used to convert the wet mass measurements to dry mass of residue for the orange, blue-speckled, and solid blue sampling areas, respectively.

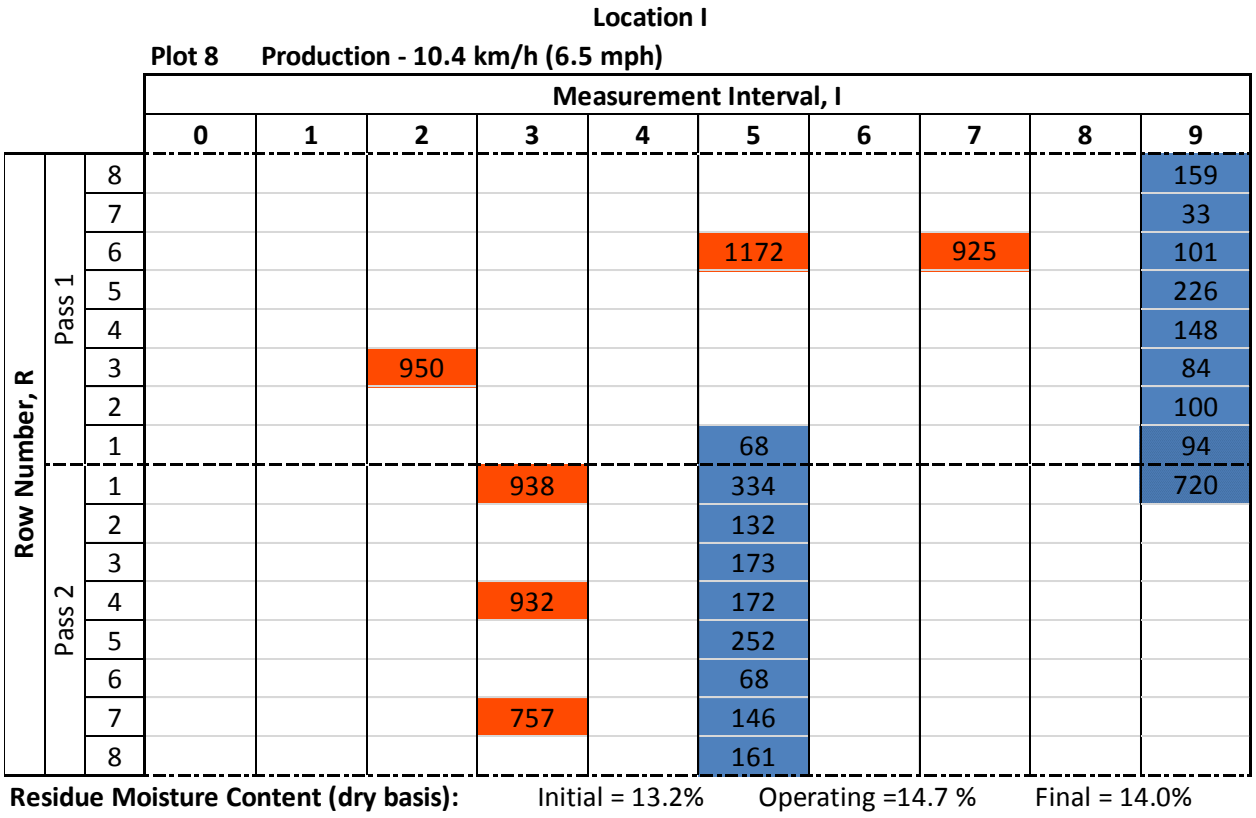

Figure A.8. Plot schematic for Plot 8 at Location I showing the initial and final residue mass measurement locations in orange and blue, respectively. The total wet mass of residue (g) measured in each sampling area is shown in its respective cell. The initial, operating and final residue moisture contents were used to convert the wet mass measurements to dry mass of residue for the orange, blue-speckled, and solid blue sampling areas, respectively.

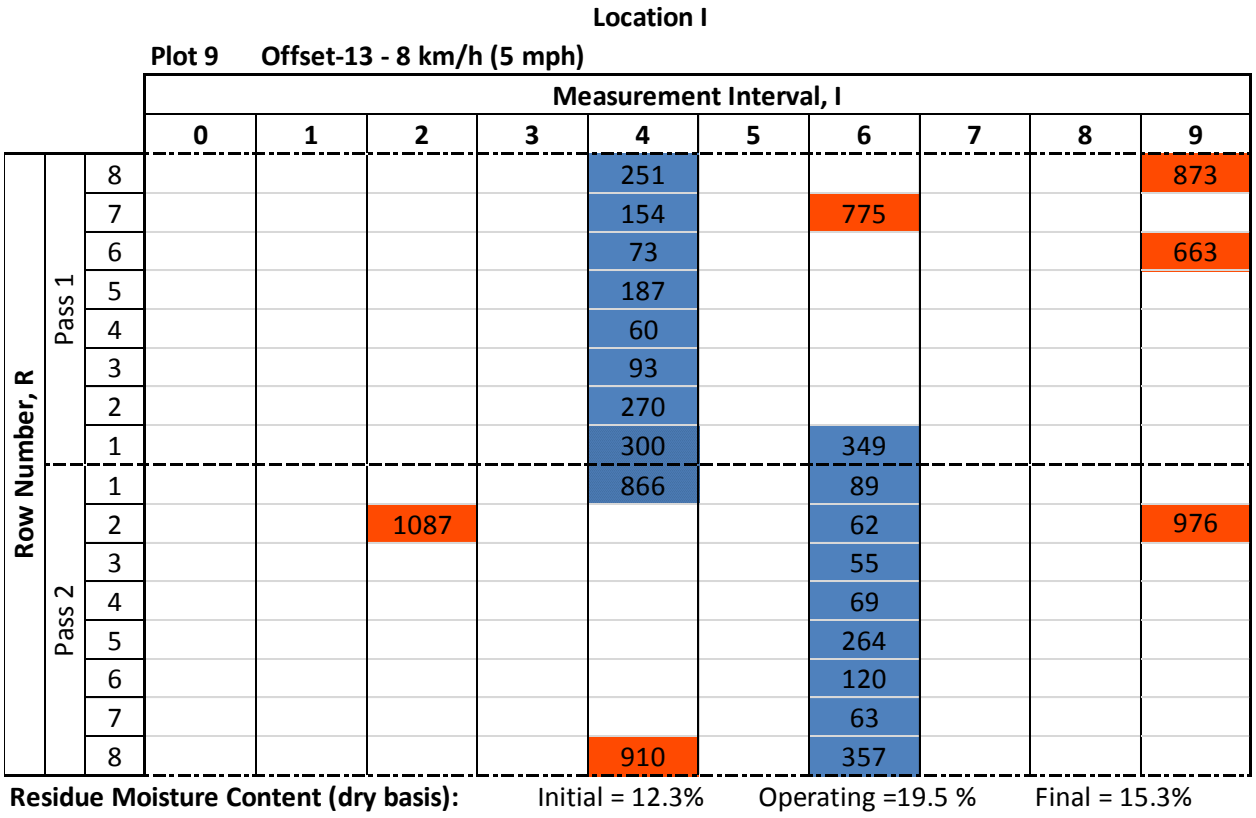

Figure A.9. Plot schematic for Plot 9 at Location I showing the initial and final residue mass measurement locations in orange and blue, respectively. The total wet mass of residue (g) measured in each sampling area is shown in its respective cell. The initial, operating and final residue moisture contents were used to convert the wet mass measurements to dry mass of residue for the orange, blue-speckled, and solid blue sampling areas, respectively.

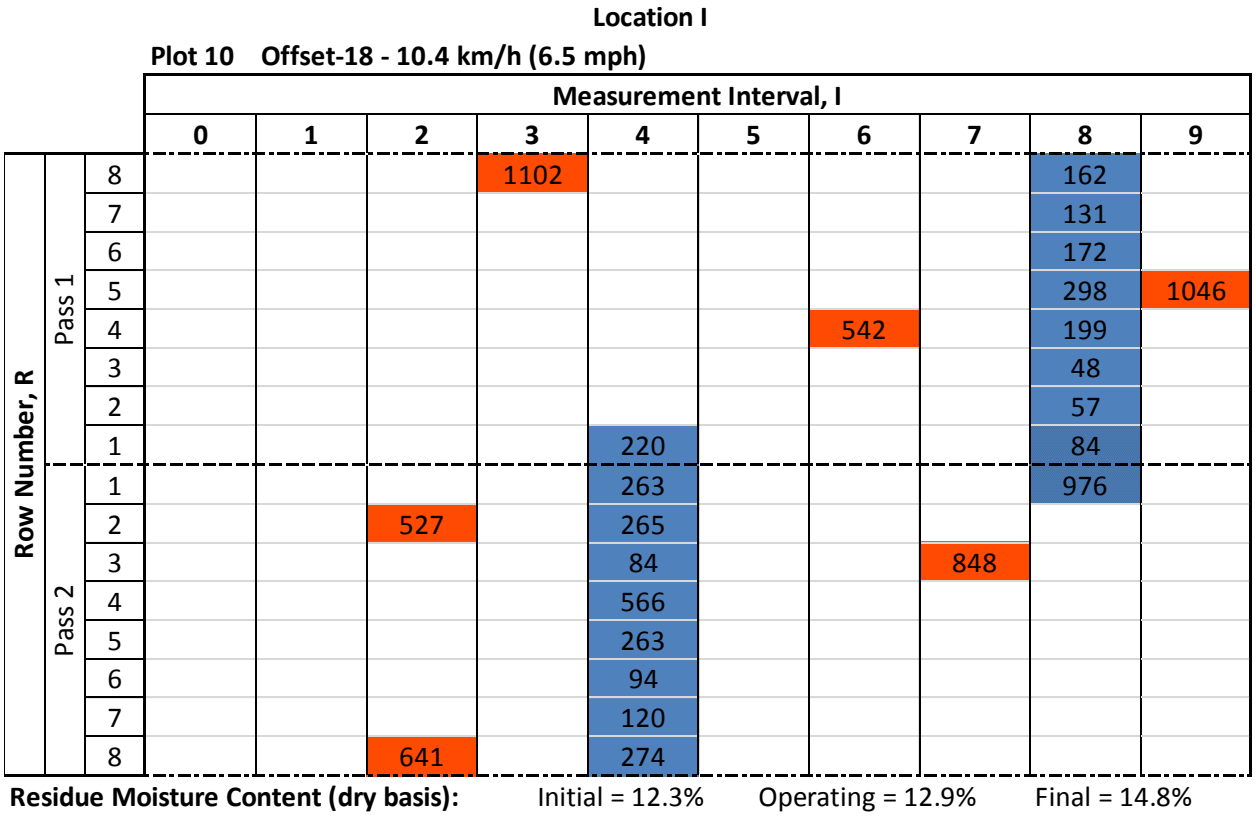

Figure A.10. Plot schematic for Plot 10 at Location I showing the initial and final residue mass measurement locations in orange and blue, respectively. The total wet mass of residue (g) measured in each sampling area is shown in its respective cell. The initial, operating and final residue moisture contents were used to convert the wet mass measurements to dry mass of residue for the orange, blue-speckled, and solid blue sampling areas, respectively.

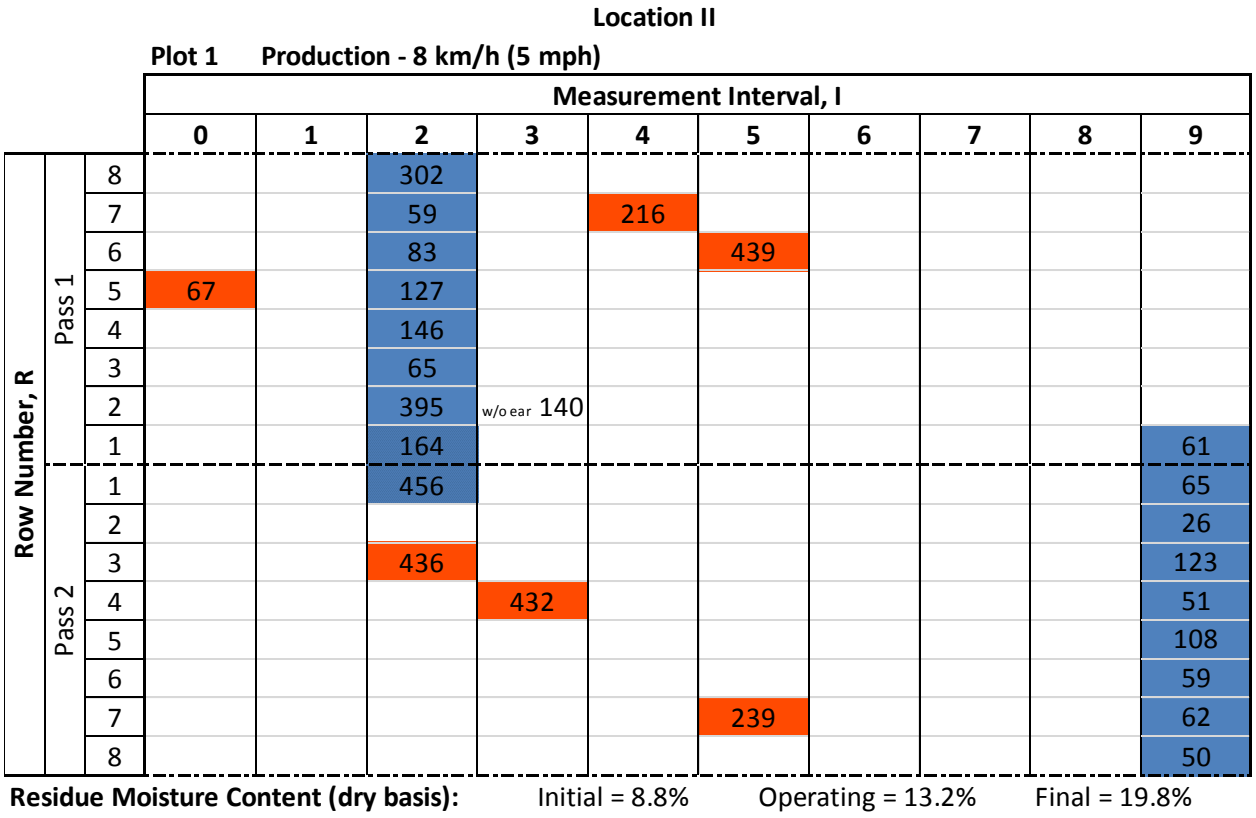

Figure A.11. Plot schematic for Plot 1 at Location II showing the initial and final residue mass measurement locations in orange and blue, respectively. The total wet mass of residue (g) measured in each sampling area is shown in its respective cell. The notation 'w/o ear' immediately adjacent to a measurement indicates the total mass of the residue excluding the ear present in the sample. The initial, operating and final residue moisture contents were used to convert the wet mass measurements to dry mass of residue for the orange, blue-speckled, and solid blue sampling areas, respectively.

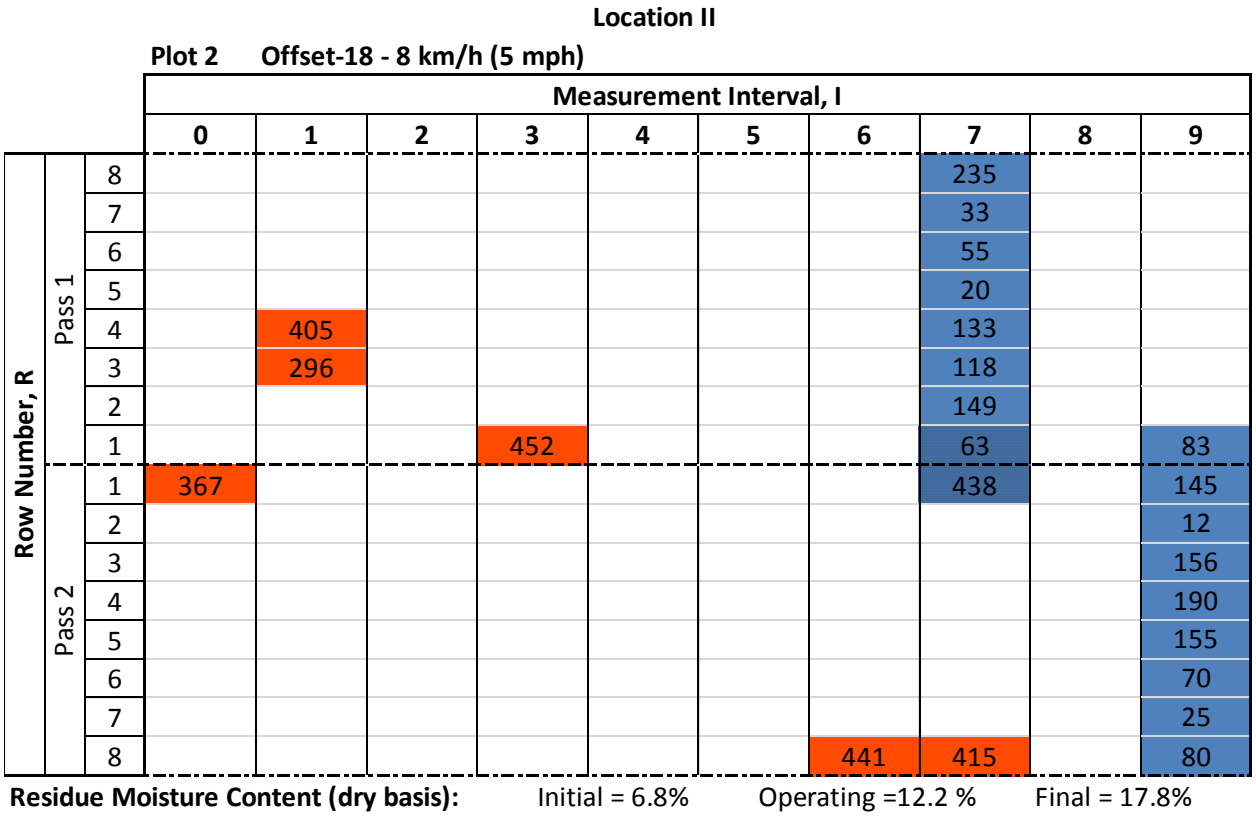

Figure A.12. Plot schematic for Plot 2 at Location II showing the initial and final residue mass measurement locations in orange and blue, respectively. The total wet mass of residue (g) measured in each sampling area is shown in its respective cell. The initial, operating and final residue moisture contents were used to convert the wet mass measurements to dry mass of residue for the orange, blue-speckled, and solid blue sampling areas, respectively.

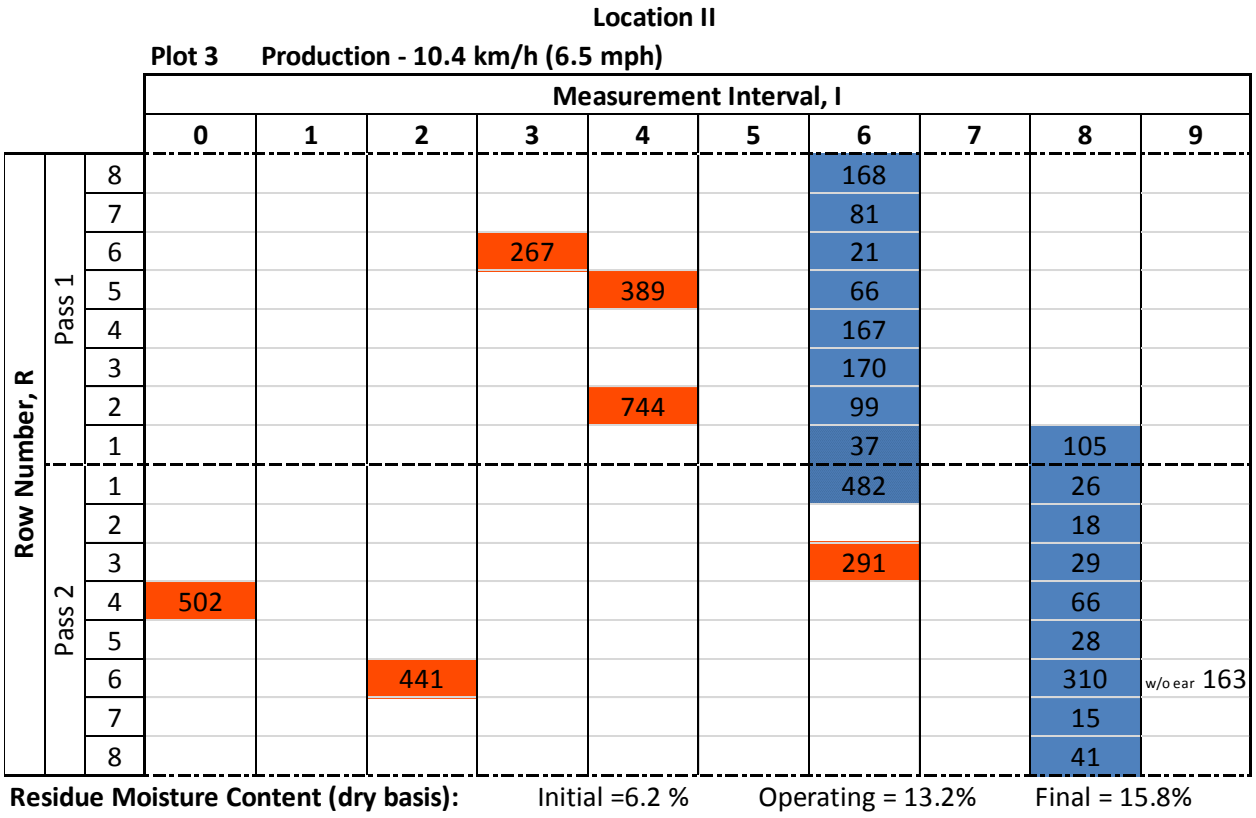

Figure A.13. Plot schematic for Plot 3 at Location II showing the initial and final residue mass measurement locations in orange and blue, respectively. The total wet mass of residue (g) measured in each sampling area is shown in its respective cell. The notation 'w/o ear' immediately adjacent to a measurement indicates the total mass of the residue excluding the ear present in the sample. The initial, operating and final residue moisture contents were used to convert the wet mass measurements to dry mass of residue for the orange, blue-speckled, and solid blue sampling areas, respectively.

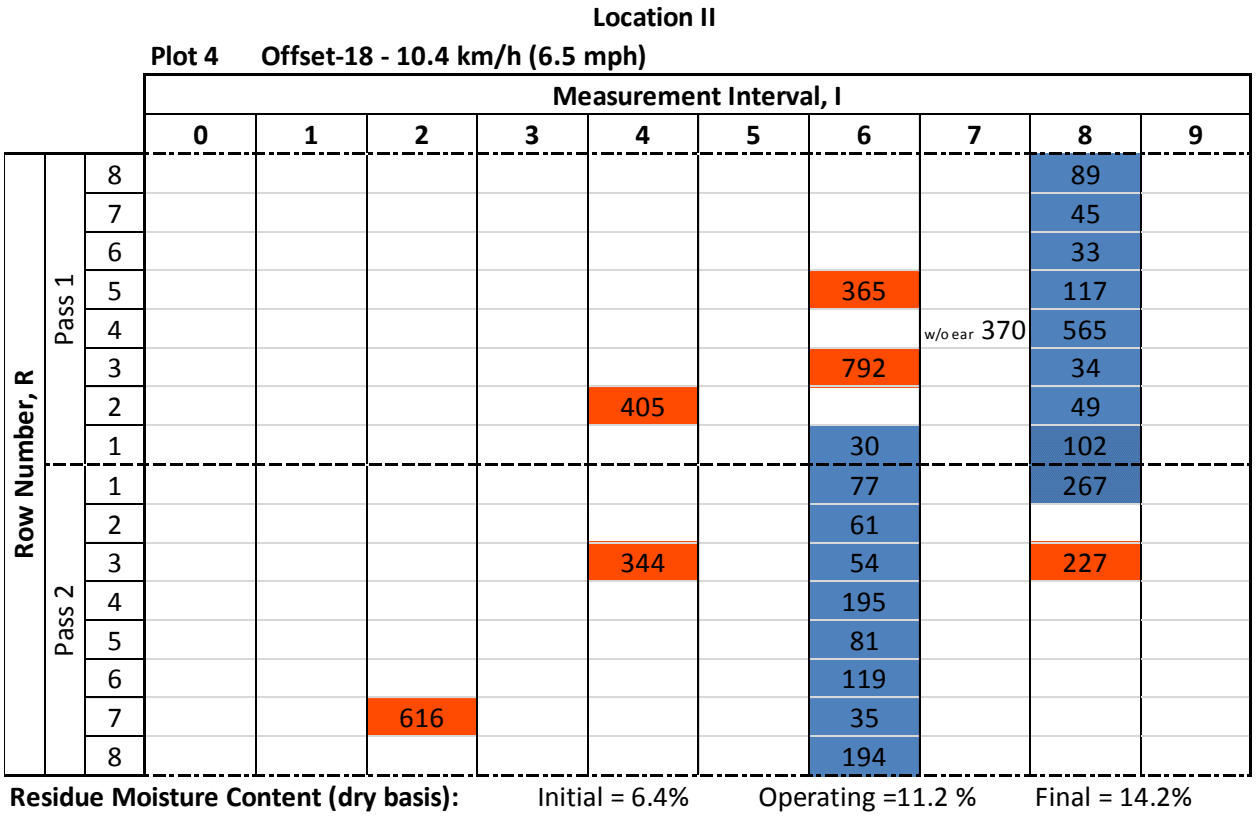

Figure A.14. Plot schematic for Plot 4 at Location II showing the initial and final residue mass measurement locations in orange and blue, respectively. The total wet mass of residue (g) measured in each sampling area is shown in its respective cell. The notation 'w/o ear' immediately adjacent to a measurement indicates the total mass of the residue excluding the ear present in the sample. The initial, operating and final residue moisture contents were used to convert the wet mass measurements to dry mass of residue for the orange, blue-speckled, and solid blue sampling areas, respectively.

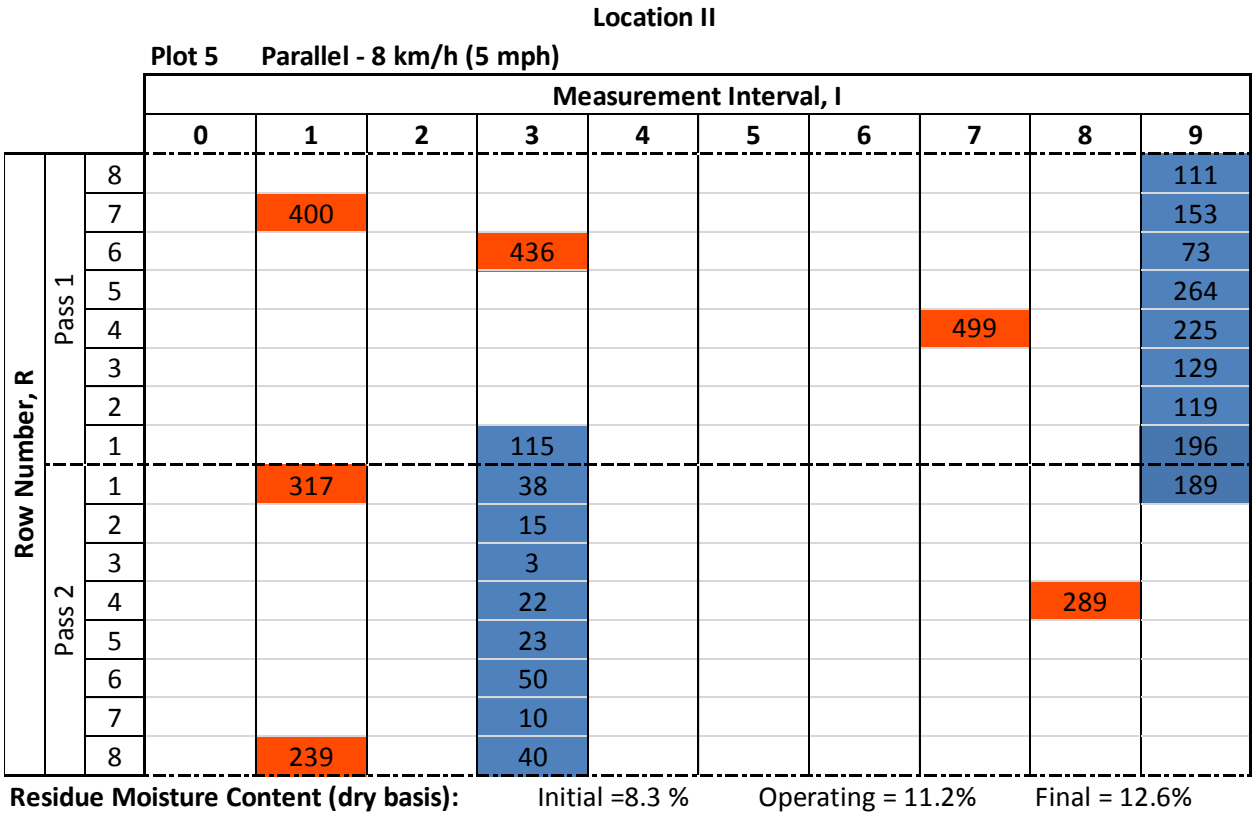

Figure A.15. Plot schematic for Plot 5 at Location II showing the initial and final residue mass measurement locations in orange and blue, respectively. The total wet mass of residue (g) measured in each sampling area is shown in its respective cell. The initial, operating and final residue moisture contents were used to convert the wet mass measurements to dry mass of residue for the orange, blue-speckled, and solid blue sampling areas, respectively.

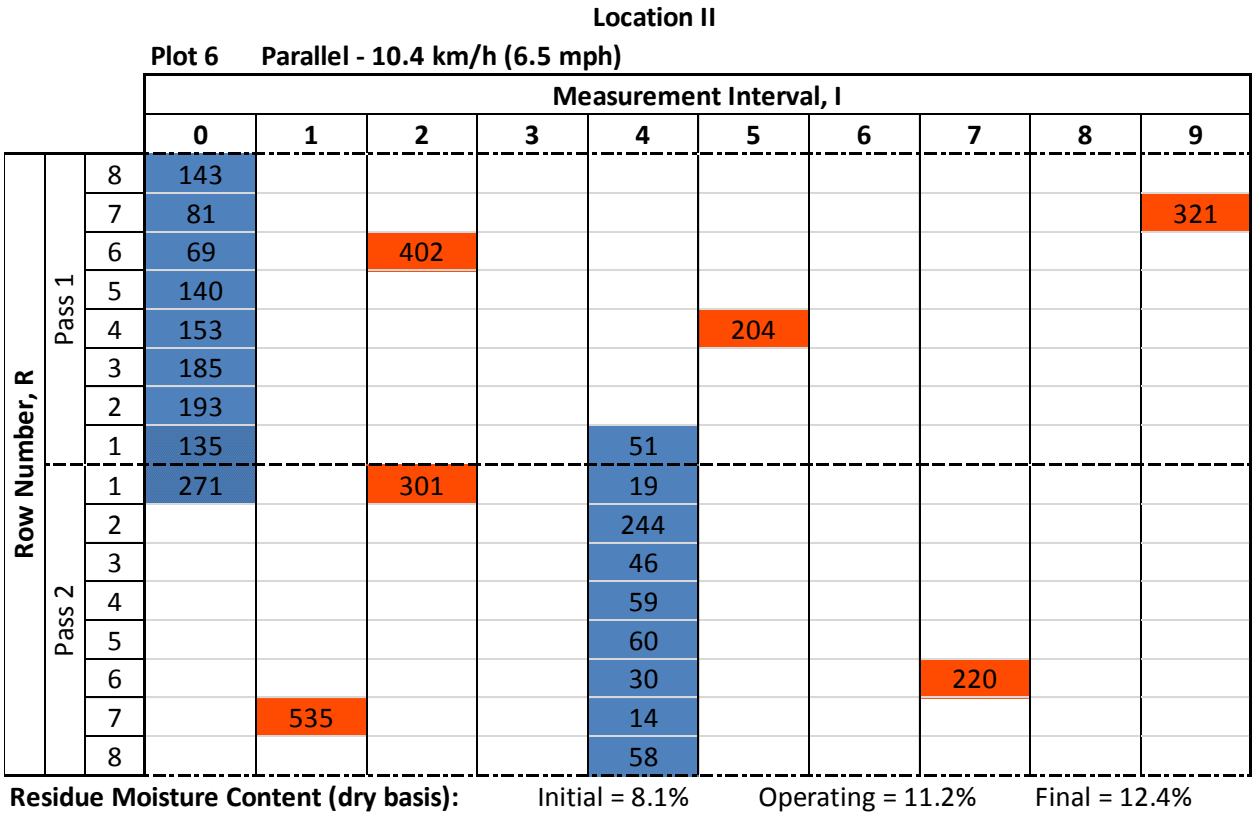

Figure A.16. Plot schematic for Plot 6 at Location II showing the initial and final residue mass measurement locations in orange and blue, respectively. The total wet mass of residue (g) measured in each sampling area is shown in its respective cell. The initial, operating and final residue moisture contents were used to convert the wet mass measurements to dry mass of residue for the orange, blue-speckled, and solid blue sampling areas, respectively.

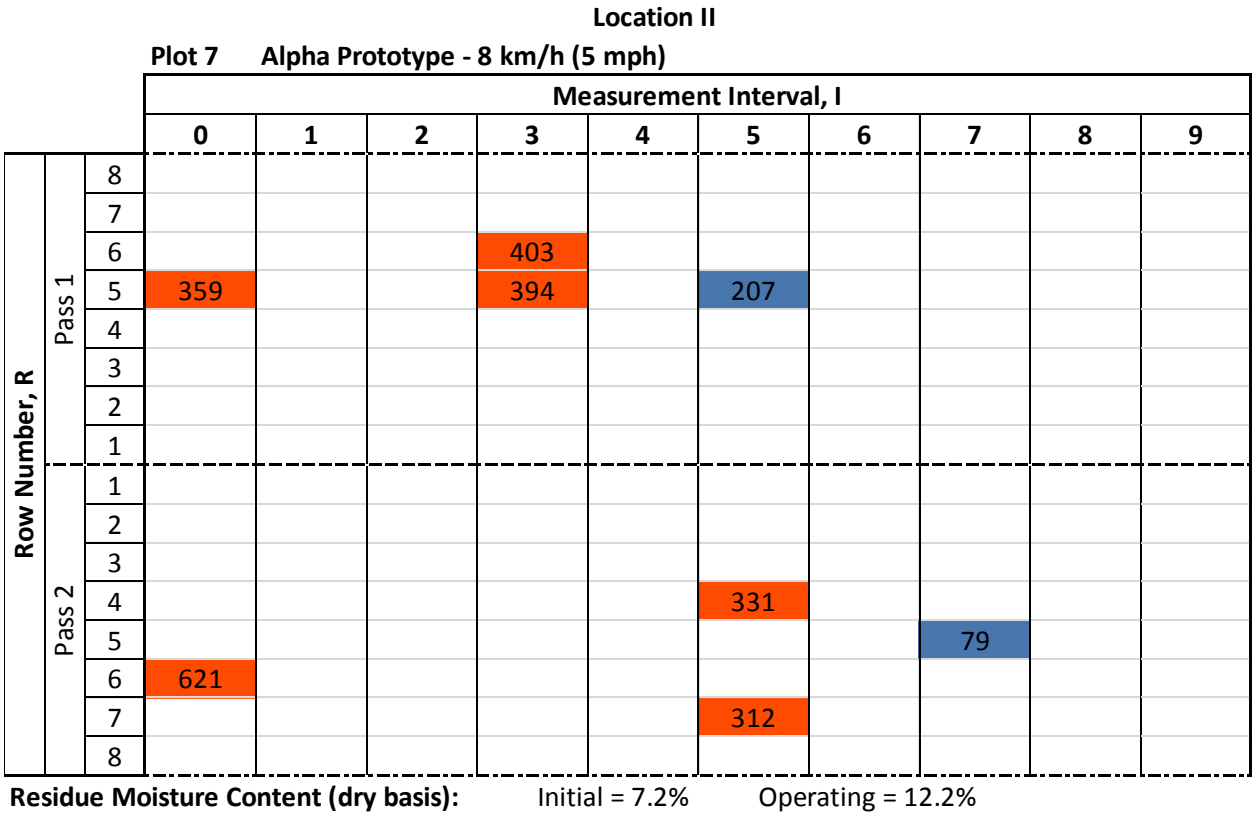

Figure A.17. Plot schematic for Plot 7 at Location II showing the initial and final residue mass measurement locations in orange and blue, respectively. The total wet mass of residue (g) measured in each sampling area is shown in its respective cell. The initial, operating and final residue moisture contents were used to convert the wet mass measurements to dry mass of residue for the orange, blue-speckled, and solid blue sampling areas, respectively.

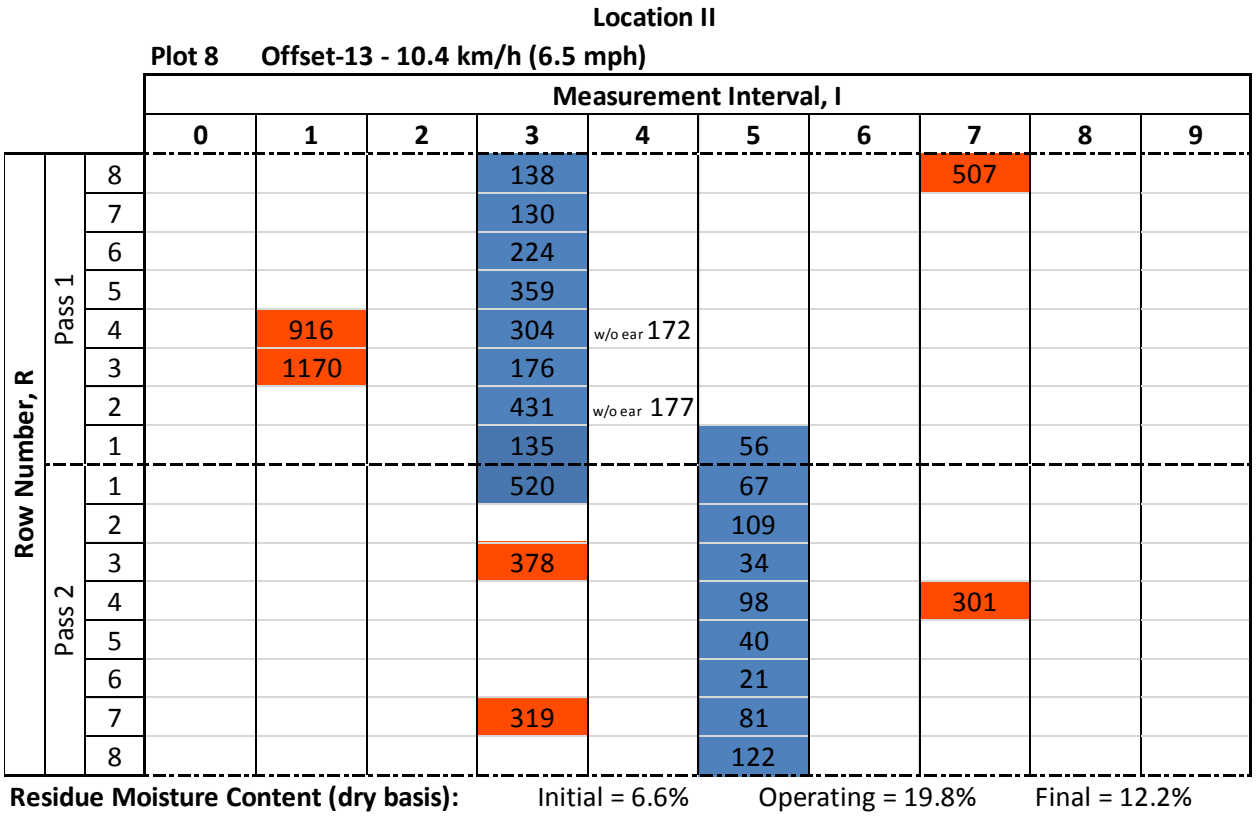

Figure A.18. Plot schematic for Plot 8 at Location II showing the initial and final residue mass measurement locations in orange and blue, respectively. The total wet mass of residue (g) measured in each sampling area is shown in its respective cell. The notation 'w/o ear' immediately adjacent to a measurement indicates the total mass of the residue excluding the ear present in the sample. The initial, operating and final residue moisture contents were used to convert the wet mass measurements to dry mass of residue for the orange, blue-speckled, and solid blue sampling areas, respectively.

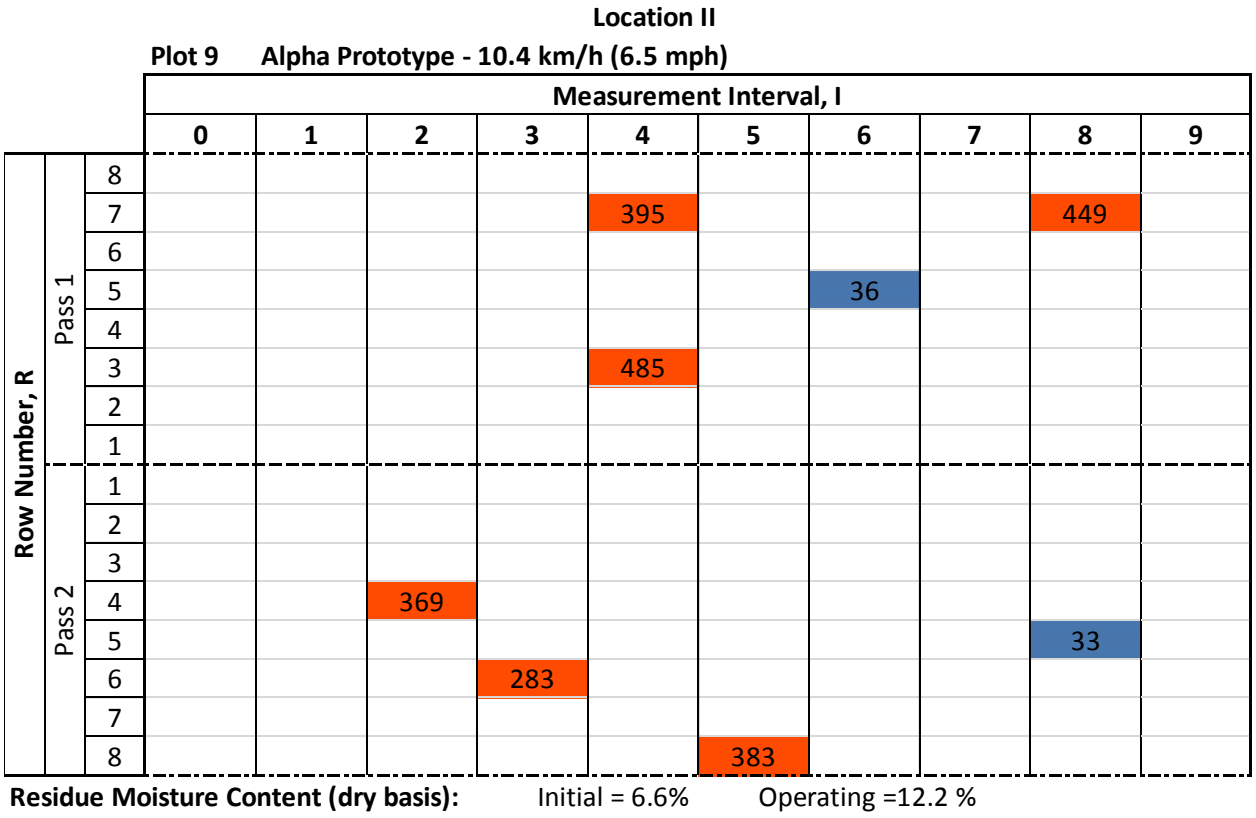

Figure A.19. Plot schematic for Plot 9 at Location II showing the initial and final residue mass measurement locations in orange and blue, respectively. The total wet mass of residue (g) measured in each sampling area is shown in its respective cell. The initial, operating and final residue moisture contents were used to convert the wet mass measurements to dry mass of residue for the orange, blue-speckled, and solid blue sampling areas, respectively.

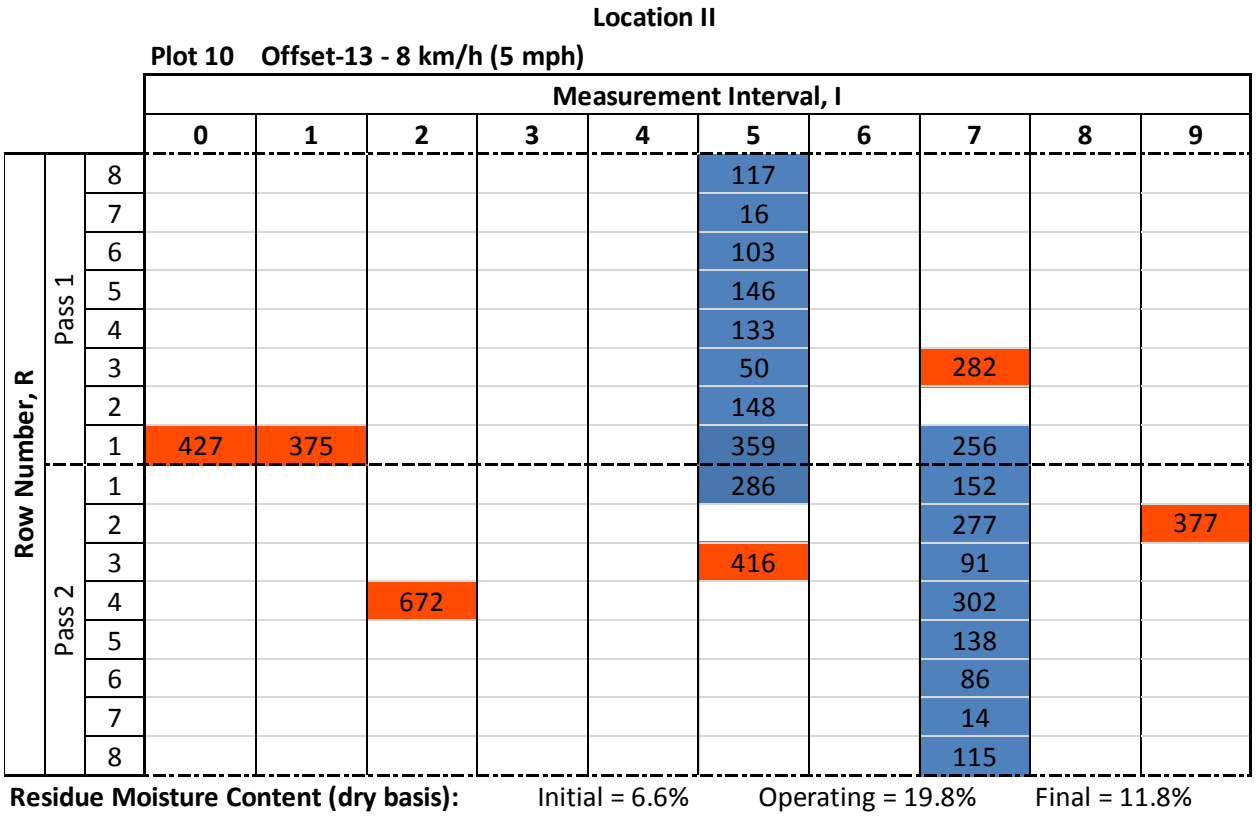

Figure A.20. Plot schematic for Plot 10 at Location II showing the initial and final residue mass measurement locations in orange and blue, respectively. The total wet mass of residue (g) measured in each sampling area is shown in its respective cell. The initial, operating and final residue moisture contents were used to convert the wet mass measurements to dry mass of residue for the orange, blue-speckled, and solid blue sampling areas, respectively.

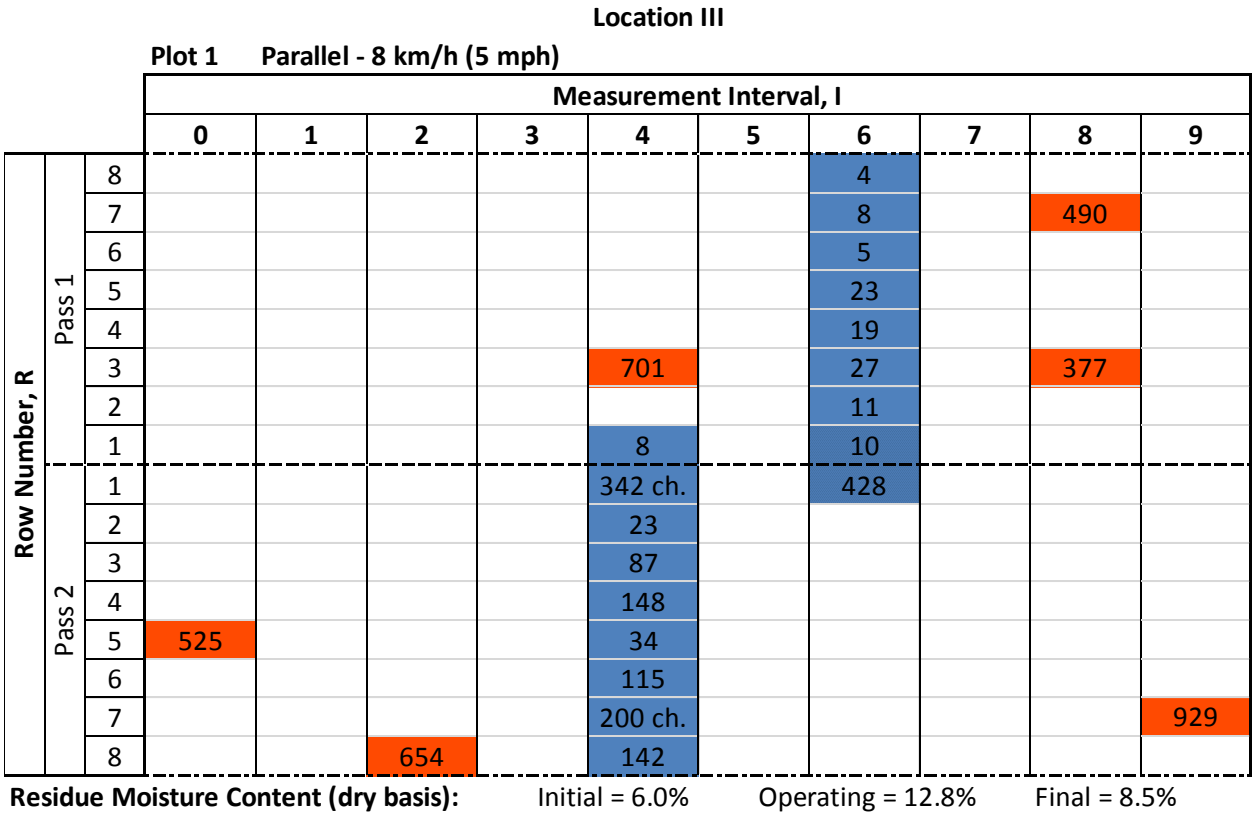

Figure A.21. Plot schematic for Plot 1 at Location III showing the initial and final residue mass measurement locations in orange and blue, respectively. The total wet mass of residue (g) measured in each sampling area is shown in its respective cell. The notation 'ch.' indicates that there was an excessive chaff layer present amongst the residue layer. The initial, operating and final residue moisture contents were used to convert the wet mass measurements to dry mass of residue for the orange, blue-speckled, and solid blue sampling areas, respectively.

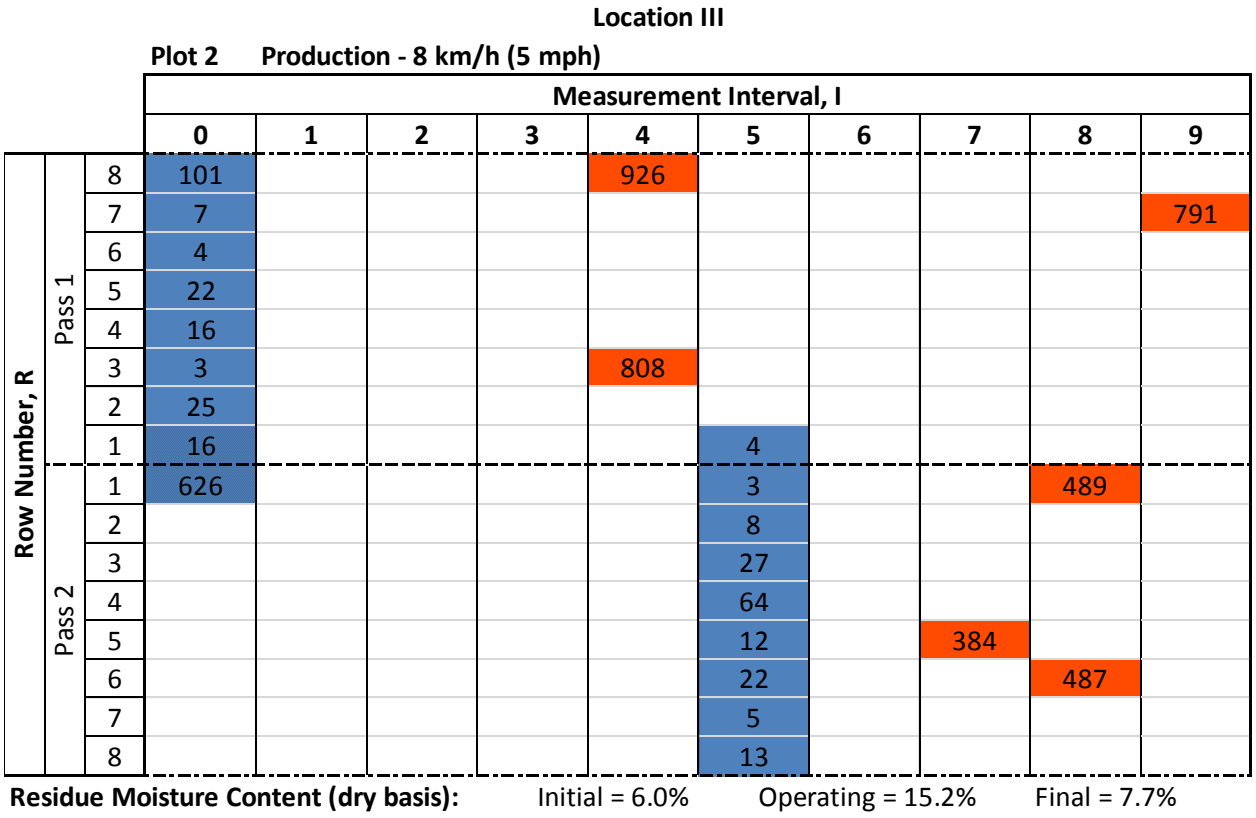

Figure A.22. Plot schematic for Plot 2 at Location III showing the initial and final residue mass measurement locations in orange and blue, respectively. The total wet mass of residue (g) measured in each sampling area is shown in its respective cell. The initial, operating and final residue moisture contents were used to convert the wet mass measurements to dry mass of residue for the orange, blue-speckled, and solid blue sampling areas, respectively.

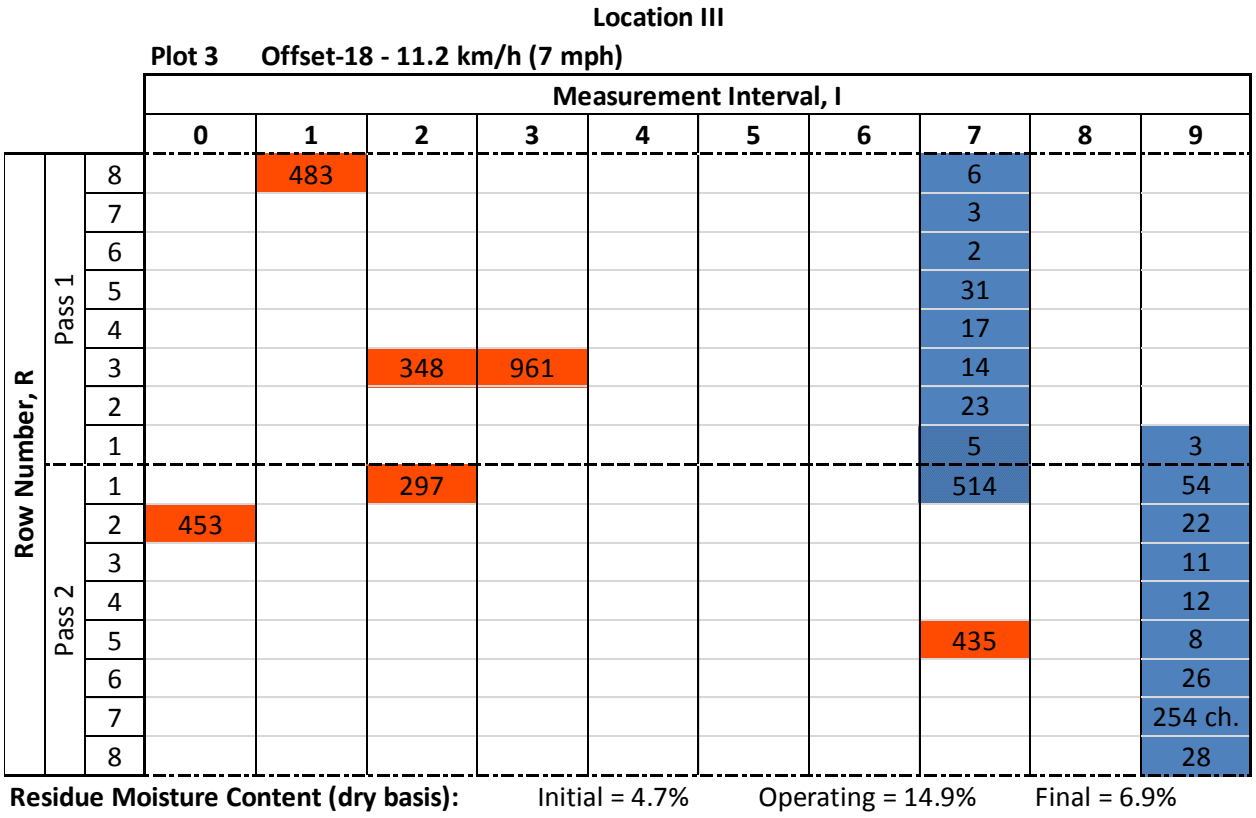

Figure A.23. Plot schematic for Plot 3 at Location III showing the initial and final residue mass measurement locations in orange and blue, respectively. The total wet mass of residue (g) measured in each sampling area is shown in its respective cell. The notation 'ch.' indicates that there was an excessive chaff layer present amongst the residue layer. The initial, operating and final residue moisture contents were used to convert the wet mass measurements to dry mass of residue for the orange, blue-speckled, and solid blue sampling areas, respectively.

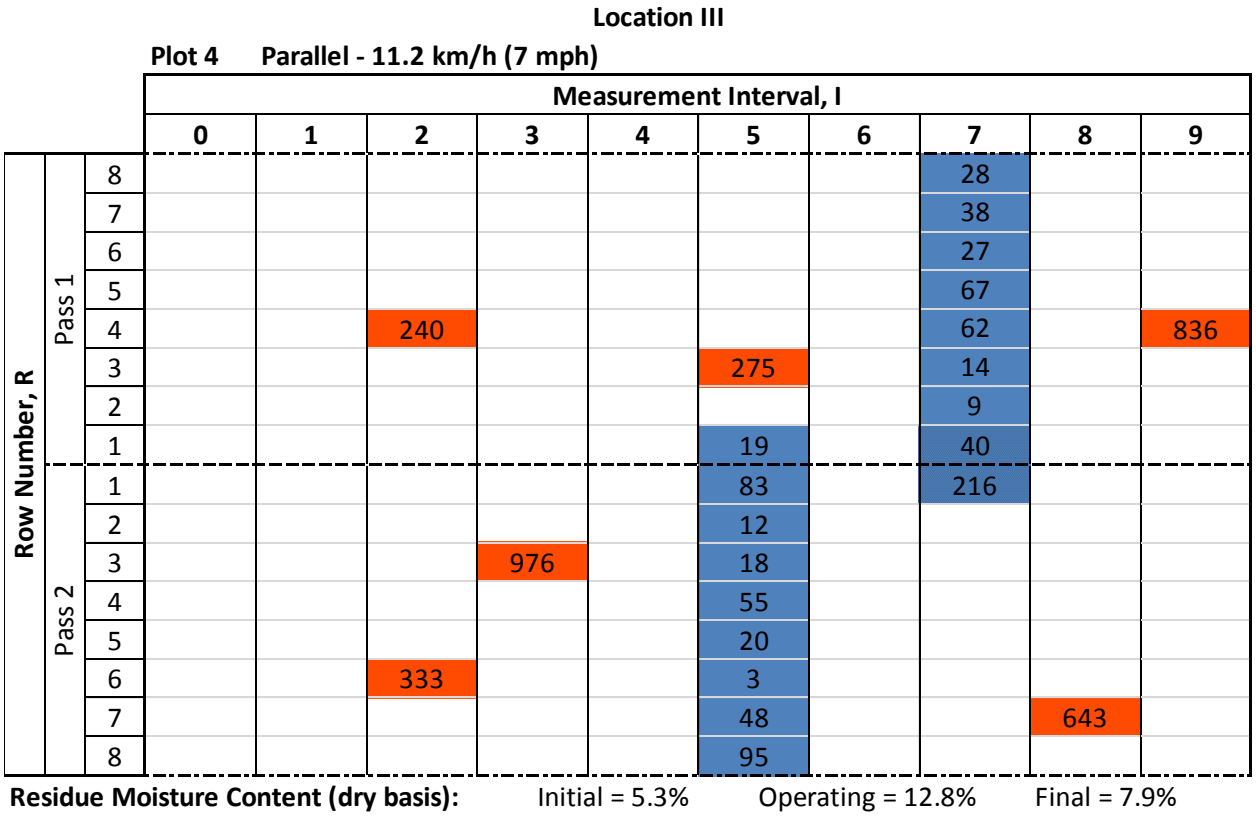

Figure A.24. Plot schematic for Plot 4 at Location III showing the initial and final residue mass measurement locations in orange and blue, respectively. The total wet mass of residue (g) measured in each sampling area is shown in its respective cell. The initial, operating and final residue moisture contents were used to convert the wet mass measurements to dry mass of residue for the orange, blue-speckled, and solid blue sampling areas, respectively.

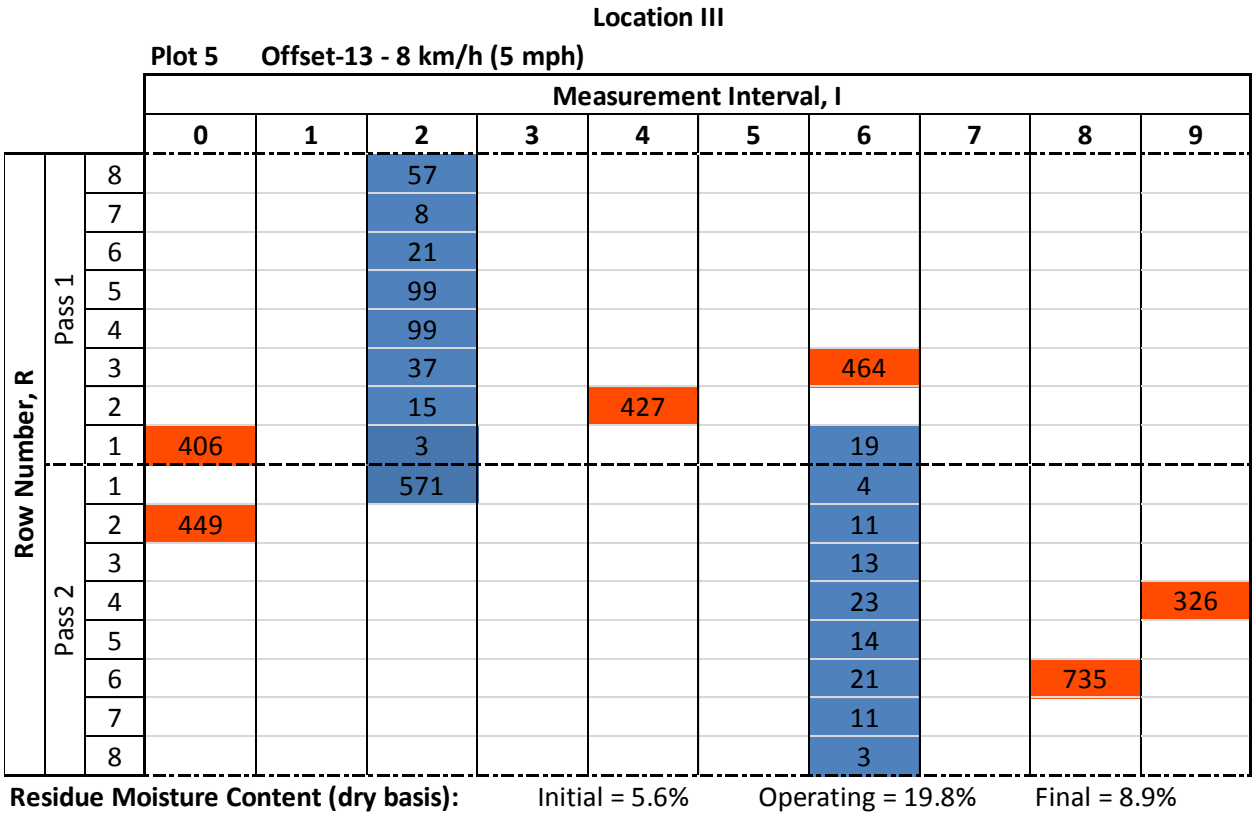

Figure A.25. Plot schematic for Plot 5 at Location III showing the initial and final residue mass measurement locations in orange and blue, respectively. The total wet mass of residue (g) measured in each sampling area is shown in its respective cell. The initial, operating and final residue moisture contents were used to convert the wet mass measurements to dry mass of residue for the orange, blue-speckled, and solid blue sampling areas, respectively.

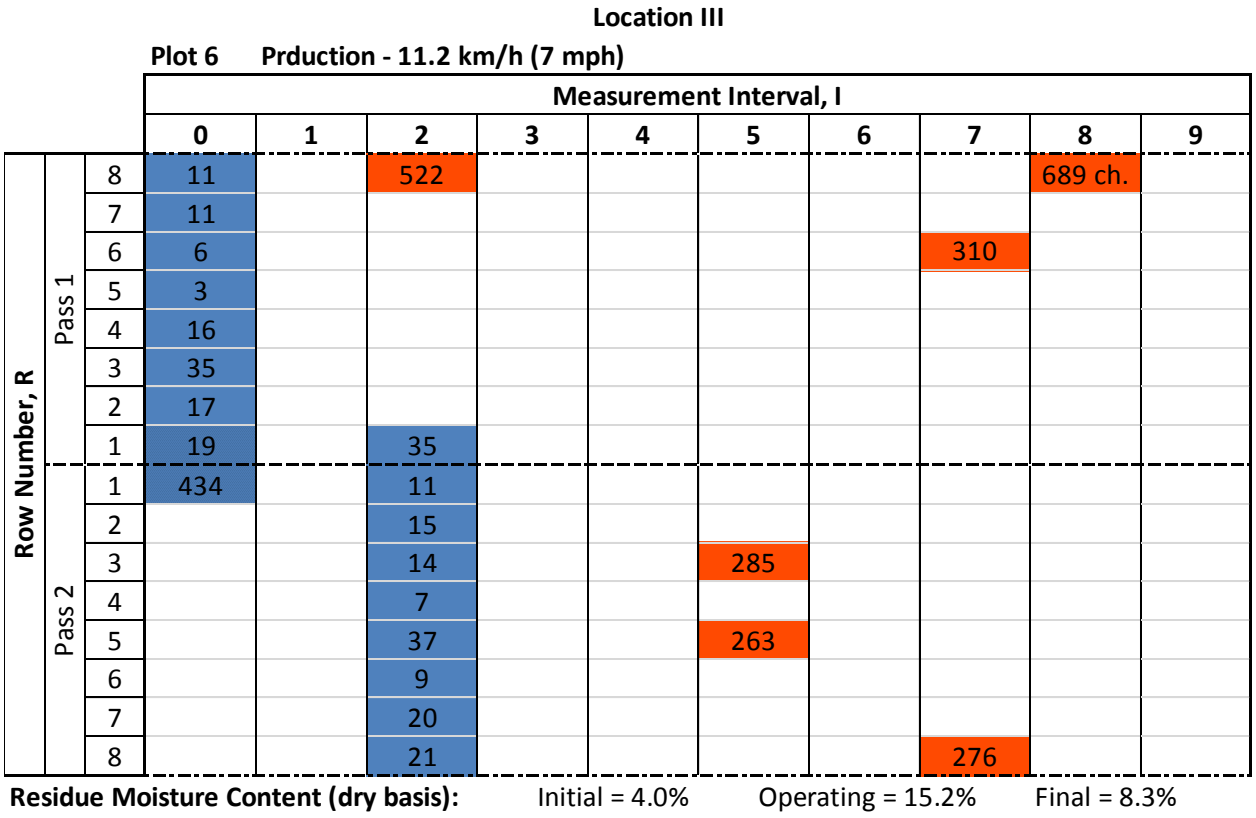

Figure A.26. Plot schematic for Plot 6 at Location III showing the initial and final residue mass measurement locations in orange and blue, respectively. The total wet mass of residue (g) measured in each sampling area is shown in its respective cell. The notation 'ch.' indicates that there was an excessive chaff layer present amongst the residue layer. The initial, operating and final residue moisture contents were used to convert the wet mass measurements to dry mass of residue for the orange, blue-speckled, and solid blue sampling areas, respectively.

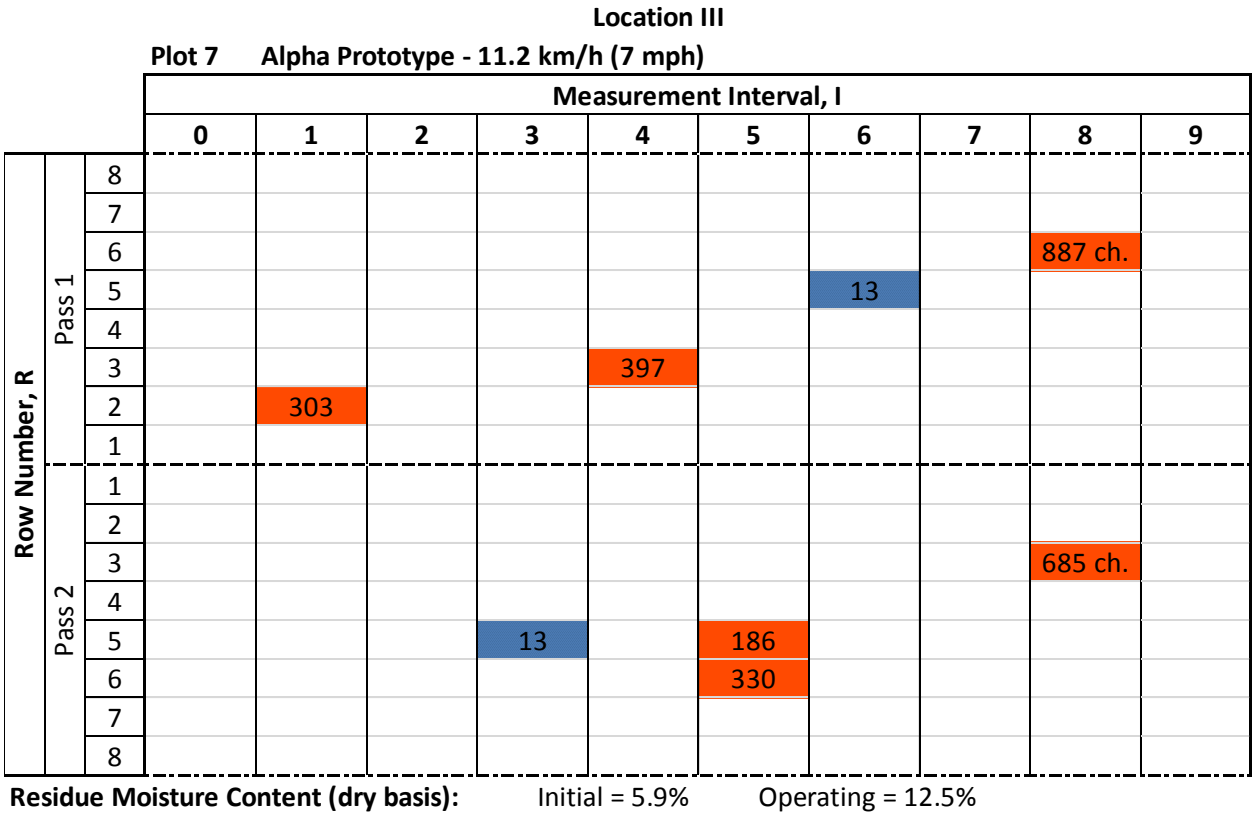

Figure A.27. Plot schematic for Plot 7 at Location III showing the initial and final residue mass measurement locations in orange and blue, respectively. The total wet mass of residue (g) measured in each sampling area is shown in its respective cell. The notation 'ch.' indicates that there was an excessive chaff layer present amongst the residue layer. The initial, operating and final residue moisture contents were used to convert the wet mass measurements to dry mass of residue for the orange, blue-speckled, and solid blue sampling areas, respectively.

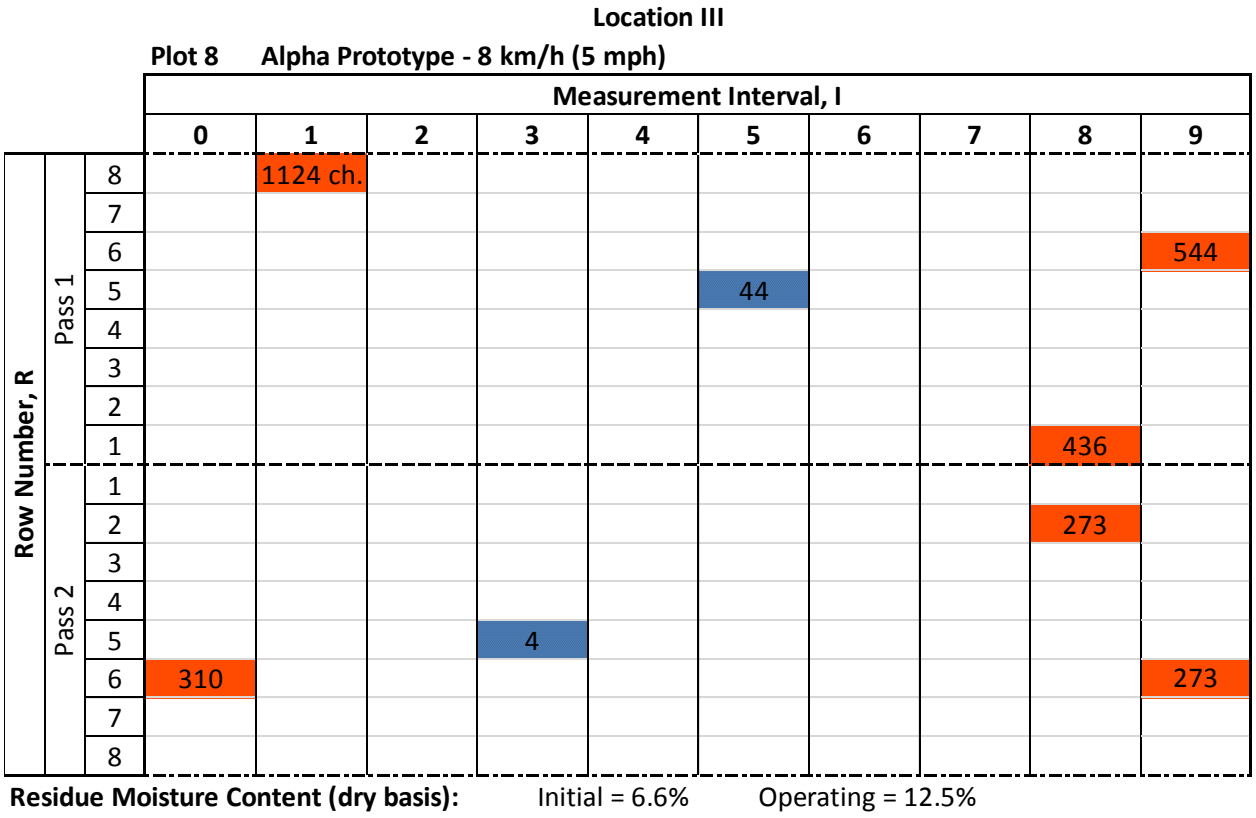

Figure A.28. Plot schematic for Plot 8 at Location III showing the initial and final residue mass measurement locations in orange and blue, respectively. The total wet mass of residue (g) measured in each sampling area is shown in its respective cell. The notation 'ch.' indicates that there was an excessive chaff layer present amongst the residue layer. The initial, operating and final residue moisture contents were used to convert the wet mass measurements to dry mass of residue for the orange, blue-speckled, and solid blue sampling areas, respectively.

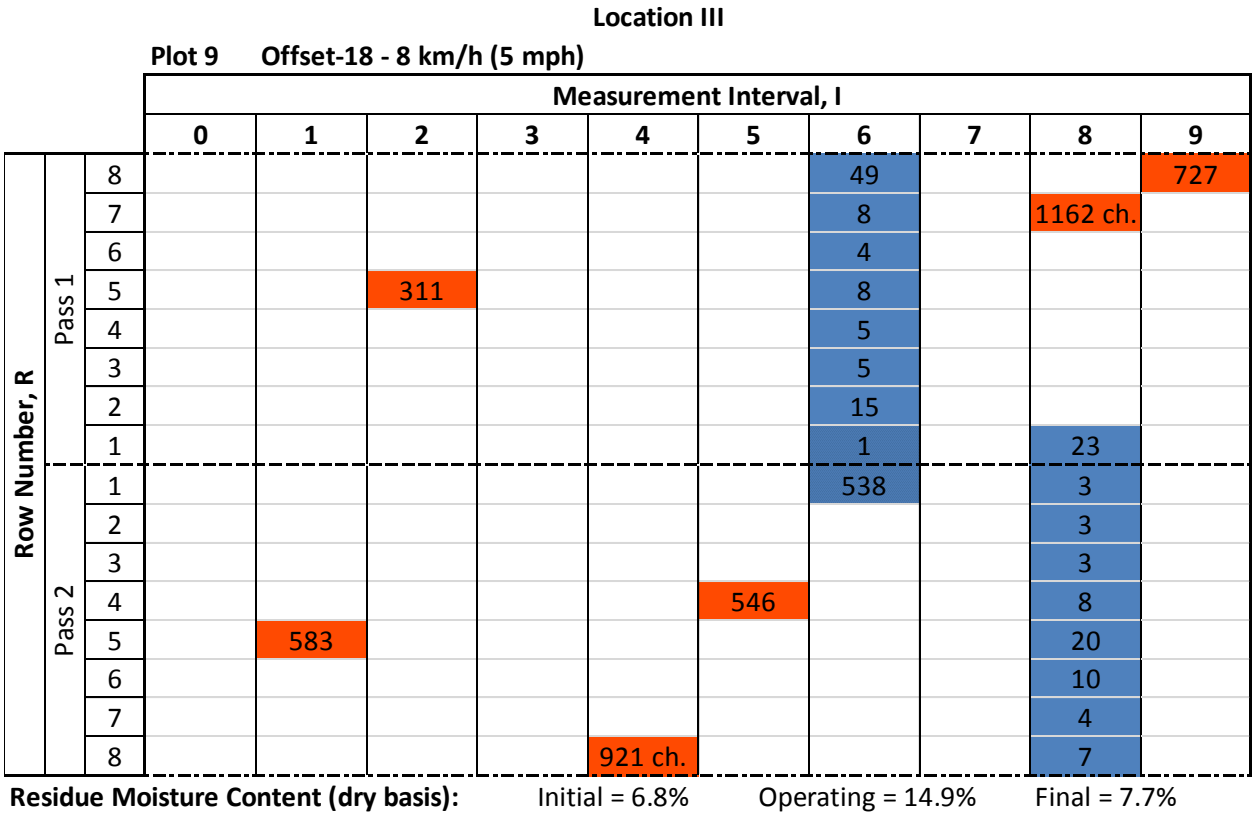

Figure A.29. Plot schematic for Plot 9 at Location III showing the initial and final residue mass measurement locations in orange and blue, respectively. The total wet mass of residue (g) measured in each sampling area is shown in its respective cell. The notation 'ch.' indicates that there was an excessive chaff layer present amongst the residue layer. The initial, operating and final residue moisture contents were used to convert the wet mass measurements to dry mass of residue for the orange, blue-speckled, and solid blue sampling areas, respectively.

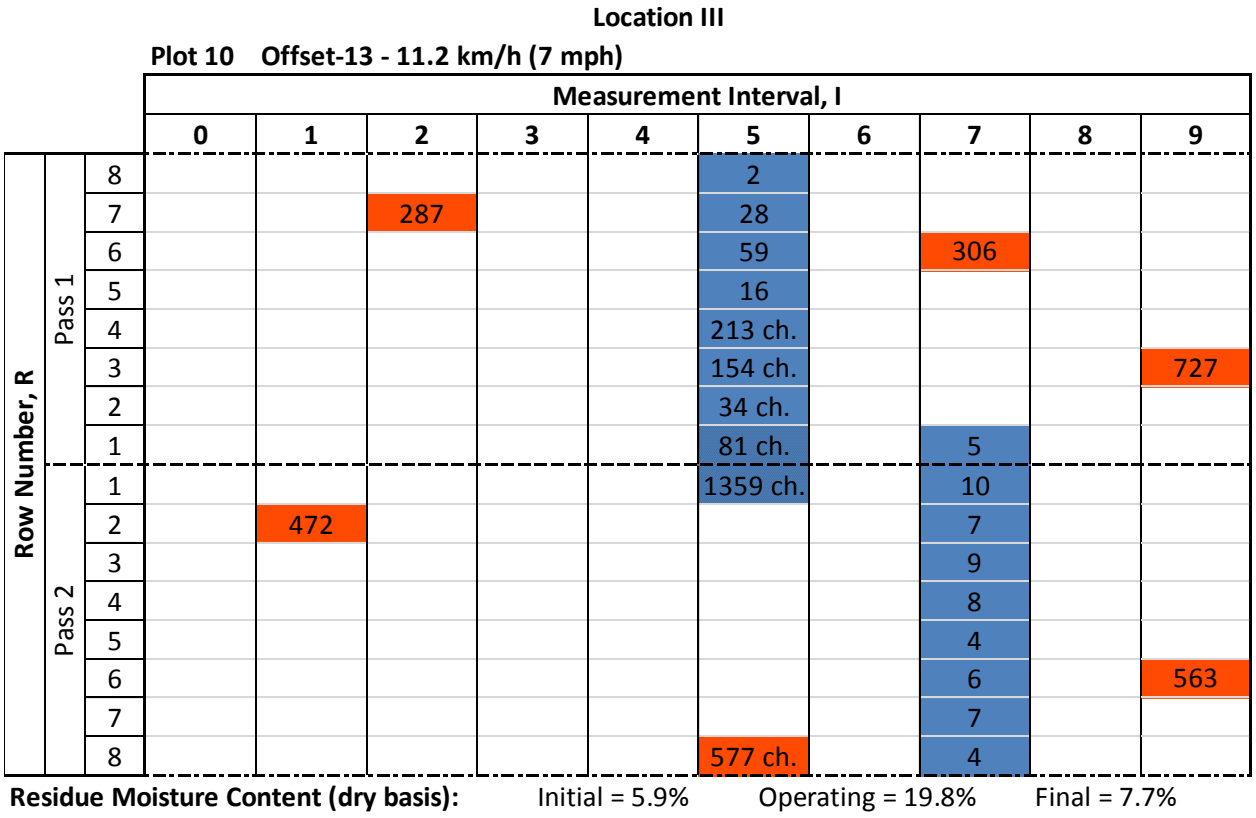

Figure A.30. Plot schematic for Plot 10 at Location III showing the initial and final residue mass measurement locations in orange and blue, respectively. The total wet mass of residue (g) measured in each sampling area is shown in its respective cell. The notation 'ch.' indicates that there was an excessive chaff layer present amongst the residue layer. The initial, operating and final residue moisture contents were used to convert the wet mass measurements to dry mass of residue for the orange, blue-speckled, and solid blue sampling areas, respectively.

APPENDIX B – R© CODE USED IN STATISTICAL ANALYSIS

This appendix contains the programming code that was implemented in R© to analyze the cleaning performance data collected during the experiment. The code used to implement the mixed model is provided first, followed by the code to extract the values of the whiskers on the box-and-whisker plots in the results section of the report.

B.1 R© code used in the mixed model to test for difference in mean performance

```
#-------------------- MASTER'S PROJECT CODE ---------- Ryan Roberge

#import the data

detach(Prodata)
Prodata <- read.table("C://Users/Ryan/Desktop/Master's Documents/Project Statistics/Corn datasets/corntotalnoalpha.txt",header=T,sep="\t", quote="")

#associate the data to a workspace and display it to confirm importation:
attach(Prodata)
names(Prodata)
list(Prodata)

#create a factor variable for Oper.MC and for Speed:
facOper.MC <- factor(Oper.MC)
facSpeed <- factor(Speed)

#-----------------------------------------------------
#setting up the Trellis parameters to better portray the graph

trellis.par.set(list(axis.text = list(cex = 2), par.ylab.text = list(cex = 2), par.xlab.text = list(cex = 2)))
trellis.par.set(list(box.rectangle = list(col="black"))) #changes box on plots to black color ->was a type of blue "#0080ff"
trellis.par.set(list(box.umbrella = list(col="black"))) #changes whiskers on plots to black color
trellis.par.set(list(plot.symbol = list(col="black"))) #changes the outliers on the plots to black
trellis.par.set(list(add.text = list(cex=2))) #changes the size of the text for the secondary and tertiary factors listed in the bands
```

```
par(mar=c(7,7.5,4,2)+0.1) #configures the position of the plot
par(mgp=c(5,1.5,0))  #spaces out the axis labels and axis titles

#Using the Trellis library to give a 2x2 series of charts giving performance vs. configuration for each orientation at each speed

bwplot(Performance~Configuration | Orientation*factor(Speed), xlab="Configuration", ylab="Cleaning Performance (dimensionless)",cex.lab=2.5,cex.axis=2,las=1,ylim = c(-0.1,1.1))
bwplot(Performance~Configuration | Orientation*factor(Speed), xlab="Configuration", ylab="Cleaning Performance (dimensionless)",cex.lab=2.5,cex.axis=2,las=1)
bwplot(Performance~Configuration | factor(Speed), xlab="Configuration", ylab="Cleaning Performance (dimensionless)",cex.lab=2.5,cex.axis=2,las=1)
bwplot(Performance~Configuration | Orientation, xlab="Configuration", ylab="Cleaning Performance (dimensionless)",cex.lab=2.5,cex.axis=2,las=1)
bwplot(Performance~Configuration, xlab="Configuration", ylab="Cleaning Performance (dimensionless)",cex.lab=2.5,cex.axis=2,las=1)
bwplot(Performance~Configuration, xlab="Configuration", ylab="Cleaning Performance (dimensionless)",cex.lab=2.5,cex.axis=2,las=1)

#-----------------------------------------------------
#Check for a Normal distribution of the Response variable "Performance"

qqnorm(Performance,cex.axis=2.5,cex.lab=2.5,cex.main=2.5)
qqline(Performance)

#the result from above is not that great - perform a ln() transform to see if this improves the situation

qqnorm(invlogPerform,cex.axis=2.5,cex.lab=2.5,cex.main=2.5)
qqline(invlogPerform)

#log transform appears to fit much better than the raw data, therefore thetransformed data will be used in the analysis
```

B.2 R© code used to obtain the box-and-whisker plot data-points for performance consistency analysis

```
#---------- MASTER'S PROJECT CODE - VARIABILITY IN CORN---------- Ryan Roberge
```

```
#--------------------------ALPHA - OVERALL ----------------------------------------
#import the data

detach(Prodata)
Prodata <- read.table("C://Users/Ryan/Desktop/Master's Documents/Project Statistics/Corn datasets/by configuration/cornalpha.txt",header=T,sep="\t", quote="")

#associate the data to a workspace and display it to confirm importation:
attach(Prodata)
names(Prodata)
list(Prodata)

boxplot.stats(Performance)
#[(lower whisker bound) (first quartile/hinge) (median) (third quartile/hinge) (upper whisker bound)]

#output
0.3687410 0.6227419 0.8320415 0.9071080 0.9268312
```

APPENDIX C - Identifying Differences in Mean Performance

This appendix contains diagnostics, an explanation of the statistical results tables with an example and the complete set of results tables from the statistical analysis for mean performance. It should be noted that for continuity in this appendix sections C.1, C.2, and C.3.1 have been copied directly from the thesis body while the remaining sections host the remainder of the results tables. To exclusively view the results tables see sections C.3 and C.4 for corn and wheat stubble results, respectively.

Before the data were analyzed using R©, they were reviewed to ensure the statistical tests would yield usable results. This included checking for goodness of fit to the normal distribution.

C.1 Using a natural logarithmic transform for cleaning performance data

Before the data were analyzed using the mixed-effects model, they were reviewed to ensure the data followed a normal distribution. This was accomplished using a normal quantile-quantile plot. On this type of plot, a solid line is shown representing where the data should lie if it follows a perfect normal distribution. The data are represented by individual points on the plot. One can compare the data and various transformations thereof to visually determine whether a certain data transformation provides a better or worse fit to a normal distribution. Figure C.1 shows the raw cleaning performance data for all three field locations plotted on a quantile-quantile plot. As can be seen, the data in the middle portion follows the normal distribution line quite well, but at the lower and upper ends, the data fall well below the normal distribution line. A logarithmic transform was then applied to the data as follows,

$$invlogPerform = \ln\left(1-(Cleaning\ \ Performance)\right). \qquad \textbf{(C.1)}$$

A difference conversion was incorporated to accommodate the two negative performance values observed during the experiment. The transformed data are shown in Figure C.2. In this case the data at the lower and upper ends of the plot were much closer to the normal distribution line. Because the transformed data more closely represented a normal distribution, they were used in all statistical tests in place of the raw data.

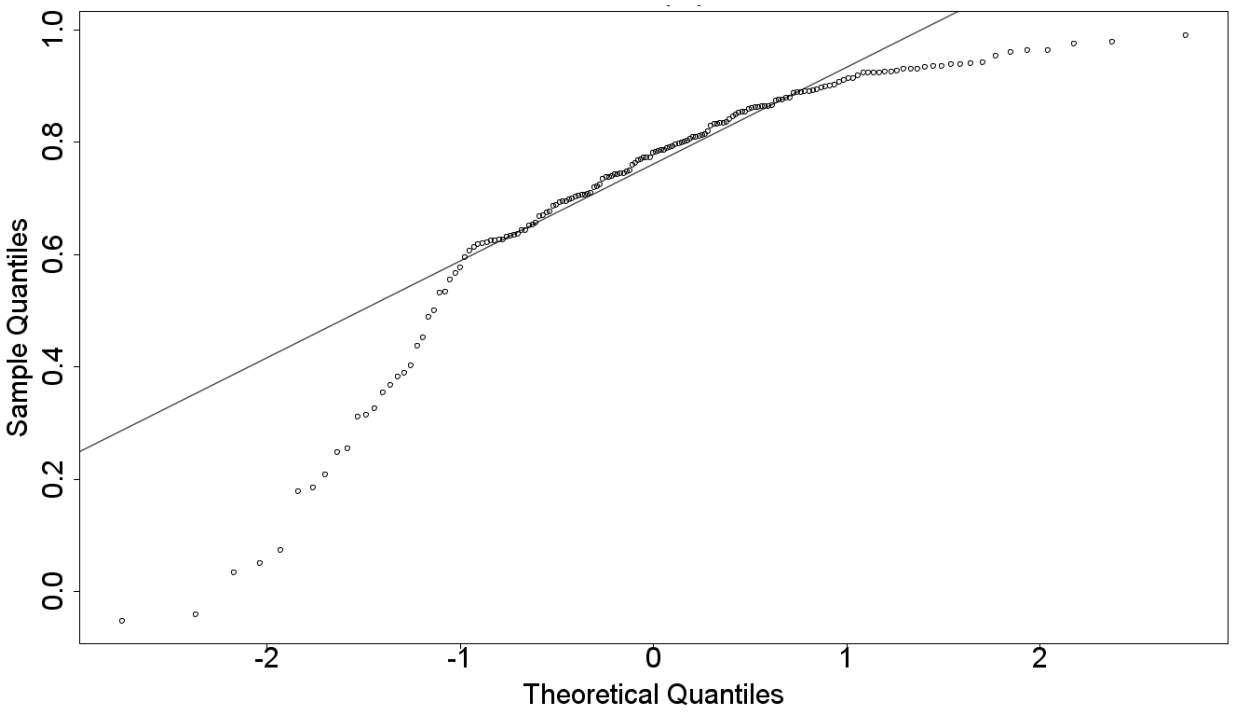

Figure C.1. Normal quantile-quantile plot of raw performance data for all three field locations.

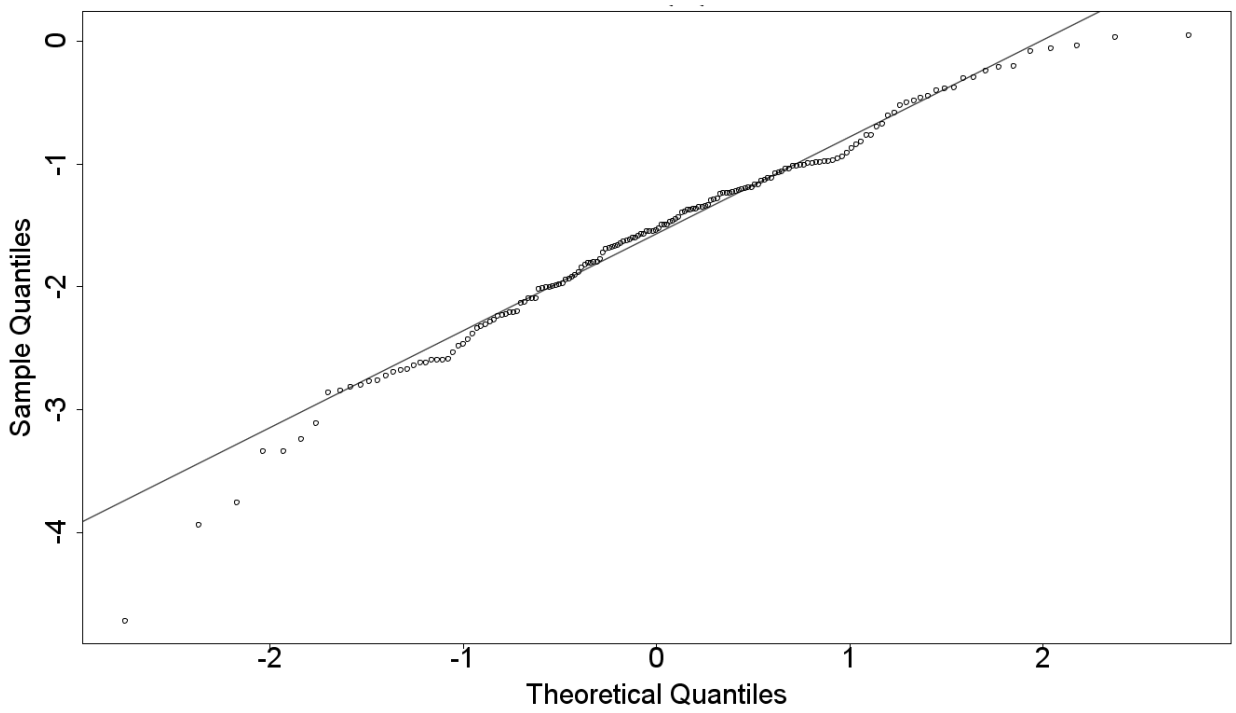

Figure C.2. Normal quantile-quantile plot of natural-logarithmic transformed data for all three field locations.

C.2 Omitting "Row" from the list of random factors

A few diagnostic tests were examined before a true analysis was performed to see whether or not the row unit number of the implement should have been included as a fourth level of nesting within the level of 'pass.' After conducting statistical tests with and without the random factor 'row,' a decision was made to omit it from the linear mixed-effects model for the reasons given below.

The first test examined was a plot of standardized residuals versus fitted values. Plots were generated for each case of including and excluding row as a random factor, examples of which are shown in Figures C.3 and C.4, respectively. In Figure C.3, a distinct linear pattern was observed as the fitted data increased in value. Alternatively, in Figure C.4, a relatively even spread of residuals above and below the y=0 axis was presented. Because a normal distribution of residuals was preferable, the model that generated Figure C.4 would be considered to be superior. Therefore with respect to this diagnostic, it was preferable for 'row' to be excluded from the random factor list.

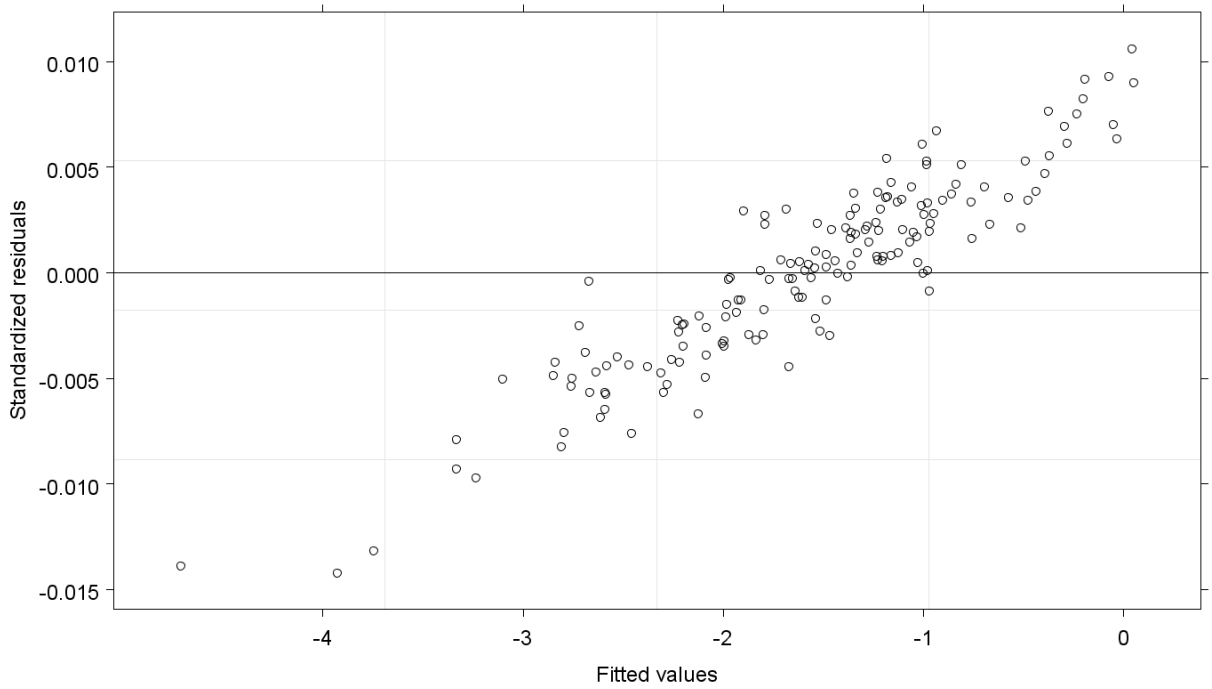

Figure C.3. Standardized residuals versus fitted values diagnostic plot for corn including "Row" in the random factor list.

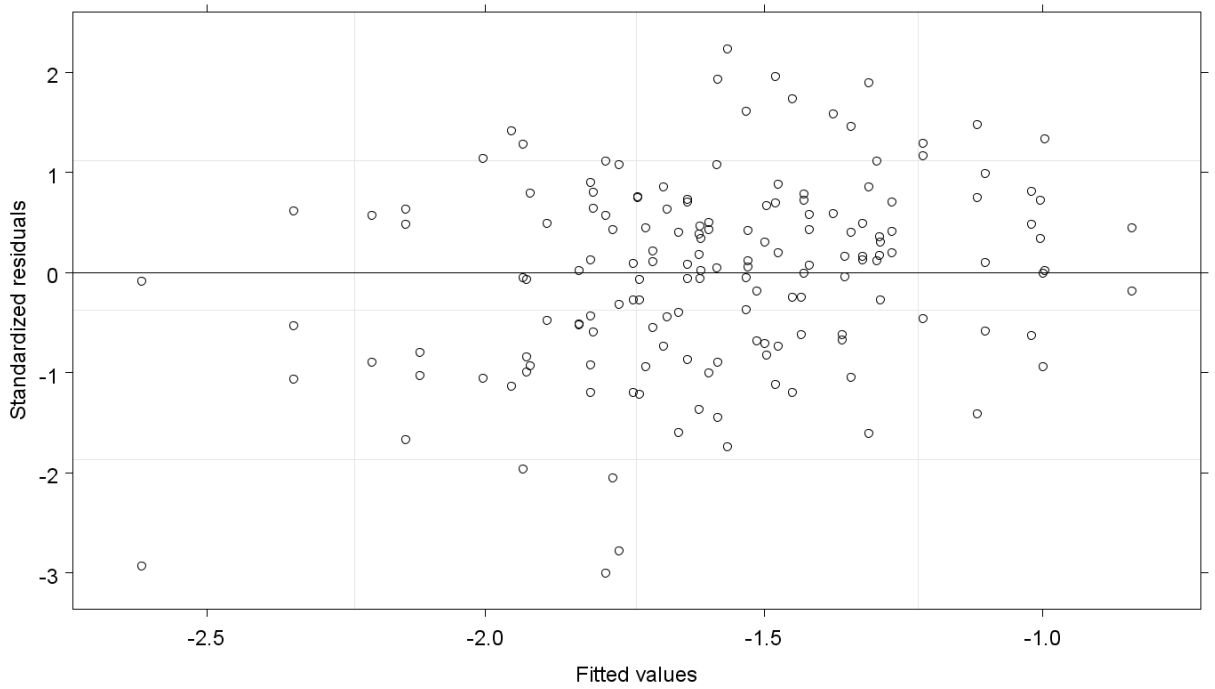

Figure C.4. Standardized residuals versus fitted values diagnostic plot for corn excluding "Row" in the random factor list.

The second diagnostic examined was a plot of the response variable (logarithmic transformed cleaning performance or *invlogPerform*) versus the fitted values of the model in question. Plots were generated for each case of including and excluding row as a random factor, examples of which are shown in Figures C.5 and C.6, respectively. One would expect that these plots should display an approximate 1:1 line indicating a high level of goodness-of-fit, as both figures do. However, the problem lies in the fact that the data displayed in Figure C.5 follow an exact 1:1 line and is suspicious, while in Figure C.6 an underlying 1:1 trend is present with a degree of variation. The cause of the trend shown in Figure C.5 was likely due to the presence of only one unique data point for each incidence of a given row number in the nesting sequence of the random factors. For 'row' to be included, it is preferable to have at least 2-3 data points for each incidence of a given row number within a nesting sequence in order for 'row' to be included as a random factor in the model. Therefore with respect to this diagnostic as well, it was preferable for 'row' to be excluded from the random factor list.

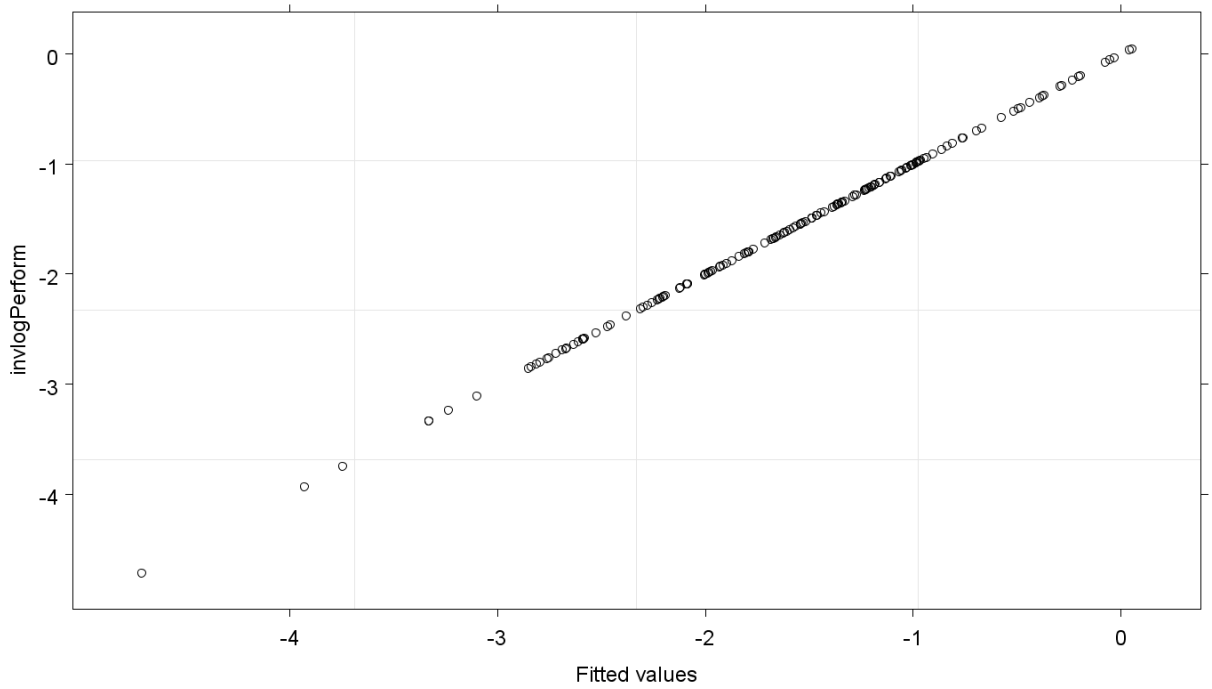

Figure C.5. Response variable versus fitted values for corn including “Row" in the random factor list.

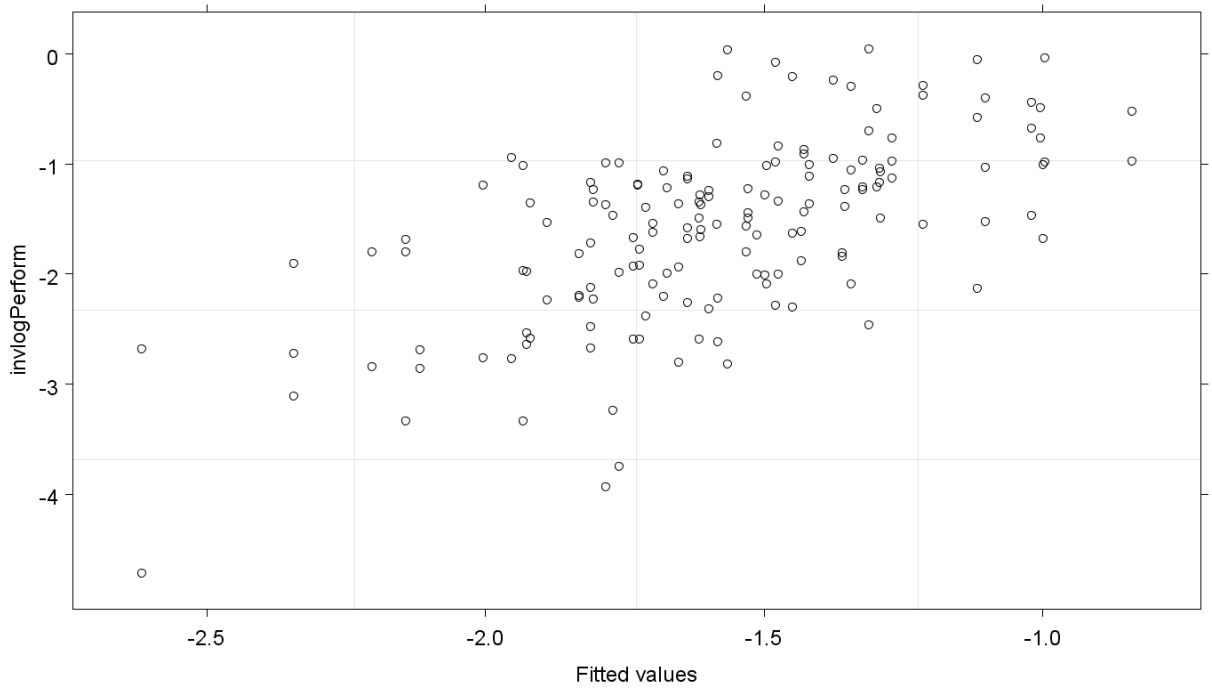

Figure C.6. Response variable versus fitted values for corn excluding "Row" in the random factor list.

C.3 Corn Stubble Results

The maximal mixed-effects model for corn stubble was constructed using main effects for configuration, speed and the residue moisture content at the time of the trial, as well as an interaction effect between configuration and speed. An interaction effect for moisture content at time of operation could not be included as singularities in the solving process could not yield a solution. A detailed explanation of tables and results is shown below for the statistical test of the front orientation, while detailed tables for the rear orientation and both orientations follow.

C.3.1 Front orientation only (four configurations)

Model simplification was used to reduce the maximal model to the minimally adequate model. This was accomplished by removing one fixed-effect model parameter at a time, evaluated by choosing the parameter with the largest p-value (continuous variable) or set of p-values (discrete value with several levels). The p-values that were evaluated are highlighted in Table C.1. The interaction effects were removed first followed by the main effects, if any. This process

continued until there were no p-values left that were greater than 0.05 or until the null model was reached. The maximal model summary from R© is shown below in Table C.1, while the minimally adequate model summary (null model) is shown in Table C.2. The standard deviation (denoted by *StdDev*) associated with each random factor is shown under the random effects section. The *(Intercept)* notation under the fixed effects heading refers to a default set of model parameters chosen as a baseline value for the response variable. In this case the *(Intercept)* notation represents main and interactive effects for the Offset-13 row cleaner configuration operating at 8 km/h with a residue moisture content of 0%. It should be noted that factors with discrete levels (such as configuration and speed) introduce a discrete change in the response variable as indicated under the column *value*. Continuous variables (such as moisture content at the time of the trial) offer a varying amount of change in the response variable where the number under the column *value* must be multiplied by the desired residue moisture content to obtain a result. It should be noted that the correlation matrix was removed from each model summary table as it was large and uninformative for this situation.

Table C.1. Maximal model summary for corn for the front orientation

Linear Mixed-effect model fit by maximum likelihood

Data: NULL

AIC	BIC	log likelihood
260.3055	293.642	-117.1528

Random Effects:

Formula: *~1 | Location*

	(Intercept)
StdDev:	2.44E-05

Formula: *~1 | Plot in Location*

	(Intercept)
StdDev:	6.89E-06

Formula: *~1 | Pass in Plot in Location*

	(Intercept)	Residual
StdDev:	0.1945217	0.7977561

Fixed Effects: **invlogPerform ~ Configuration * facSpeed + Oper.MC**

	Value	Std.Error	DF	t-value	p-value
(Intercept)	-0.915798	1.123038	64	-0.81546	0.4178
Configurationoffset18	-0.326944	0.54217	6	-0.60303	0.5686
Configurationparallel	-0.262325	0.473205	6	-0.55436	0.5994
Configurationproduction	-0.155353	0.488244	6	-0.31819	0.7611
facSpeed11.2	-0.107604	0.371374	6	-0.28975	0.7818
Oper.MC	-3.449207	5.556849	6	-0.62071	0.5576
Configurationoffset18:facSpeed11.2	0.260049	0.525967	6	0.49442	0.6386
Configurationparallel:facSpeed11.2	0.367829	0.525202	6	0.700357	0.5099
Configurationproduction:facSpeed11.2	0.118139	0.525202	6	0.224941	0.8295

Standardized Within-Group Residuals:

Min	Q1	Med	Q3	Max
-2.8521282	-0.7089884	0.0895918	0.6439797	2.15702

Number of Observations: 96

Number of Groups:

Location	Plot in Location	Pass in Plot in Location
2	16	32

Table C.2. Minimally adequate model summary for corn for the front orientation

Linear Mixed-effect model fit by maximum likelihood

Data: NULL

AIC	BIC	log likelihood
245.7812	258.6029	-117.8906

Random Effects:

Formula: *~1 | Location*

	(Intercept)
StdDev:	0.03731743

Formula: *~1 | Plot in Location*

	(Intercept)
StdDev:	4.40E-05

Formula: *~1 | Pass in Plot in Location*

	(Intercept)	Residual
StdDev:	0.2197652	0.797756

Fixed Effects: **invlogPerform ~ 1**

	Value	Std.Error	DF	t-value	p-value
(Intercept)	-1.582071	0.09448749	64	-16.7437	0

Standardized Within-Group Residuals:

Min	Q1	Med	Q3	Max
-2.81354919	-0.6757066	0.04670678	0.62824714	1.929394

Number of Observations: 96

Number of Groups:

Location	Plot in Location	Pass in Plot in Location
2	16	32

Tables C.3 and C.4 display a compact summary of the detailed results shown above in Tables C.1 and C.2 using generalized p-values for each factor.

Table C.3. Summary table for the maximal model for corn for the front orientation

MAXIMAL MODEL	Numerator DF	Denominator DF	F-value	p-value
(Intercept)	1	64	290.3688	< 0.0001
Configuration	3	6	0.06803	0.9749
facSpeed	1	6	0.20126	0.6695
Oper.MC	1	6	0.40598	0.5475
Configuration:facSpeed	3	6	0.18782	0.9009

Table C.4. Summary table for the null model for corn for the front orientation

NULL MODEL	Numerator DF	Denominator DF	F-value	p-value
(Intercept)	1	64	280.3518	< 0.0001

A comparison between the maximal and minimally adequate (null) models is shown in Table C.5. The p-value on the right hand side was much greater than 0.05 which meant that there was no statistically significant difference in the results between the two models. The null model could therefore be used to predict cleaning performance with very little difference from the maximal model with much greater simplicity. This meant that none of the fixed factors used in the experiment had a statistically significant impact on the mean cleaning performance of the various row cleaner configurations.

Table C.5. Comparison table between the maximal model and the null model for corn for the front orientation

Model Type	Model Number	Degrees of Freedom	AIC	BIC	logLik	Test	L. Ratio	p-value
maximal	1	13	260.306	293.642	-117.15			
null	2	5	245.781	258.603	-117.89	1 vs 2	1.47567	0.9931

C.3.2 Rear orientation only (all five configurations)

There were no statistically significant differences within each the five configurations, and the two travel speeds. In addition there were no statistically significant differences between the factors of configuration, travel speed and moisture content at time of operation. The mean cleaning performance for the rear orientation for corn residue could therefore be considered to be equal regardless of the configuration or travel speed chosen within the statistical bounds of this experiment. The statistical output is shown below in Tables C.6 through C.10.

Table C.6. Maximal model summary for corn for the rear orientation

Linear Mixed-effect model fit by maximum likelihood

Data: NULL

AIC	BIC	log likelihood
196.8153	230.9653	-83.40764

Random Effects:

Formula: *~1 | Location*

	(Intercept)
StdDev:	1.87E-05

Formula: *~1 | Plot in Location*

	(Intercept)
StdDev:	4.10E-06

Formula: *~1 | Pass in Plot in Location*

	(Intercept)	Residual
StdDev:	0.2894121	0.7179141

Fixed Effects: **invlogPerform ~ Configuration * facSpeed + Oper.MC**

	Value	Std.Error	DF	t-value	p-value
(Intercept)	-1.5670517	0.837226	32	-1.87172	0.0704
Configurationoffset13	-0.0507886	0.765887	8	-0.06631	0.9488
Configurationoffset18	-0.0408044	0.534966	8	-0.07627	0.9411
Configurationparallel	-0.3402759	0.567949	8	-0.59913	0.5657
Configurationproduction	0.4816357	0.55817	8	0.862884	0.4133
facSpeed11.2	-0.2096365	0.594645	8	-0.35254	0.7335
Oper.MC	-0.2676478	6.513471	8	-0.04109	0.9682
Configurationoffset13:facSpeed11.2	0.2036744	0.745064	8	0.273365	0.7915
Configurationoffset18:facSpeed11.2	0.0072988	0.745805	8	0.009787	0.9924
Configurationparallel:facSpeed11.2	0.7580866	0.745064	8	1.017479	0.3387
Configurationproduction:facSpeed11.2	-0.0893319	0.745064	8	-0.1199	0.9075

Standardized Within-Group Residuals:

Min	Q1	Med	Q3	Max
-3.26587965	-0.5598731	0.06577441	0.53500867	2.254223

Number of Observations: 72

Number of Groups:

Location	Plot in Location	Pass in Plot in Location
2	20	40

Table C.7. Minimally adequate model summary for corn for the rear orientation

Linear Mixed-effect model fit by maximum likelihood

Data: NULL

AIC	BIC	log likelihood
182.4053	193.7886	-86.20263

Random Effects:

Formula: *~1 | Location*

	(Intercept)
StdDev:	1.80E-05

Formula: *~1 | Plot in Location*

	(Intercept)
StdDev:	5.14E-06

Formula: *~1 | Pass in Plot in Location*

	(Intercept)	Residual
StdDev:	0.3777558	0.7163533

Fixed Effects: **invlogPerform ~ 1**

	Value	Std.Error	DF	t-value	p-value
(Intercept)	-1.604552	0.1047943	32	-15.3114	0

Standardized Within-Group Residuals:

Min	Q1	Med	Q3	Max
-3.2965319	-0.5385025	0.07787143	0.54708414	2.18531

Number of Observations: 72

Number of Groups:

Location	Plot in Location	Pass in Plot in Location
2	20	40

Table C.8. Summary table for the maximal model for corn for the rear orientation

MAXIMAL MODEL	Numerator DF	Denominator DF	F-value	p-value
(Intercept)	1	32	233.3001	< 0.0001
Configuration	4	8	0.71412	0.6052
facSpeed	1	8	0.00643	0.9381
Oper.MC	1	8	0.00011	0.9917
Configuration:facSpeed	4	8	0.56406	0.6959

Table C.9. Summary table for the null model for corn for the rear orientation

NULL MODEL	Numerator DF	Denominator DF	F-value	p-value
(Intercept)	1	32	234.4403	< 0.0001

Table C.10. Comparison table between the maximal model and the null model for corn for the rear orientation

Model Type	Model Number	Degrees of Freedom	AIC	BIC	logLik	Test	L. Ratio	p-value
maximal	1	15	196.815	230.965	-83.408			
null	2	5	182.405	193.789	-86.203	1 vs 2	5.58999	0.8485

C.3.3 Both front and rear orientations (four configurations)

Because there were no significant differences within the datasets for each orientation, the two datasets were combined and tested as a single dataset. When completed, there were no statistically significant differences in mean cleaning performance. The statistical output is shown in Tables C.11 through C.15.

Table C.11. Maximal model summary for corn for both orientations (no alpha prototype)

Linear Mixed-effect model fit by maximum likelihood

Data: NULL

AIC	BIC	log likelihood
403.6109	443.5882	-188.8055

Random Effects:

Formula: *~1 | Location*

(Intercept)

StdDev: 2.53E-05

Formula: *~1 | Plot in Location*

(Intercept)

StdDev: 5.92E-07

Formula: *~1 | Pass in Plot in Location*

	(Intercept)	Residual
StdDev:	0.3612696	0.7266023

Fixed Effects: **invlogPerform ~ Configuration * facSpeed + Oper.MC**

	Value	Std.Error	DF	t-value	p-value
(Intercept)	-1.2088351	1.069531	128	-1.13025	0.2605
Configurationoffset18	-0.1877518	0.516338	6	-0.36362	0.7286
Configurationparallel	-0.2699076	0.450659	6	-0.59892	0.5711
Configurationproduction	0.1233051	0.464981	6	0.265183	0.7997
facSpeed11.2	-0.0669472	0.35368	6	-0.18929	0.8561
Oper.MC	-2.1143916	5.292094	6	-0.39954	0.7033
Configurationoffset18:facSpeed11.2	0.0777963	0.500907	6	0.155311	0.8817
Configurationparallel:facSpeed11.2	0.442462	0.500178	6	0.884609	0.4104
Configurationproduction:facSpeed11.2	-0.0463189	0.500178	6	-0.0926	0.9292

Standardized Within-Group Residuals:

Min	Q1	Med	Q3	Max
-3.1958069	-0.59026	0.1252315	0.5923238	2.239478

Number of Observations: 160

Number of Groups:

Location	Plot in Location	Pass in Plot in Location
2	16	32

Table C.12. Minimally adequate model summary for corn for both orientations (no alpha prototype)

Linear Mixed-effect model fit by maximum likelihood

Data: NULL

AIC	BIC	log likelihood
390.0979	405.4738	-190.0489

Random Effects:

Formula: *~1 | Location*

(Intercept)

StdDev: 3.61E-05

Formula: *~1 | Plot in Location*

(Intercept)

StdDev: 2.54E-07

Formula: *~1 | Pass in Plot in Location*

	(Intercept)	Residual
StdDev:	0.3867782	0.7266023

Fixed Effects: **invlogPerform ~ 1**

	Value	Std.Error	DF	t-value	p-value
(Intercept)	-1.585154	0.08958106	128	-17.6952	0

Standardized Within-Group Residuals:

Min	Q1	Med	Q3	Max
-3.14529969	-0.546438	0.09004296	0.60099261	2.18499

Number of Observations: 160

Number of Groups:

Location	Plot in Location	Pass in Plot in Location
2	16	32

Table C.13. Summary table for the maximal model for corn for both orientations

MAXIMAL MODEL	Numerator DF	Denominator DF	F-value	p-value
(Intercept)	1	128	321.398	< 0.0001
Configuration	3	6	0.3372	0.7996
facSpeed	1	6	0.0941	0.7694
Oper.MC	1	6	0.1534	0.7089
Configuration:facSpeed	3	6	0.3939	0.7623

Table C.14. Summary table for the null model for corn for both orientations

NULL MODEL	Numerator DF	Denominator DF	F-value	p-value
(Intercept)	1	128	313.1199	< 0.0001

Table C.15. Comparison table between the maximal model and the null model for corn for both orientations

Model Type	Number	Degrees of Freedom	AIC	BIC	logLik	Test	L. Ratio	p-value
maximal	1	13	403.611	443.588	-188.81			
null	2	5	390.098	405.474	-190.05	1 vs 2	2.48699	0.9623

C.4 Wheat Stubble Results

The maximal mixed-effects model for wheat stubble was constructed using main effects for configuration, and speed. An interaction effect for configuration and speed as well as main and interactive effects for moisture content at time of operation could not be included as singularities in the solving process could not yield any solutions. Because a detailed explanation example of tables and results was shown for corn and because the same analysis was used for wheat stubble, only the detailed tables of statistical results are found below. Generally, the smaller range of data values for wheat stubble led to smaller p-values as compared to corn, however not to the point where there was a statistically significant difference ($p \leq 0.05$). In all three statistical tests, using datasets for the front orientation only (four configurations), the rear orientation only (five configurations), and both orientations combined, respectively, similar results to the corn stubble were obtained. In all three cases there were no statistically significant differences within each of the five configurations and the two travel speeds. This meant that the mean cleaning performance for the front and rear orientations could be considered to be equal regardless of the configuration or travel speed chosen within the statistical bounds of the experiment.

C.4.1 Front orientation only (four configurations)

The statistical output for the front orientation for wheat is shown in Tables C.16 through C.20.

Table C.16. Maximal model summary for wheat for the front orientation

Linear Mixed-effect model fit by maximum likelihood

Data: NULL

AIC	BIC	log likelihood
148.664	165.5048	-65.332

Random Effects:

Formula: *~1 | Location*

	(Intercept)
StdDev:	2.10E-05

Formula: *~1 | Plot in Location*

	(Intercept)
StdDev:	7.27E-09

Formula: *~1 | Pass in Plot in Location*

	(Intercept)	Residual
StdDev:	0.4085343	0.86678

Fixed Effects: **invlogPerform ~ Configuration + facSpeed**

	Value	Std.Error	DF	t-value	p-value
(Intercept)	-3.13762	0.3815526	32	-8.22331	0
Configurationoffset18	-1.0834	0.4826301	3	-2.24477	0.1105
Configurationparallel	-0.25415	0.4826301	3	-0.5266	0.6349
Configurationproduction	-0.61811	0.4826301	3	-1.28071	0.2903
facSpeed11.2	0.164354	0.341271	3	0.481594	0.663

Standardized Within-Group Residuals:

Min	Q1	Med	Q3	Max
-2.1071368	-0.6808778	0.043783	0.67662392	1.949578

Number of Observations: 48

Number of Groups:

Location	Plot in Location	Pass in Plot in Location
1	8	16

Table C.17. Minimally adequate model summary for wheat for the front orientation

Linear Mixed-effect model fit by maximum likelihood

Data: NULL

AIC	BIC	log likelihood
146.2078	155.5638	-68.1039

Random Effects:

Formula: *~1 | Location*

	(Intercept)
StdDev:	3.10E-05

Formula: *~1 | Plot in Location*

	(Intercept)
StdDev:	1.03E-07

Formula: *~1 | Pass in Plot in Location*

	(Intercept)	Residual
StdDev:	0.5828513	0.86678

Fixed Effects: **invlogPerform ~ 1**

	Value	Std.Error	DF	t-value	p-value
(Intercept)	-3.544361	0.194086	32	-18.2618	0

Standardized Within-Group Residuals:

Min	Q1	Med	Q3	Max
-1.99085647	-0.4921603	-0.03563	0.44851516	2.009503

Number of Observations: 48

Number of Groups:

Location	Plot in Location	Pass in Plot in Location
1	8	16

Table C.18. Summary table for the maximal model for wheat for the front orientation

MAXIMAL MODEL	Numerator DF	Denominator DF	F-value	p-value
(Intercept)	1	32	431.4567	< 0.0001
Configuration	3	3	1.9011	0.3055
facSpeed	1	3	0.2319	0.663

Table C.19. Summary table for the null model for wheat for the front orientation

NULL MODEL	Numerator DF	Denominator DF	F-value	p-value
(Intercept)	1	32	333.4948	< 0.0001

Table C.20. Comparison table between the maximal model and the null model for wheat for the front orientation

Model Type	Model Number	Degrees of Freedom	AIC	BIC	logLik	Test	L. Ratio	p-value
maximal	1	9	148.664	165.505	-65.332			
null	2	5	146.208	155.564	-68.104	1 vs 2	5.5438	0.2359

C.4.2 Rear orientation only (all five configurations)

The statistical output for the front orientation for wheat is shown in Tables C.21 through C.25.

Table C.21. Maximal model summary for wheat for the rear orientation

Linear Mixed-effect model fit by maximum likelihood

Data: NULL

AIC	BIC	log likelihood
112.8087	128.6439	-46.40433

Random Effects:

Formula: *~1 | Location*

	(Intercept)
StdDev:	1.73E-05

Formula: *~1 | Plot in Location*

	(Intercept)
StdDev:	5.04E-08

Formula: *~1 | Pass in Plot in Location*

	(Intercept)	Residual
StdDev:	2.81E-05	0.878158

Fixed Effects: **invlogPerform ~ Configuration + facSpeed**

	Value	Std.Error	DF	t-value	p-value
(Intercept)	-3.97149	0.5070045	16	-7.83325	0
Configurationoffset13	0.817678	0.5890859	4	1.388045	0.2374
Configurationoffset18	-0.15525	0.5890859	4	-0.26354	0.8052
Configurationparallel	0.917413	0.5890859	4	1.55735	0.1944
Configurationproduction	-0.17516	0.5890859	4	-0.29733	0.781
facSpeed11.2	0.112818	0.3206578	4	0.351834	0.7427

Standardized Within-Group Residuals:

Min	Q1	Med	Q3	Max
-2.03236215	-0.5420077	-0.0845	0.74694902	2.125498

Number of Observations: 36

Number of Groups:

Location	Plot in Location	Pass in Plot in Location
1	10	20

Table C.22. Minimally adequate model summary for wheat for the rear orientation

Linear Mixed-effect model fit by maximum likelihood

Data: NULL

AIC	BIC	log likelihood
112.1259	120.0435	-51.06295

Random Effects:

Formula: *~1 | Location*

(Intercept)

StdDev: 0.00059162

Formula: *~1 | Plot in Location*

(Intercept)

StdDev: 0.00666794

Formula: *~1 | Pass in Plot in Location*

	(Intercept)	Residual
StdDev:	0.4876966	0.88657

Fixed Effects: **invlogPerform ~ 1**

	Value	Std.Error	DF	t-value	p-value
(Intercept)	-3.610788	0.187474	16	-19.2602	0

Standardized Within-Group Residuals:

Min	Q1	Med	Q3	Max
-1.95509567	-0.45151	0.020033	0.49178886	2.19338

Number of Observations: 36

Number of Groups:

Location	Plot in Location	Pass in Plot in Location
1	10	20

Table C.23. Summary table for the maximal model for wheat for the rear orientation

MAXIMAL MODEL	Numerator DF	Denominator DF	F-value	p-value
(Intercept)	1	16	504.9964	< 0.0001
Configuration	4	4	2.4347	0.2049
facSpeed	1	4	0.1238	0.7427

Table C.24. Summary table for the null model for wheat for the rear orientation

NULL MODEL	Numerator DF	Denominator DF	F-value	p-value
(Intercept)	1	16	370.9544	< 0.0001

Table C.25. Comparison table between the maximal model and the null model for wheat for the rear orientation

Model Type	Model Number	Degrees of Freedom	AIC	BIC	logLik	Test	L. Ratio	p-value
maximal	1	10	112.809	128.644	-46.404			
null	2	5	112.126	120.044	-51.063	1 vs 2	9.31724	0.0971

C.4.3 Both front and rear orientations (four configurations)

The statistical output for the front orientation for wheat is shown in Tables C.26 through C.30.

Table C.26. Maximal model summary for wheat for both orientations (no alpha prototype)

Linear Mixed-effect model fit by maximum likelihood

Data: NULL

AIC	BIC	log likelihood
226.9555	248.3937	-104.4777

Random Effects:

Formula: *~1 | Location*

	(Intercept)
StdDev:	2.08E-05

Formula: *~1 | Plot in Location*

	(Intercept)
StdDev:	1.14E-08

Formula: *~1 | Pass in Plot in Location*

	(Intercept)	Residual
StdDev:	0.4723014	0.808547

Fixed Effects: **invlogPerform ~ Configuration + facSpeed**

	Value	Std.Error	DF	t-value	p-value
(Intercept)	-3.13361	0.3434231	64	-9.12463	0
Configurationoffset18	-1.03921	0.4343996	3	-2.39229	0.0965
Configurationparallel	-0.1126	0.4343996	3	-0.2592	0.8122
Configurationproduction	-0.768	0.4343996	3	-1.76795	0.1752
facSpeed11.2	0.122753	0.3071669	3	0.39963	0.7162

Standardized Within-Group Residuals:

Min	Q1	Med	Q3	Max
-2.26984671	-0.5449259	0.027983	0.75202034	1.928242

Number of Observations: 80

Number of Groups:

Location	Plot in Location	Pass in Plot in Location
1	8	16

Table C.27. Minimally adequate model summary for wheat for both orientations (no alpha prototype)

Linear Mixed-effect model fit by maximum likelihood

Data: NULL

AIC	BIC	log likelihood
225.9509	237.861	-107.9754

Random Effects:

Formula: *~1 | Location*

	(Intercept)
StdDev:	3.61E-05

Formula: *~1 | Plot in Location*

	(Intercept)
StdDev:	4.58E-07

Formula: *~1 | Pass in Plot in Location*

	(Intercept)	Residual
StdDev:	0.6458295	0.808547

Fixed Effects: **invlogPerform ~ 1**

	Value	Std.Error	DF	t-value	p-value
(Intercept)	-3.552182	0.186209	64	-19.0763	0

Standardized Within-Group Residuals:

Min	Q1	Med	Q3	Max
-2.3323528	-0.5823184	0.114128	0.6927044	1.933545

Number of Observations: 80

Number of Groups:

Location	Plot in Location	Pass in Plot in Location
1	8	16

Table C.28. Summary table for the maximal model for wheat for both orientations

MAXIMAL MODEL	Numerator DF	Denominator DF	F-value	p-value
(Intercept)	1	64	534.9355	< 0.0001
Configuration	3	3	2.6887	0.2191
facSpeed	1	3	0.1597	0.7162

Table C.29. Summary table for the null model for wheat for both orientations

NULL MODEL	Numerator DF	Denominator DF	F-value	p-value
(Intercept)	1	64	363.9062	< 0.0001

Table C.30. Comparison table between the maximal model and the null model for wheat for both orientations

Model Type	Model Number	Degrees of Freedom	AIC	BIC	logLik	Test	L. Ratio	p-value
maximal	1	9	226.956	248.394	-104.48			
null	2	5	225.951	237.861	-107.98	1 vs 2	6.99365	0.1361

APPENDIX D - Evaluation of Edge Effects

This appendix contains the detailed data table results for the edge effects of the outside row unit of the machine. In all cases the mean and standard deviation were calculated from the raw data. Upper and lower limits of a 95% confidence interval (CI) were then calculated based on a normal distribution of the initial amount of residue on the field. The mass of residue of the neighboring row, immediate of the outside row unit on the machine was then compared to see if its value resided within the range provided by the confidence interval. If it did the "test" resulted in a value of "TRUE." Conversely, if the value was outside the 95% CI, the "test" returned a value of "FALSE."

D.1 Corn – Location I

The edge effects results for Location I are shown below in Tables D.1 and D.2. From these it can be concluded that residue throw-over does not occur.

Table D.1. Edge effects results for location I for plots 1 through 4

Plot	1	2	3	4
Configuration	Offset-18	Production	Offset-13	Parallel
Speed	8 km/h	8 km/h	11.2 km/h	8 km/h
Mean Mass of Residue (dry basis) (g)	738.57	752.65	749.99	780.63
Sample Standard Deviation (g)	107.75	92.48	80.25	201.14
Lower Limit of Confidence Interval (g)	527.37	571.40	592.70	386.40
Upper Limit of Confidence Interval (g)	949.76	933.90	907.28	1174.87
Outside Row Residue Mass (g)	630.00	875.69	823.28	696.53
Test	TRUE	TRUE	TRUE	TRUE

Table D.2. Edge effects results for location I for plots 7 through 10

Plot	7	8	9	10
Configuration	Parallel	Production	Offset-13	Offset-18
Speed	11.2 km/h	11.2 km/h	8 km/h	11.2 km/h
Mean Mass of Residue (dry basis) (g)	859.49	781.58	733.06	648.65
Sample Standard Deviation (g)	138.52	114.81	130.78	221.58
Lower Limit of Confidence Interval (g)	587.99	556.57	476.75	214.37
Upper Limit of Confidence Interval (g)	1130.98	1006.60	989.38	1082.93
Outside Row Residue Mass (g)	699.83	614.52	696.93	850.22
Test	TRUE	TRUE	TRUE	TRUE

D.2 Corn – Location II

The edge effects results for Location I are shown below in Tables D.3 and D.4. In most cases it can be concluded that throw-over does not occur except in the case of the Production configuration at high-speed. The reason for this anomaly though was likely due to an abnormally low initial mass measurement distribution. In plot eight, highlighted in green is a negative value for the lower limit of the 95% CI. This is highlighted to show the wide degree of variation in the initial mass measurements of the plot and the fact that it is physically impossible to have a negative mass.

Table D.3. Edge effects results for location II for plots 1 through 4

Plot	1	2	3	4
Configuration	Production	Offset-18	Production	Offset-18
Speed	8 km/h	8 km/h	11.2 km/h	11.2 km/h
Mean Mass of Residue (dry basis) (g)	277.92	418.92	148.37	386.73
Sample Standard Deviation (g)	141.34	120.88	65.44	193.80
Lower Limit of Confidence Interval (g)	0.90	181.99	20.11	6.90
Upper Limit of Confidence Interval (g)	554.95	655.84	276.62	766.56
Outside Row Residue Mass (g)	395.62	384.59	418.18	237.16
Test	TRUE	TRUE	HIGH	TRUE

Table D.4. Edge effects results for location II for plots 5, 6, 8, & 10

Plot	5	6	8	10
Configuration	Parallel	Parallel	Offset-13	Offset-13
Speed	8 km/h	11.2 km/h	11.2 km/h	8 km/h
Mean Mass of Residue (dry basis) (g)	291.77	262.43	516.94	354.79
Sample Standard Deviation (g)	89.96	113.40	337.01	122.75
Lower Limit of Confidence Interval (g)	115.46	40.16	-143.58	114.20
Upper Limit of Confidence Interval (g)	468.08	484.69	1177.46	595.37
Outside Row Residue Mass (g)	167.88	240.72	417.16	229.44
Test	TRUE	TRUE	TRUE	TRUE

D.3 Wheat – Location III

The edge effects results for Location I are shown below in Tables D.5 and D.6. In most cases it can be concluded that throw-over does not occur except in the case of the Offset-13 configuration at high-speed. The reason for this anomaly though, was likely due to an abnormally large outside-row residue mass measurement which was situated in heavy chaff. In plots four and nine, highlighted in green are negative values for the lower limits of the 95% CI. This is highlighted to show the wide degree of variation in the initial mass measurements of the plot and the fact that it is physically impossible to have a negative mass.

Table D.5. Edge effects results for location III for plots 1 through 4

Plot	1	2	3	4
Configuration	Parallel	Production	Offset-18	Parallel
Speed	8 km/h	8 km/h	11.2 km/h	11.2 km/h
Mean Mass of Residue (dry basis) (g)	575.62	608.35	472.80	521.44
Sample Standard Deviation (g)	182.11	207.65	226.89	296.75
Lower Limit of Confidence Interval (g)	218.69	201.36	28.10	-60.17
Upper Limit of Confidence Interval (g)	932.55	1015.33	917.50	1103.05
Outside Row Residue Mass (g)	373.36	530.71	437.53	188.43
Test	TRUE	TRUE	TRUE	TRUE

Table D.6. Edge effects results for location III for plots 5, 6, 9, & 10

Plot	5	6	9	10
Configuration	Offset-13	Production	Offset-18	Offset-13
Speed	8 km/h	11.2 km/h	8 km/h	11.2 km/h
Mean Mass of Residue (dry basis) (g)	441.72	375.52	610.25	460.06
Sample Standard Deviation (g)	131.75	167.69	327.79	160.02
Lower Limit of Confidence Interval (g)	183.49	46.84	-32.20	146.43
Upper Limit of Confidence Interval (g)	699.94	704.20	1252.70	773.69
Outside Row Residue Mass (g)	457.92	367.94	422.74	1089.87
Test	TRUE	TRUE	TRUE	HIGH